Hydrologic Functioning of Low-Relief, Deep Soil Watersheds and Hydrologic Legacies of Intensive Agriculture in the Calhoun Critical Zone Observatory, South Carolina, USA
by

John Mallard

Earth and Ocean Sciences
Duke University

Date:_______________________
Approved:

____
Brian McGlynn, Advisor

____
Allen Murray

____
Martin Doyle

____
Lincoln Pratson

____
Daniel Richter

Dissertation submitted in partial fulfillment of the requirements for the degree of
Doctor of Philosophy in Earth and Ocean Sciences
in the Graduate School of Duke University
2020

ABSTRACT

Hydrologic Functioning of Low-Relief, Deep Soil Watersheds and Hydrologic Legacies of Intensive Agriculture in the Calhoun Critical Zone Observatory, South Carolina, USA
by

John Mallard

Earth and Ocean Sciences
Duke University

Date:_______________________
Approved:

____
Brian McGlynn, Advisor

____
Allen Murray

____
Martin Doyle

____
Lincoln Pratson

____
Daniel Richter

An abstract of a dissertation submitted in partial fulfillment of the requirements for the degree of Doctor of Philosophy in Earth and Ocean Sciences
in the Graduate School of Duke University
2020

Abstract

Watersheds are complex, three dimensional structures that partition water between the components of the water balance and multiple storage pools within the watershed. This partitioning function, however, remains poorly understood in a broadly transferable way despite decades of research. Perhaps one reason for this is the disciplinary bias towards studying pristine, mountainous watersheds with steep terrain and shallow soil. Although the relative simplicity of such systems has made them ideal hydrologic laboratories, understanding how the diversity of watersheds function globally will require the incorporation of new types of landscapes into the studies of hillslope and watershed hydrology.

The Southern Piedmont region of the United States stretches from Alabama to Maryland between the Appalachian Mountains and Atlantic coastal plain. It's generally rolling terrain is widely underlain by deeply weathered and highly stratified soil characterized by relatively shallow clay-rich Bt horizons while weathered saprolite can extend tens of meters below. Although a low-relief landscape overall, headwaters of the Southern Piedmont are often highly dissected with steep narrow valleys containing temporary streams surrounded by diverse topography. The deep soils and low overall relief of the region represent an ideal opportunity to incorporate more diverse landscapes into our studies of watershed hydrology.

As part of the NSF funded Calhoun Critical Zone Observatory, we intensively instrumented a 6.9 ha headwater (watershed 4, WS4), along with other targeted sensor locations including discharge in the 322 ha watershed that contains it (Holcombe's Branch, HLCM), a nearby meteorological station, a deep groundwater well on a relatively

flat interfluve, and a network of shallow groundwater wells in the buried floodplain. Sensors were continuously monitored for over 3 years while logging at 5 minute intervals. This sensor network allowed us to quantify the timing and magnitude of precipitation, soil moisture, deep and shallow water tables, and runoff. By doing so we were able to 1) describe the interactions between water balance components in WS4, 2) compare these watershed-scale measurements to internal hydrologic dynamics to determine what parts of the watershed are responsible for distinct watershed functions, and 3) explore how headwaters connect to higher order streams.

Using the monthly water balance in WS4, we calculated changes in integrated watershed storage and then derived a cumulative monthly storage time series from its running integral. We estimate that storage changes within the year by hundreds of millimeters (~25% of annual precipitation) in conjunction with seasonal peaks in evapotranspiration. Additionally, of all the potential variables that correlated to runoff magnitudes at the watershed scale, we found storage to be the best, particularly above a threshold value which remained remarkably consistent across all three years even with substantial differences in precipitation.

However, despite the storage threshold dependence of runoff, when we calculated daily storage we found that while runoff increased primarily in response to major precipitation events and then decreased again shortly thereafter, storage primarily wet up and dried down seasonally. Similarly, individual measurements of internal watershed hydrology like depth-dependent soil moisture and water tables displayed either seasonal or event-scale changes. We determined that measurements taken at watershed positions with more convergent hillslopes, or farther from the watershed divide, or installed deeper in the soil are more likely to display seasonal changes, and vice versa for event-scale changes. These three gradients (convergence, hillslope position, and depth) are proxies for vertical, lateral, and longitudinal distances, and so it appeared that the underlying gradient being measured was contributing volume. We determined the functions of different landscape components based on this analysis, and came to understand that storage-linked sites wet up first and then stay consistently so, setting threshold conditions for runoff. Subsequently, when runoff-linked sites wet-up, they mobilize significant runoff fluxes either by hydraulic displacement, or interflow, or a transmissivity feedback, or likely some combination of them all. During these times of high storage, a substantial portion of the watershed is connected before drying down again with the exception of more storage-linked locations. The resulting runoff outputs from WS4 are extremely flashy (i.e., high runoff peaks shortly after precipitation followed rapidly declining runoff), but only under conditions when the storage threshold is exceeded.

In contrast, we found HLCM to be far less flashy and relatively less sensitive to year to year fluctuations in precipitation. Further, we observed that except in the most extreme storms, surface flow from WS4 across the former floodplain in between it and HLCM always fully infiltrates into the sandy, legacy sediments deposited along the entire former floodplain. These sediments are the legacy of centuries of intensive and poorly managed agriculture across the Southern Piedmont. Wells in these sediments along HLCM and at the outlet of WS4 revealed a highly dynamic water table that was very responsive to outflow from WS4. A geometric simplification of the shape of this sediment packet and an estimate of their porosity revealed that these sediments had ~900 m^3 of available storage space, space that was constantly filling and draining. Interestingly, that available storage volume level was sufficient to absorb discharge from WS4 through 97% of the study period. Through most WS4 flow states, this storage buffered HLCM from flashier runoff coming from WS4 by converting runoff to slower subsurface flow. However, when storage reached volumes within 15% of maximum, usually in conjunction with large fluxes coming from WS4, runoff in HLCM behaved similarly to WS4. So, the storage volume in legacy sediments serves as an effective buffer from flashy upstream hydrology, but when they reach or approach saturation they become effective at transmitting surface flow, likely via saturation excess overland flow. Although we observed this phenomenon at a single location, such features are likely quite common locally and regionally and represent a heretofore underappreciated legacy of historic agriculture.

Taken together, these findings describe a hydrologic system that is much more dynamic seasonally than its abundant rainfall and surface water resources might suggest. Further, they indicate that even a century or more after agricultural land abandonment and forest regrowth, legacies of the 18th and 19th century remain in the landforms and soils of the region.

Contents

Abstract iv

List of Tables xii

List of Figures xiii

1. Introduction 1

1.1 Background – Runoff Generation in Watershed Hydrology 1

2. Storage dynamics buffer apparent water limitation and facilitate flashy, threshold-mediated runoff response. 5

2.1 Introduction 5

2.2 Methods 10

2.2.1 Study Site 10

2.2.2 Hydrologic and hydroclimatic data 12

2.2.3 Watershed storage 15

2.3 Results 17

2.3.1 Long-term regional hydroclimatic conditions 17

2.3.2 Annual and seasonal-scale hydrology 18

2.3.2.1 Precipitation, PET, and runoff 18

2.3.2.2 Storage dynamics 20

2.3.3 Deep groundwater and storage dynamics 23

2.3.4 Event-scale storage and runoff dynamics 25

2.3.5 Flow duration and regime 27

2.4 Discussion 31

2.4.1 What are the long-term hydroclimatic conditions of the Southern Piedmont and what do they suggest about water or energy limitation at multiple time scales?

– Seasonal and aseasonal hydroclimatic forcing lead to intra-annual switching between apparent water and energy limitation 31

2.4.2 How does integrated watershed storage vary at multiple time scales, and how does it reflect coupling to or buffering of hydroclimatic forcing? – Watershed storage varies seasonally, with high storage during the dormant season, suggesting its role in buffering stochastic precipitation and high growing season evapotranspiration . 34

2.4.3 What does the manifestation of storage dynamics in runoff suggest about the role of storage in mediating hydroclimatic forcing? – Runoff dynamics suggest threshold behavior in response to watershed storage, where higher runoff ratios, longer duration runoff, and less ephemeral flow are indicative of higher storage states regardless of immediate hydroclimatic forcing. 37

2.4.3.1 Runoff generation efficiency reflects seasonal changes in watershed storage 39

2.4.3.2 Flow regime changes interannually and seasonally in reflection of seasonal changes in storage. 43

2.4.3.3 Summary of 2.4.3 45

2.5 Implications for Critical Zone hydrology and ecohydrology 46

2.5.1 How does subsurface critical zone structure organize storage and its connections to runoff three-dimensionally? 46

2.5.2 Ecohydrologic functioning and future of the Southern Piedmont 49

2.6 Conclusion 55

3. Watershed scale storage and runoff generation reflect hillslope hydrology and watershed structural heterogeneity 58

3.1 Introduction 58

3.2 Methods 61

3.2.1 Study Site: WS4 of the Calhoun Critical Zone Observatory 61

3.2.2 Surface and Subsurface Hydrologic Measurements 63

3.2.3 Water Balance Calculation of Storage 66

3.3. Results 68

3.3.1 Water Balance 68

3.3.2 Deep groundwater 70

3.3.3 WS4 subsurface and terrain structure 73

3.3.4 Soil moisture and shallow groundwater connections to runoff dynamics 75

3.3.4.1 Soil Moisture 76

3.3.4.2 Shallow groundwater 78

3.4 Discussion 83

3.4.1 Water tables and soil moisture display primarily either event- or seasonal-scale dynamics 83

3.4.1.1 Subsurface hydrologic dynamics correspond to longitudinal, lateral, and vertical watershed structural gradients, suggesting an underlying relationship with contributing volume. 83

3.4.1.2 Individual water table and soil moisture locations generally correspond to either runoff or storage. 88

3.4.1.3 An evolving understanding of storage heterogeneity and runoff generation with deeply-weathered, vertically-stratified landscapes 93

3.5 Conclusion 100

4. Connectivity between intermittent headwaters and higher order streams mediated by dynamic storage in legacy anthropogenic sediments deposited on floodplains. 103

4.1 Introduction 103

4.1.1 Hydrologic connectivity across mountain fronts and alluvial fans in arid and semi-arid zones. 103

4.1.2 Legacy sediments in the Southern Piedmont 105

4.2 Methods 106

4.2.1 Study Site: nested watersheds within the Calhoun Critical Zone Observatory 106

4.2.2 Hydrologic measurements and flow characteristics 109

4.2.3 Estimation of legacy sediment pore volume 111

4.3 Results 114

4.3.1 Flow characteristics of watershed 4 and Holcombe's Branch 114

4.3.2 Hydrologic dynamics in legacy sediments between Holcombe's Branch and watershed 4. 116

4.4 Discussion 120

4.4.1 Importing hydrologic process from arid landscapes: mountain-front recharge mediates connectivity across scale in humid, low-relief landscapes 120

4.4.2 Implications for hydrologic functioning in the Southern Piedmont 122

4.5 Conclusion 125

5. Conclusions 127

References 130

Biography 148

List of Tables

Table 1: Annual and mean annual water balance components 18

Table 2: Physical characteristics of well nests. 64

Table 3: Physical characteristics of soil moisture pits. 64

Table 4: Physical and flow characteristics of watershed 4 (WS4) and Holcombe's Branch (HLCM) for water years (WY) 2016, 2017. 109

List of Figures

Figure 1: Site Map 11

Figure 2: Monthly Precipitation and Evapotranspiration; 19

Figure 3: Monthly water balance components for WS4 22

Figure 4: Runoff ratio and wetness index 23

Figure 5: Relationships between monthly runoff and monthly precipitation, evapotranspiration, and storage for WS4 25

Figure 6: Time series of daily storage in WS4 26

Figure 7: Monthly water balance components for WS4 30

Figure 8: Cumulative daily water balance components in WS4 30

Figure 9: Flow duration curves for WS4 31

Figure 10: Site Map 62

Figure 11: Water balance components for WS4 70

Figure 12: Storage and water table depth 71

Figure 13: Relationship between depth to water table in deep groundwater well and runoff 73

Figure 14: Depth profiles of saturated hydraulic conductivity (Ksat). 76

Figure 15: Lateral depth profiles of transects 1-3 in WS4. 80

Figure 16: Hourly runoff and soil moisture 83

Figure 17: Hourly runoff and shallow/deep water table along transect 1 86

Figure 18: Hourly runoff and shallow/deep water table along transect 2 90

Figure 19: Hourly runoff and shallow/deep water table along transect 3 93

Figure 20: Continuity of each subsurface hydrologic measurement through the study period 97

Figure 21: Continuity of each subsurface hydrologic measurement through the study period weighted by its relative value. 99

Figure 22: Conceptual model of storage and runoff conditions through the transition from dry to wet season in early fall. 99

Figure 23: Site Map 108

Figure 24: General well installation within legacy sediments on alluvial fan between WS4 and HLCM. 111

Figure 25: Precipitation and runoff for HLCM and WS4 113

Figure 26: Flow duration curves 115

Figure 27: Flood plain wells 118

Figure 28: Volume over time for both WS4 discharge and air volume 119

Figure 29: Scatter of mean flood plain well depth and runoff in HLCM. 122

Figure 30: Location of WS4 floodplain sediments and four other examples of different levels of a defined surface channel across them. 123

1. Introduction

1.1 Background – Runoff Generation in Watershed Hydrology

One of the earliest scientific models of runoff generation was proposed by Horton (1933) and separated watershed contributions to streamflow into two components: groundwater flow and surface runoff. He proposed that flat or minimally varying parts of the hydrograph corresponded to "groundwater flow" and that peaks in response to storms were caused by surface runoff generated when rainfall intensity exceeds the infiltration capacity of the soils. Infiltration-excess overland flow, now termed Hortonian overland flow, was further expanded (Horton 1945) to propose a definite connection between the depth of water stored on the surface and the rate of surface runoff and incidentally to propose linkages between that runoff mechanism and the geomorphic evolution of a watershed. Although it was later shown that Hortonian flow is both rare and one of many runoff generating process, the concept of dividing streamflow into contributions from two distinct sources was crucial in laying the groundwork for many subsequent models.

Betson (1964) showed that the circumstances under which Horton's model of overland runoff generation could be met exist primarily at locations proximal to the stream channel. This analysis was expanded upon by Kirkby & Chorley (1967) and others (Hewlett & Hibbert, 1963; Tsukamoto, 1963; Weyman, 1970) to incorporate the concept of throughflow as another form of runoff generation. At this stage, throughflow was defined broadly as flow occurring within the soil column, which shifted the focus of hydrologists studying runoff generation from surface to subsurface flow. Kirkby & Chorley (1967) emphasize that although the model of runoff generation proposed by

Horton (1933, 1945) is not incorrect, it is usually only applicable to end-member catchments with very low infiltration capacity.

Prior and concurrent to the development of the concept of throughflow as an important runoff generating process was the variable source area (VSA) concept (Hewlett & Hibbert, 1967; Hursh, 1936). VSA refers to the saturated zones adjacent to the stream that expand and contract in response to precipitation inputs. The concept allowed hydrologists to explain how throughflow, previously considered primarily as much slower unsaturated flow, could rapidly reach the stream as saturated flow when it intersects an expanding source area. In conjunction with the incorporation of the VSA concept into the model of runoff generation, Dunne & Black (1970) proposed the exfiltration of subsurface flow at these saturated area, also termed “return flow,” as a mechanism for delivering water to the stream rapidly and an explanation for observed overland flow in addition to Hortonian overland flow.

Rapid subsurface flow through pore spaces large enough that flow is much less affected by capillary forces, known as macropore flow, was recognized as early as the 19th century (Lawes & Gilbert, 1888; Schumacher, 1864), and then revisited in the mid 20th century (Horton, 1942; Hursh, 1944). It was not until Beven & Germann (1982), however, that it was rigorously described as a distinct runoff generation process. They describe macropores as connected pore space large enough that capillary flow (Richards, 1931) is not an accurate model of flow within them. Beven and Germann (1982) explain the conditions when macropores would be thought to either dominate runoff generation (saturated conditions with minimal capillary forces) or be mostly irrelevant (dry conditions where precipitation would infiltrate into the micropores due to higher capillary pressure). Subsequent studies have focused around relating macropore flow to specific structural characteristics of macropores (Tsuboyama et al., 1994) or developing models to incorporate their heterogeneity and non-Richards flow behavior (Weiler & McDonnell, 2007).

Because contributions to runoff generation from any one portion of the watershed are often dependent on saturation or some other threshold in soil moisture, watershed response to precipitation can often be highly threshold-dependent and sensitive to antecedent conditions (Detty & McGuire, 2010). Hydrologic connectivity, generally defined as the connection between or within elements of the water cycle by hydrologic fluxes, was introduced as an ecological concept by Pringle (2001, 2003). It has been of broad use to multiple fields since then, including watershed hydrology (Jencso et al., 2009; McGlynn & McDonnell, 2003a; Vidon & Hill, 2004). Connectivity is generally driven by the development of shallow subsurface water tables, which have been linked to surface topography (Detty & McGuire, 2010; Jencso et al., 2009; Rinderer et al., 2014), soil characteristics (Gannon et al., 2014; McGlynn et al., 2004), or the presence of confining layers (Tromp-van Meerveld & McDonnell, 2006; Weyman, 1973; Zimmer & McGlynn, 2017b).

Since the majority of studies around runoff generation have been completed in steep catchments with relatively shallow, homogeneous soils; subsurface water table development has been well explained by topography (Jencso et al., 2009; McGuire et al., 2005; Montgomery & Dietrich, 1988). Although there has been scattered work in lower relief systems with deeper soils where additional structural characteristics of watersheds may be important (Jackson et al., 2014; Sklash & Farvolden, 1979; Zimmer & McGlynn, 2017b), this area remains a significant opportunity for expanding the scope of our understanding of runoff generation processes and watershed hydrology more broadly. Deeper soils generally facilitate greater storage volumes, suggesting the possibility that seasonal variability in storage may play an important role in these watersheds (Zimmer & McGlynn, 2017a). Although watershed storage has been recognized as an important control on runoff (Kirchner, 2009) and a potentially fruitful means of cross-site comparison (McNamara et al., 2011), it has been less well recognized in terms of seasonal or shorter changes outside of Mediterranean regions (though see Nippgen et al., 2016; Pfister et al., 2017; Zimmer & McGlynn, 2017a) where phase shifted peaks in annual precipitation and primary production create clear conditions for it to exhibit such changes (Dralle et al., 2018; Hahm, Rempe, et al., 2019).

The focus of this dissertation is to incorporate the CCZO and therefore similar systems into our current understanding of watershed hydrology. To do so we focus on three goals, each connected to one of three chapters:

1. How do water balance components relate to each other and vary through time at annual, seasonal, and monthly time scales?
2. How do these watershed scale measurements relate to internal, direct measurements of a point in the watershed? What characteristics of the watershed can help interpret those relationships?
3. How is headwater hydrology expressed in higher order streams in these systems?

2. Storage dynamics buffer apparent water limitation and facilitate flashy, threshold-mediated runoff response.

2.1 Introduction

Watershed storage plays a crucial role in buffering climatic inputs of water (Hartmann et al., 2013). Despite this, the magnitudes and dynamics of storage at seasonal and event scales remain poorly understood in many parts of the world. This is partially due to the difficulties in quantifying it over time. However, understanding watershed storage dynamics and their linkages to runoff generation timing and magnitude are critical to managing stream ecosystem health (Jaeger et al., 2014), water availability for human use (Wang & Cai, 2009), and anticipating the effects of extreme events such as extreme precipitation leading to floods (Marchi et al., 2010) or droughts (Hellwig & Stahl, 2018). Furthermore, the importance of expanding our understanding of the connections between subsurface hydrology, subsurface structure, and terrestrial ecosystems is becoming increasingly recognized as a crucial hurdle to incorporating storage into earth systems models (Fan et al., 2019).

Although spatial heterogeneity of watershed storage, or proxies thereof, has been broadly studied as a driver of runoff generation, less research has focused on the temporal dynamics of storage, particularly at time scales longer than single storm events (Nippgen et al., 2016). There remains an outstanding need to understand the linkage between the dynamic aspects of watershed storage and watershed runoff characteristics, especially in warm, humid landscapes with deeper soils and low overall relief that are less well represented in the current literature despite their prevalence worldwide.

Implicit connections between watershed storage and other components of the terrestrial water balance have been recognized for decades by incorporating its effects in the form of antecedent precipitation indices or similar approaches. As early as the middle of the twentieth century, studies linked antecedent precipitation or soil moisture to runoff (Hamon, 1963; Kohler & Linsley, 1951), and used indices of antecedent precipitation (Fedora & Beschta, 1989; Kim et al., 2005; Sidle et al., 2000; Sittner et al., 1969) or soil moisture (Buttle & McDonald, 2002; Detty & McGuire, 2010; Penna et al., 2011) prior to runoff or lateral flow events as de facto surrogates for watershed storage. However, these and similar studies have generally limited themselves to focus on antecedent time scales of days to weeks and their effects on stormflow during individual events, although more recent work by Nippgen et al. (2016) has elucidated linkages between antecedent conditions and runoff at monthly, seasonal, and annual time scales.

A substantial body of research has focused on describing the effects of subsurface soil moisture, modeled or measured, on runoff. Although not explicitly addressing watershed storage, they provide valuable context for metrics of watershed storage in terms of both threshold behavior and heterogeneity in hydrologic state within the watershed. These numerous and diverse studies have related runoff dynamics to subsurface moisture (Hewlett & Hibbert, 1963; Tsukamoto, 1963), to variable source areas (Dunne & Black, 1970; Hewlett & Hibbert, 1967), to redistribution and accumulation of water due to surface topography (K. J. Beven & Kirkby, 1979; Nippgen et al., 2015; Smith et al., 2013) or subsurface topography (Tromp-van Meerveld & McDonnell, 2006), to the development of saturated hydrologic connectivity that dynamically extends up the entire stream-riparian-hillslope continuum (Jencso et al., 2009; McGlynn & McDonnell, 2003b), or to metrics of connectivity derived from time series analysis of shallow groundwater wells (Rinderer et al., 2019). Although these studies do not focus explicitly on watershed storage, their findings emphasize the role of threshold behavior in mediating both surface or subsurface flow, and by illustrating spatiotemporal heterogeneity of watershed storage they provide important context for interpreting integrated watershed data.

Studies focused explicitly on catchment storage have found ranges in storage depths over two orders of magnitude across a diverse range of watersheds (Buttle, 2016; McNamara et al., 2011; Peters & Aulenbach, 2011; Staudinger et al., 2017). Setting aside simulations of storage from modelling-based upscaling of point measurements like water tables or soil moisture (e.g., Seibert et al., 2011), or large scale measurements using remote sensing platforms (Adusumilli et al., 2019; Landerer & Swenson, 2012; Rodell et al., 2007), metrics of storage dynamics have been calculated from empirical studies either using stream tracer data or recession analysis of the stream hydrograph. Stream tracer data can be used to calculate the transit time distribution of a watershed, whose product with runoff yields a storage estimate (Birkel et al., 2011; Buttle, 2016; Soulsby et al., 2009; Tetzlaff et al., 2014). Alternatively, the recession curve of the hydrograph can be used to calculate a relationship between storage and discharge, which can then be inverted to directly calculate storage from discharge or estimate a dynamic storage range (Birkel et al., 2011; Buttle, 2016; Kirchner, 2009). However, these methods are both limited to perennial watersheds because they assume the relationships between streamflow and/or streamflow chemistry and storage are invertible; in other words, that the full range of watershed storage states can be represented by streamflow characteristics. If a stream dries but storage continues to decrease, as the case would likely be in a temporary stream, then this assumption no longer holds. As such, both of these methods capture only the storage dynamics that correspond directly to runoff, alternatively called “dynamic storage” (Kirchner, 2009; Staudinger et al., 2017) or “direct storage” (Dralle et al., 2018). Combining water balance calculations of storage with recession analysis has been used to calculate and distinguish between storage pools directly or indirectly related to runoff dynamics either implicitly (Peters & Aulenbach, 2011; Sayama et al., 2011) or explicitly (Dralle et al., 2018; Hale et al., 2016). However, these and similar studies generally confine their analysis to wet/dormant seasons where either precipitation far outweighs evapotranspiration, or evapotranspiration is minimized, or both. Analyzing storage using a parsimonious water balance approach remains a relatively underutilized tool and also stands to yield complimentary analyses to the bulk of studies of storage dynamics, including insight into storage dynamics in temporary streams and dynamics through entire years.

In addition to fairly robust literature addressing storage dynamics directly or indirectly in watersheds with Mediterranean climates (Dralle et al., 2018; Hahm, Rempe, et al., 2019; Hale et al., 2016; Rempe & Dietrich, 2018; Sayama et al., 2011; Swarowsky et al., 2011), watersheds whose water balances are dominated by seasonal melt of snow or glacial ice have been also sites of seasonal-scale storage research (Cochand et al., 2019; Hood & Hayashi, 2015). Both of these types of watersheds have clear seasonality that allows simplifying assumptions about components of the water balance or relevant portions of the year to study. However, the seasonal dynamics of watershed storage have been less recognized outside of such regions that clearly exhibit strong seasonality in storage. Humid regions, with more consistent and more substantial precipitation, represent an opportunity to explore the central role of storage in watershed hydrology and have been poorly studied until recently (Nippgen et al., 2016; Pfister et al., 2017; Zimmer & McGlynn, 2017a). Such regions, and particularly the Southern Piedmont of the United States, are ideal locations to expand our understanding of storage dynamics because of minimal seasonality in precipitation, no significant snow influence, deeply weathered regolith, largely energy limited evapotranspiration, and strong seasonality in energy availability. All of these factors combine to create a landscape with potential for highly dynamic storage, while runoff dynamics observed in similar landscapes (Zimmer & McGlynn, 2017a) suggest linkages with dynamic storage. To advance understanding of the role of dynamic watershed storage in mediating hydroclimatic controls on runoff dynamics across temporal scales, we address the following questions:

1. What are the long-term hydroclimatic conditions of the Southern Piedmont and what do they suggest about water or energy limitation at multiple time scales?
2. How does integrated watershed storage vary at annual, seasonal, and event scales, and how does it reflect coupling to or buffering of hydroclimatic inputs?
3. What does the manifestation of storage dynamics in runoff suggest about the role of storage in mediating hydroclimatic forcing?

2.2 Methods

2.2.1 Study Site

The Calhoun Critical Zone Observatory (CCZO) is located in northern South Carolina in the United States. It is situated within the Southern Piedmont region of the southeastern United States, which stretches from Maryland to Alabama between the Appalachian Mountains and the eastern coastal plain (Figure 1a). The CCZO is situated within a humid subtropical climate zone, which is globally located in southeastern regions of continents between the latitudes of 25° and 35°. These regions experience hot, humid summers and mild winters. In the summer, precipitation is primarily in the form of convective thunderstorms or high-intensity tropical storms; in the winter it is generated primarily by large frontal systems that extend into subtropical latitudes from westerlies.

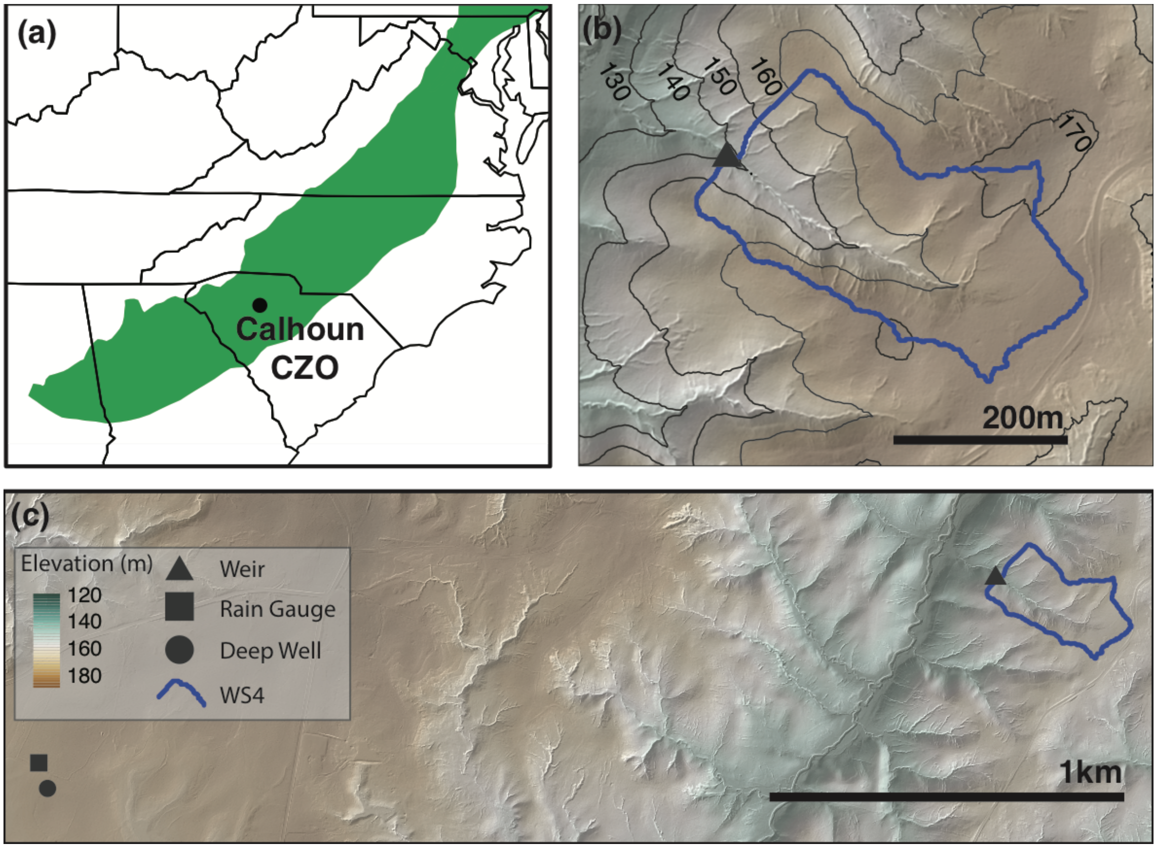

Figure 1: Site Map (a) Regional location of the Calhoun Critical Zone Observatory within the Southern Piedmont physigraphic region (shaded green) of the southeastern united states. (b) Watershed 4 DEM (shaded color) and 10m elevation contours (grey lines). (c) Watershed 4 area map including location of deep groundwater well on relatively flatter interfluve adjacent to 3rd order watershed containing Watershed 4.

The Calhoun Experimental Forest was founded as a USFS research forest within the Sumter National Forest in 1947 and was in active operation until 1962 hosting a suite of experiments centered around hydrology, forest ecology, and pedology. Although it was officially deactivated in 1962, infrastructure built during this time period remains, including multiple 90° v-notch weirs installed in small, headwater watersheds (Figure 1b) that formed the backbone of a substantial re-instrumentation that began in 2013 when the Calhoun Experimental Forest was recommissioned as the NSF-sponsored Calhoun Critical Zone Observatory.

This study focuses on the 6.9 ha Research Watershed 4 (WS4, Figure 1b). WS4 is primarily forested in mixed hardwoods (e.g., *Carya* spp. and *Quercus* spp.) with minimal pine stands (*Pinus* spp.). It has a total relief of 50 m, with elevation ranging from 173 m to 124 m, and a median slope of 19% with a standard deviation of 13%. Underlying geology is granitic gneiss, the most common bedrock of the Southern Piedmont. Soils are primarily Ultisols of the Appling, Cecil, and Madison soil series, which collectively represent roughly one third of the Southern Piedmont. These soils can be generally described as loamy sands overlying clay-rich argillic horizons, underlain by deeply weathered saprolitic material (Richter et al., 2000). We approximated soil depth by hand auguring (AMS; 2.75" auger diameter) to refusal. These depths (inclusive of C-horizon but not of less-weathered bedrock) were determined by spatially distributed hand auguring in WS4, and range from <1 m in or adjacent to stream channels to >4 m on narrow ridge tops to 9 m at the upper divide of WS4 where it connects to a broader interfluve. Depth increases moving away from the stream channel in WS4. WS4 contains a temporary stream which dries completely in the summer through early fall and flows primarily in late winter and early spring.

2.2.2 Hydrologic and hydroclimatic data

Our study focused on hydrologic data from water years 2015-2017 in WS4 (Figure 1). WS4 is one of four watersheds within the CCZO that had been instrumented previously by the Forest Service when the Calhoun Experimental Forest was founded. Each of these watersheds was originally fitted with a concrete stilling pool and v-notch weir. In the decades since the USFS decommissioned the Calhoun Experimental Forest, the weirs had filled in with sediment and their blades have rusted; however, the concrete pools remained intact. We removed sediment from each pool and replaced the weir blades with new blades made in the same dimensions as the originals. We measured stage in the weir pool with redundant capacitance rods (TruTrack, ±1 mm) at five-minute intervals. Manual measurements of stage above the v-notch were taken bi-weekly to monthly and used to offset and drift-correct the continuous measurements as necessary. Discharge was derived from the rating curve for a 90° v-notch weir (USBR, 2001) and periodically verified by measuring the time to fill a container of known volume held beneath the weir notch.

Deep groundwater dynamics were measured in a 65 m well co-located with the precipitation gauge, 2.8 km from WS4. This well is on a broad, low-gradient interfluve directly adjacent to the third-order watershed that contains WS4 and within 10 meters of elevation of the highest point in WS4 (Figure 1). It is completed in competent bedrock and cased to ~17 m, extending through the entire regolith profile. Water level was measured at twenty-minute intervals using a pressure transducer (Solinst Levelogger LTC M10, ±5 mm) and corrected to barometric pressure using a co-located barometric pressure sensor (Solinst Barologger, ±0.05 kPa).

The hydroclimate of a region is the portion of the climate system directly affecting its hydrologic cycle. These components can be succinctly summarized as fluxes of energy and water. In this study we use measurements of potential evapotranspiration (PET) to characterize energy input and precipitation (P) to characterize water input. Hereafter, references to hydroclimate refer to these two variables or their difference.

Precipitation was measured using a tipping bucket rain gauge (TE525MM, Texas Instruments) with a 24.5 cm diameter funnel, 0.1 mm rainfall depth per tip, and nominal accuracy of 1% at intensities of up to 2.5 cm/hr. Cumulative tips were recorded at five-minute intervals. It was placed in a clearing with an approximately 45° cone of no intercepting vegetation and was located 2.8 km from WS4. We obtained daily temperature and precipitation data for the period 1950-2015 from the Spartanburg Memorial airport climate station (NCDC ID: 20017544), located ~40 km from WS4.

Potential evapotranspiration (PET) was calculated from the Thornthwaite equation (Thornthwaite, 1948) using temperature data from WS4 or historic data (1950-present) from Spartanburg Memorial airport, as available. Rather than the more typical method to calculate actual evapotranspiration (ET) as the annual difference between precipitation and runoff, we assume ET ≅ PET based on the assumption that this region is annually energy-limited.

We chose the parsimonious Thornthwaite method because it requires only air temperature, for which we have high-quality data dating back decades in the area, therefore facilitating robust comparisons between our study period and the historic record. Although it has well known limitations, including substantial underestimates in arid climates (Pereira & De Camargo, 1989) and a lack of generalized applicability across diverse climates (Vorosmarty et al., 1998), it is more robust in humid climates similar to those in the NE United States in which it was developed (Thornthwaite, 1948), and in uncultivated, deciduous forests (Vorosmarty et al., 1998). Although Lu et al. (2005) in a study of 36 watersheds in the southeastern United States suggested it may be the least desirable method for PET estimation among six common methods, their recommendation was due to its relatively lower estimates with mean and standard deviation nearly equivalent to that of ET at the same sites. This potential limitation for other studies can be viewed as a strength here.

Our assumption of energy-limitation for calculating ET was similarly based on a desire to use consistent metrics for comparison between our study and historic records, and we found our ET estimates to be consistent with other regional ET values reported from a variety of methods. Annual numbers based on this method were comparable to those directly measured by latent heat flux in Southern Piedmont site in North Carolina (Novick et al., 2016), and agree with the interannual consistency observed in hardwood forests at the same location (Stoy et al., 2006) and in other southeastern locations (Hanson et al., 2004; Nippgen et al., 2016; K. B. Wilson & Baldocchi, 2000). Additionally, the subset of sites reported by Lu et al. (2005) that were in the Southern Piedmont exhibited very similar mean annual numbers. In contrast, if we assumed no net annual change in storage and calculated ET as the difference of precipitation and runoff, the resulting ET would exhibit a much greater range of interannual variability inconsistent with these studies. Other studies have used comparably parsimonious methods for approximating ET from PET (Dralle et al., 2018; Pfister et al., 2017; Staudinger et al., 2017) and found results were sufficient to capture relevant storage dynamics.

2.2.3 Watershed storage

The basic watershed mass balance relates hydrologic influx and efflux to changes in storage within the watershed:

(1) $$\frac{dS_{tot}}{dt} = P_{tot} - Q_{tot} - ET$$

where S_{tot} [L] is storage of water within all storage components of the watershed, P_{tot} [L/T] is the sum of liquid and frozen precipitation, Q_{tot} [L/T] is total surface and subsurface watershed discharge normalized to watershed area (i.e., runoff), and ET [L/T] is evapotranspiration.

S_{tot} is indeterminate from a water balance due to challenges in observation and a poorly defined lower boundary condition. Integrating equation 1 with respect to time and defining S_{tot} as the sum of initial total storage condition (i.e., prior to measurement) and accumulated storage over a studied period of time yields:

$$(2) \quad S_{tot} = S + S_0 = \int_0^{\tau} (P_{tot} - Q_{tot} - ET)dt$$

where S [L] is cumulative storage over the time period, τ [T], and S_0 [L] is the initial storage. If we set the initial time (t = 0) in equation 2 to a time when it can be assumed that the watershed is at an approximate storage minimum (i.e., at the end of the driest season), then we can define S as the dynamic component of storage and focus only on this component of storage. In the CCZO, the start of the water year, as defined by the USGS (October 1) is generally within the driest part of the year, so here we adopt this time as the starting point for integration of equation 2.

Here we assume that in the CCZO, P is predominantly liquid, ignoring precipitation in the form of snow or ice, and that surface runoff is much greater than subsurface runoff. We additionally assume that the CCZO behaves generally as an energy-limited system, and therefore make the simplifying assumption that ET $\cong$ PET. Based on these assumptions and the focus on relative rather than total storage, equation 2 can be rewritten as:

(3) $$S = \int_{0}^{\tau} (P - Q - PET)dt$$

We have measured both P and Q in WS4, and use a PET estimate based on air temperature to calculate dynamic storage for our study period at monthly and daily time steps.

2.3 Results

2.3.1 Long-term regional hydroclimatic conditions

Long-term annual precipitation and PET at the CCZO (Figure 2) was approximated from 65 years of data at the Greenville-Spartanburg International Airport (1950-2015), located within 35 kilometers of the CCZO. Annual precipitation was ~1200 mm and annual PET was ~800 mm (Table 1). Despite precipitation at the CCZO being controlled by different drivers seasonally, mean monthly precipitation for each month was approximately constant at ~100 mm; however, monthly variability was high relative to mean values, with a ±1 standard deviation range of approximately 100 mm in each month (Figure 2a). In contrast, monthly mean PET exhibited distinct seasonality, with summer peaks >150 mm and winter lows <10 mm. Monthly PET variability was extremely low; ± 1 standard deviation range in each month was approximately 1 mm (Figure 2b).

Because precipitation and PET had different patterns of seasonality over the period of record (Figure 2a, c), the difference between the two switched from positive (apparent energy limitation) to negative (apparent water limitation) from winter to summer (Figure 2c). On a mean monthly basis over the period of record, five months (May- September) exhibited apparent water limitation, though considering the substantial month to month variability of precipitation (Figure 2a) this period differed by several months from year to year (Figure 2c).

Table 1: Annual and mean annual water balance components for nearby Spartanburt Memorial Airport (NCDC ID: 20017544) and WS4. Evapotranspiration estimated via Thornthwaite method.

	Precipitation (mm)	Evapotranspiration (mm)	Runoff (mm)	Runoff ratio (Q/P)
Historic (67 yrs) Annual mean	1247	864	-	-
Study (3 yrs) Annual mean	1120	809	277	0.22
Water year 2015	1159	782	200	0.17
Water year 2016	1409	822	554	0.39
Water year 2017	791	823	78	0.10

2.3.2 Annual and seasonal-scale hydrology

2.3.2.1 Precipitation, PET, and runoff

During our study period (water years 2015-2017), annual precipitation varied around its mean value of ~1200 mm; 2015 was an approximately average year, 2016 a wetter than average year, and 2017 a much drier than average year (Table 1). Annual runoff varied similarly; the highest runoff was measured in the wettest year and vice versa (Figure 3a). Annual runoff ratio increased with wetness index (P/PET) from a value of 0.10 in the driest year to 0.39 in the wettest year (Table 1, Figure 3, Figure 4).

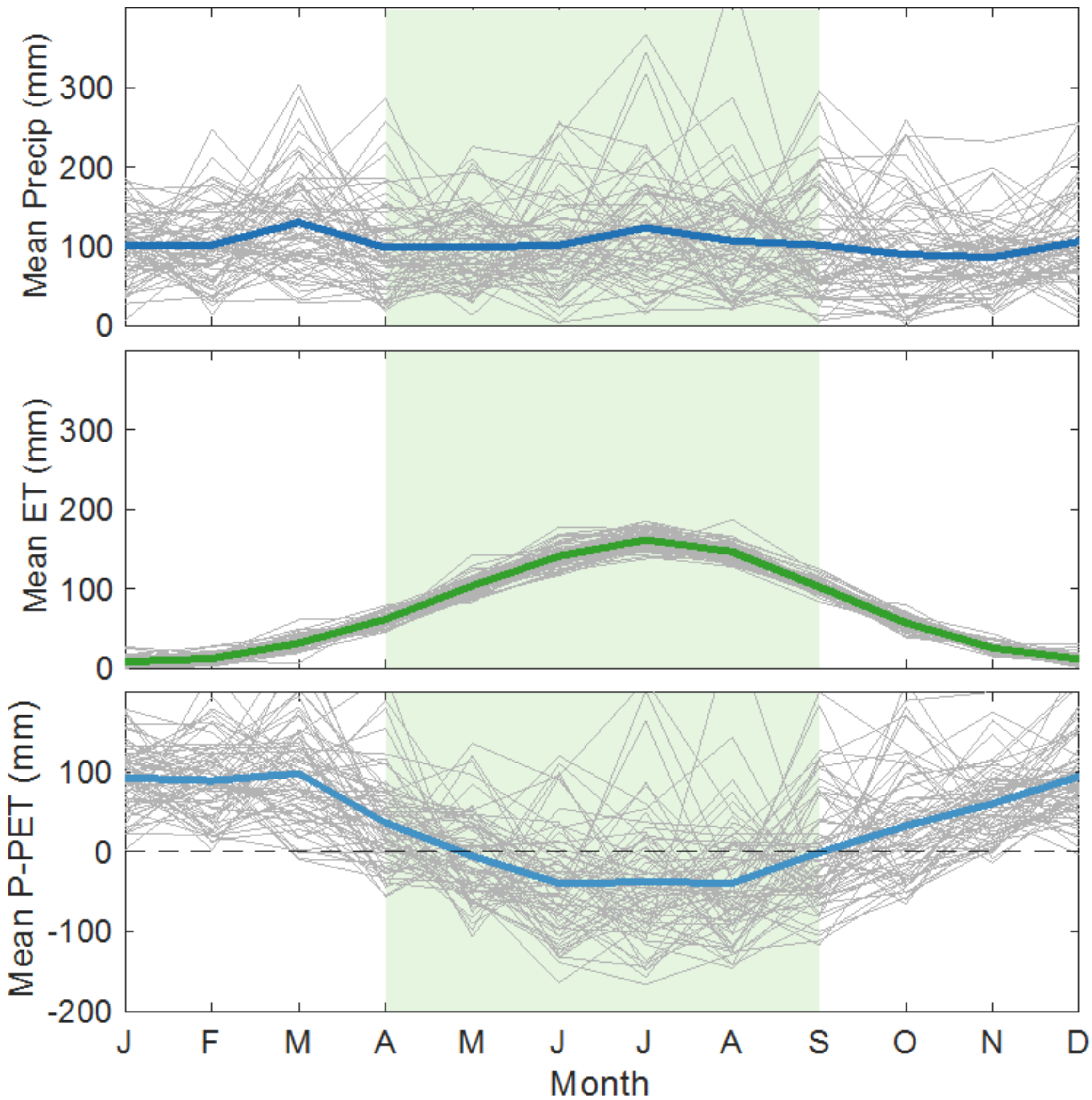

Figure 2: Monthly Precipitation and Evapotranspiration; Monthly (grey lines) and monthly mean (thicker colored lines) precipitation, evapotranspiration, and their difference at the Spartanburg Memorial Airport (NCDC ID: 20017544) from 1950-2017. Green shaded area represents approximate growing season.

Monthly precipitation during the study period exhibited high variability between months and a lack of clear seasonality (Figure 3b). Monthly values range between ~10 mm and >300 mm. The wettest months in each of the three water years, respectively, were April, October, and May while the driest months were October, April, and February.

There was measurable precipitation in every month. Monthly PET during the study period exhibited clear seasonality due to its temperature dependence, with only slight differences from year to year (Figure 3c). Monthly runoff (Figure 3d) displays quasi-seasonality: it decreased consistently in the late spring and summer months, and peaked somewhere in the late fall through spring; however, the peak months varied widely from year to year. Over the study period, the month with the highest runoff varied from April to December to June. In contrast, summer months were consistently dry regardless of precipitation.

The relationships between monthly runoff and either monthly precipitation or PET were complex. Monthly runoff generally increased with monthly precipitation, but at values below mean monthly precipitation (~100 mm) the relationship between runoff and precipitation was unclear while above this value there is a general positive relationship (Figure 5a). PET had little direct relationship with runoff, but rather set an envelope of runoff variability that tightens as PET increased (Figure 5b).

2.3.2.2 Storage dynamics

The residual of the monthly water balance created by precipitation, PET, and runoff represents a monthly change in integrated watershed storage (ΔS, Equation 2). This storage is undifferentiated between distinct storage pools. Negative changes correspond to draining storage, while positive values correspond to filling storage (light orange bars, Figure 3e). Similar to runoff, a quasi-seasonal behavior was seen with generally more negative values in summer months and generally more positive values in non-summer months, but the aseasonal effect of precipitation was apparent as well.

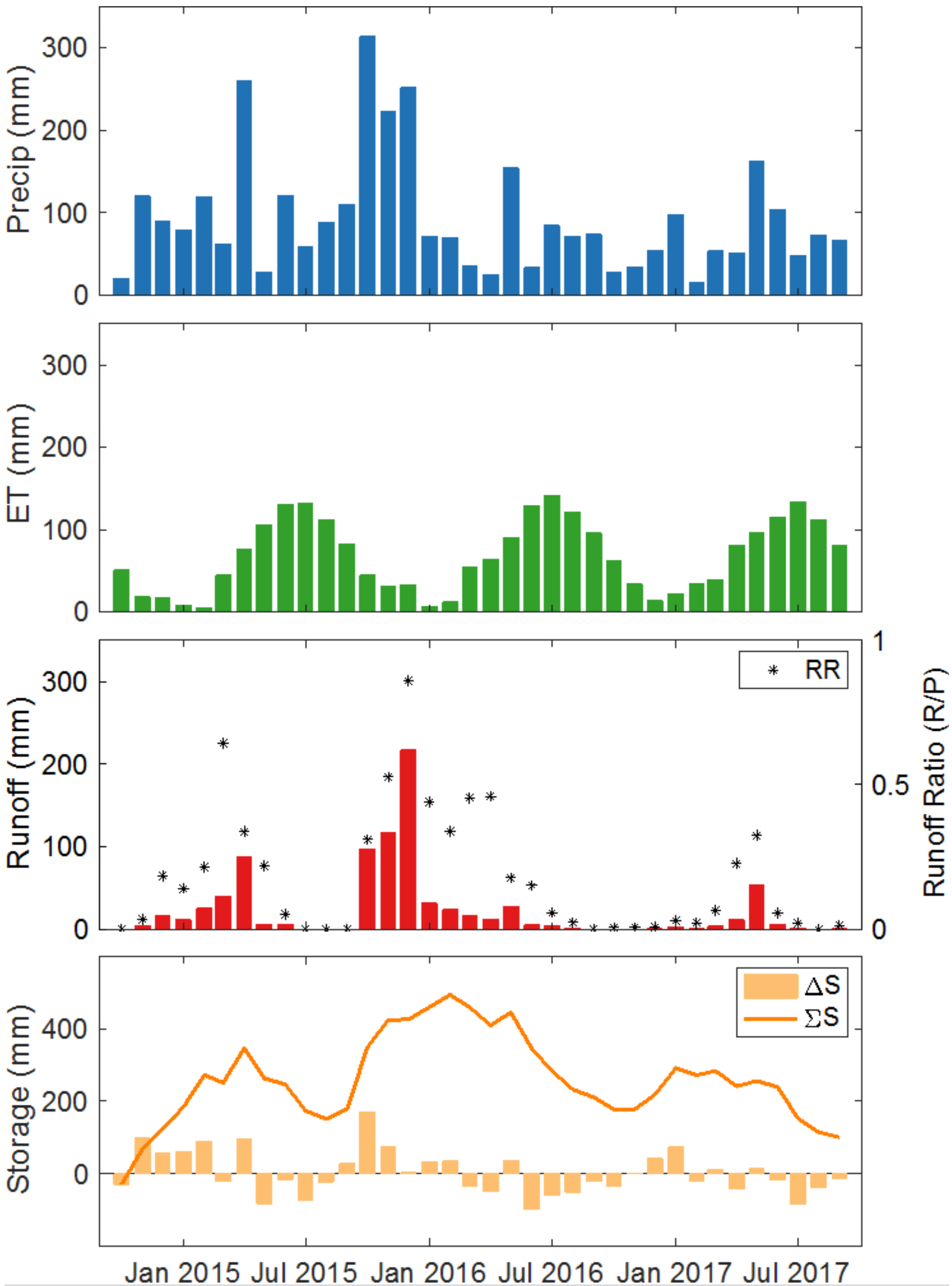
Precip (mm)
ET (mm)
Runoff (mm)
Runoff Ratio (R/P)
RR
Storage (mm)
ΔS
ΣS
Jan 2015 Jul 2015 Jan 2016 Jul 2016 Jan 2017 Jul 2017

Figure 3: Monthly water balance components for WS4 from October 2014 to September 2017, water years 2015-2017. Runoff ratio is the monthly ratio of total WS4 runoff to monthly precipitation. ΔS is the monthly residual of precipitation, evapotranspiration, and runoff (i.e., P-ET-Q), and ΣS is the cumulative sum of ΔS.

The cumulative sum of monthly storage values through the study period revealed the magnitude of relative watershed storage (S_r, Equations 5, 6) from the conditions at the start of the study period (dark orange line, Figure 3d). We observed a clear seasonal signal in this relative storage, with peak values of cumulative storage around midwinter and low values in late summer. Over the three years of this study, total change in cumulative storage was <100 mm; for this period, this change was approximately 3% of the total precipitation inputs, 4% of total PET, and 12% of total runoff (Figure 3). Total range of cumulative storage was 530 mm across the three-year period.

When comparing our calculated cumulative storage to runoff and runoff ratios, we observed a storage threshold of ~200 mm above which runoff generation typically occurred (Figure 3d). When plotted against each other, this threshold was revealed to be robust, with positive response of runoff to storage above 200 mm and minimal response below (Figure 5c). Additionally, we observed higher runoff ratios above this threshold even when the magnitude of runoff was relatively small (size of markers; Figure 5c). Although the relationship between storage and runoff above the threshold was not a simple linear one, the two distinct arms of this relationship correspond to two different flow states: with the steeper one representing months dominated by stormflow and the more gradual one by baseflow (Figure 5c).

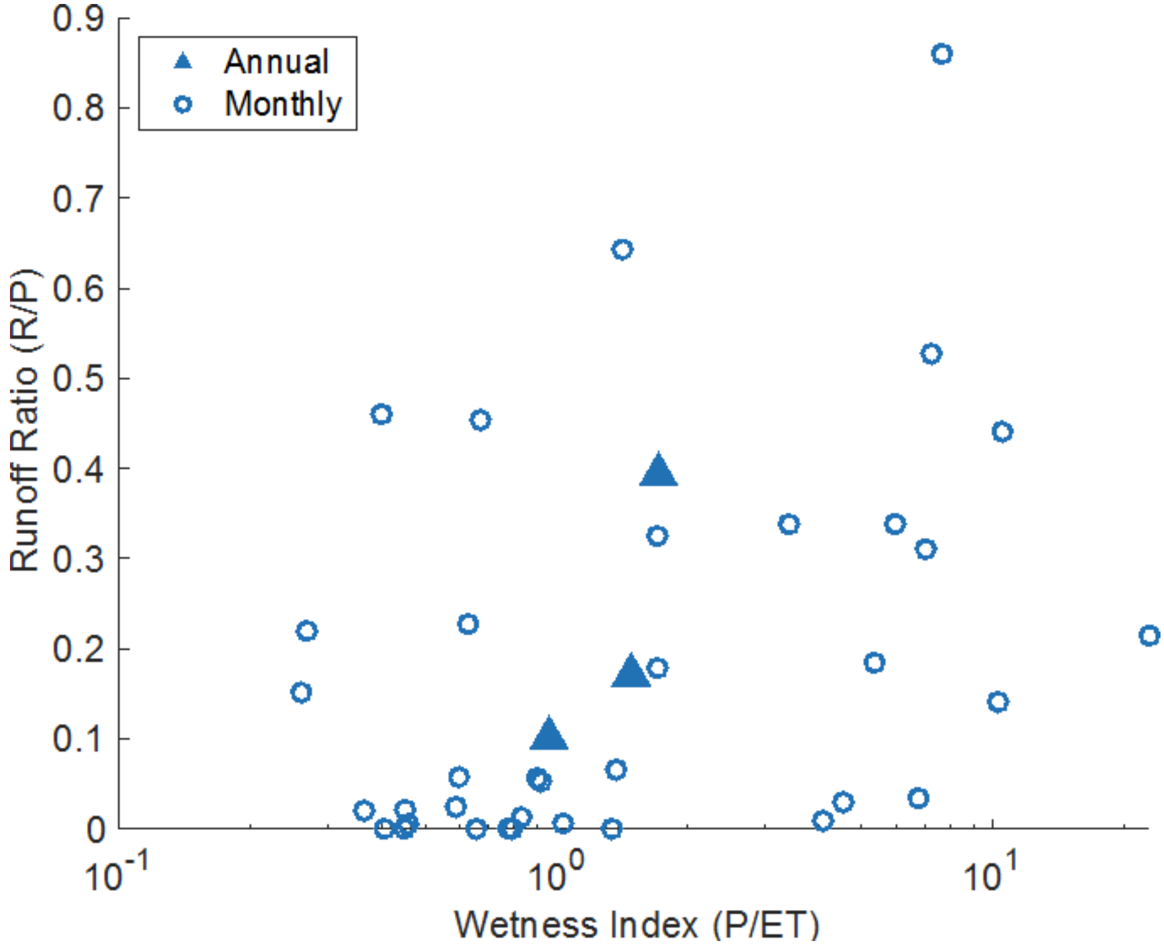

Figure 4: Runoff ratio and wetness index; Annual (filled triangles) and monthly (open circles) relationship between runoff ratio and wetness index for WS4 from October 2014 to September 2017, water years 2015-2017.

2.3.3 Deep groundwater and storage dynamics

We measured daily groundwater levels in a 70m deep well situated on a low gradient interfluve. Its location is <3 km from WS4 and adjacent to the 3rd-order watershed containing it. The elevation of this interfluve is comparable to that of the upper watershed divides of WS4 and similar watersheds in the immediate area. The interfluve is roughly 1.5 km wide between identifiable, higher-gradient watersheds like WS4. Its width and elevation suggest it is representative of groundwater dynamics at a more regional scale (Figure 1).

Over the course of the study period (water years 2015-2017), groundwater depth ranged from -2.3 m in the late winter of 2016 to -6.5 m in the early fall of 2017, a range of more than 4 m over 18 months. These times were during the dormant season of the wettest year and growing season of the driest year over the study period. Predominant changes in groundwater level were seasonal increases starting some time from the early winter to spring and seasonal decreases starting in early summer (Figure 6). The annual range for each year corresponded to annual precipitation for that year, with a range of 0.7 m in 2017 (791 mm P), 1.4 m in 2015 (1159 mm P), and 3.7 m in 2016 (1409 mm p).

We observed general agreement in both direction and timing of changes in groundwater level and daily storage for the three-year study period (Figure 6). When plotted against each other they showed a significant, positive relationship (Figure 6 inset). Peaks in both of these time series occurred within days of each other in each of the three years, as does the timing of summer dry-down. Magnitudes of change relative to each y-scale aligned. However, we also observed notable differences between the time series. Although the timing of the start of wet-up in water year 2016 was the same for both storage and groundwater (corresponding to several high-magnitude precipitation events), it was not for the other two years. In water year 2015 increase in storage preceded groundwater by roughly six weeks, and in water year by almost six months. Both of these lags in time corresponded to increases in storage of between 100 and 150 mm. In both cases groundwater was still drying down while storage was beginning to increase (Figure 6). The broad similarity between the two time series emphasized the robustness of our calculated storage relative to a measurable component of storage.

The differences we observed point to the distinct pools that comprise watershed storage, of which deep groundwater is only one.

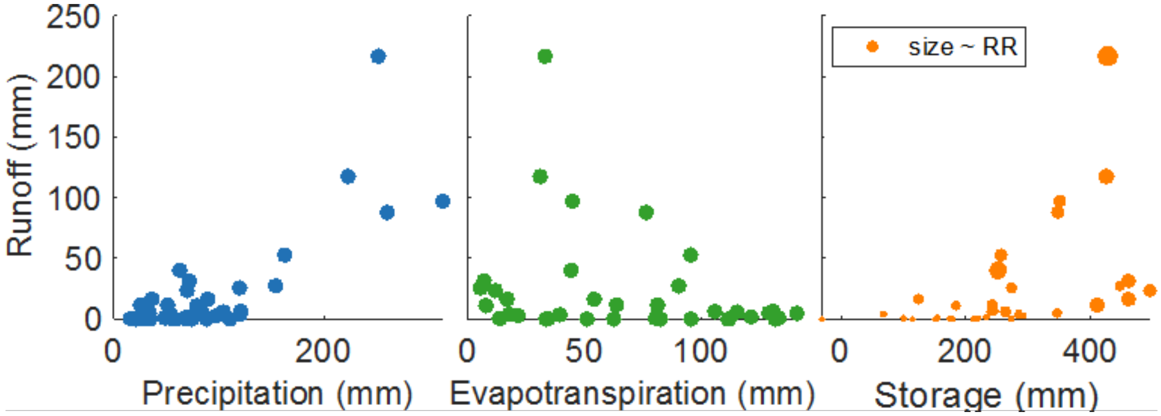

Figure 5: Relationships between monthly runoff and monthly precipitation, evapotranspiration, and storage for WS4 from October 2014 to September 2017, water years 2015-2017. Symbol size in far right is proportional to runoff ratio in that month. Storage refers to cumulative sum of monthly changes in storage.

2.3.4 Event-scale storage and runoff dynamics

We observed a high degree of temporal variability in precipitation inputs and runoff response to these inputs (Figures 7a,b). Multiple precipitation events occurred in each month of the three year study period. They varied strongly in total magnitude, intensity, and duration. In contrast, the hydrograph was dominated by a few strong responses to precipitation events, weaker response to most events (Figure 7a), and negligible response to other rainfall events or no response at all relative to baseflow (Figure 7b). WS4 is a temporary stream that dries down for at least some portion of each year (Figures 7a,b). However, over the three-year period studied we observed flow regimes that were both ephemeral (response to events followed by full drying) and intermittent (seasonally persistent flow with response to events on top of baseflow). Flow duration, or the percentage of active flow days during the year, differed widely between the three water years, with substantial duration, 73%, during water year 2016, and much more limited duration for water years 2015 and 2017 (51% and 48%, respectively).

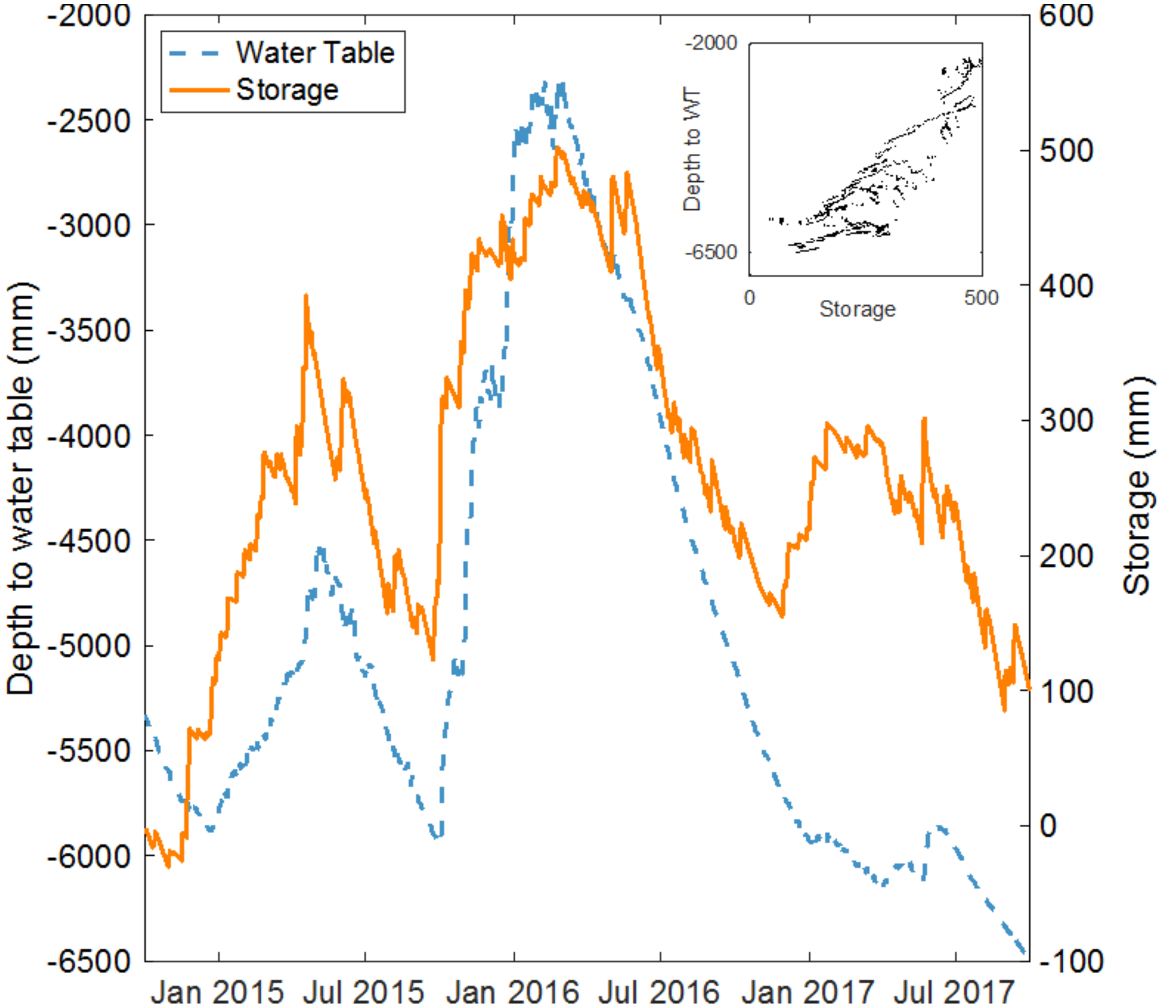

Figure 6: Time series of daily storage in WS4 (orange solid line) and depth to water table in deep groundwater well (blue dashed line) from October 2014 to September 2017, water years 2015-2017. Inset depicts relationship between the two, a significant linear relationship (R^2 = 0.64; p << 0.01).

We also calculated daily storage and cumulative storage as the sum of the daily water balance residual (Figure 7,7d). At this time scale, event-scale changes in storage became apparent and exhibited rapid filling of storage in response to large precipitation inputs, but with their magnitude mediated by the degree of concurrent increases in stormflow runoff. Draining of storage was more gradual than precipitation induced increases because it was driven by moderate, daily PET and baseflow runoff.

Cumulative distributions of each of the water balance components for water year 2016 (Figure 8) reveal the response magnitude and timing of runoff and storage to inputs of precipitation. In the three highlighted storm events we observed 1) Storage responding more strongly to precipitation events than runoff (events 1), storage and runoff responding with roughly the same magnitude (event 2), and runoff responding without concurrent storage response (event 3). These three conditions represent variable partitioning between runoff and storage as a function of storage echoing threshold behavior observed in monthly data (Figure 3c).

2.3.5 Flow duration and regime

Flow duration curves (FDCs) for each water year and for the entire study period provide a succinct summary of the differences and similarities in flow characteristics from year to year. The steepness of the lowest-duration part of each curve indicated the predominance of shorter duration, higher flows in the annual hydrograph for each of these water years (Figure 9). Although accounting for only 3% of the year, these short-duration flows accounted for 91%, 92%, and 97% of annual runoff for water years 2015, 2016, and 2017, respectively. Across all three years, despite a large range in precipitation magnitudes (Figure 3), the average runoff production during short-duration flows was 95% of annual runoff.

Baseflow is represented by the broad middle portion of the FDC, roughly centered on the inflection point in each curve. This portion of the curve has a much lower slope, indicating temporal persistence of that flow range, with lower slopes corresponding to more persistent baseflow. For WS4, this portion of the FDC was between 0.5 mm/d and 1 mm/d in water years 2015 and 2016, although the duration of baseflow was longer in water year 2016 (Figure 7b). Water year 2017 exhibited a much higher slope through this portion of the curve. This difference between 2017 and the two previous water years corresponded to a lack of persistent baseflow for any portion of the year (Figure 7a,b).

Since WS4 is a temporary stream, meaning it flows only part of the year, its x-intercept on the FDC is less than 100 and its value indicates the proportion of each year that measurable flow occurred. While over the whole time period this watershed was flowing 57% of the year, when separated by water year it ranges from 48% to 73%. The average precipitation year (2015, 51%) was much closer to the low end of that range (Figure 9). We observed two different types of flow regime in WS4 in different years: intermittent (flow through an entire season) during water years 2015-2016 and ephemeral (flow only in response to precipitation followed by drying) during water year 2017. In all years no flow was observed during late summer.

Flow duration and flow regime are two different metrics to characterize temporary streams, and the three study years illustrate how they do not necessarily change concurrently. For example, water year 2015 has roughly the same flow duration as water year 2017 (~50%) but exhibits an intermittent flow regime more similar to water year 2016 but in contrast to the ephemeral flow regime observed in water year 2017.

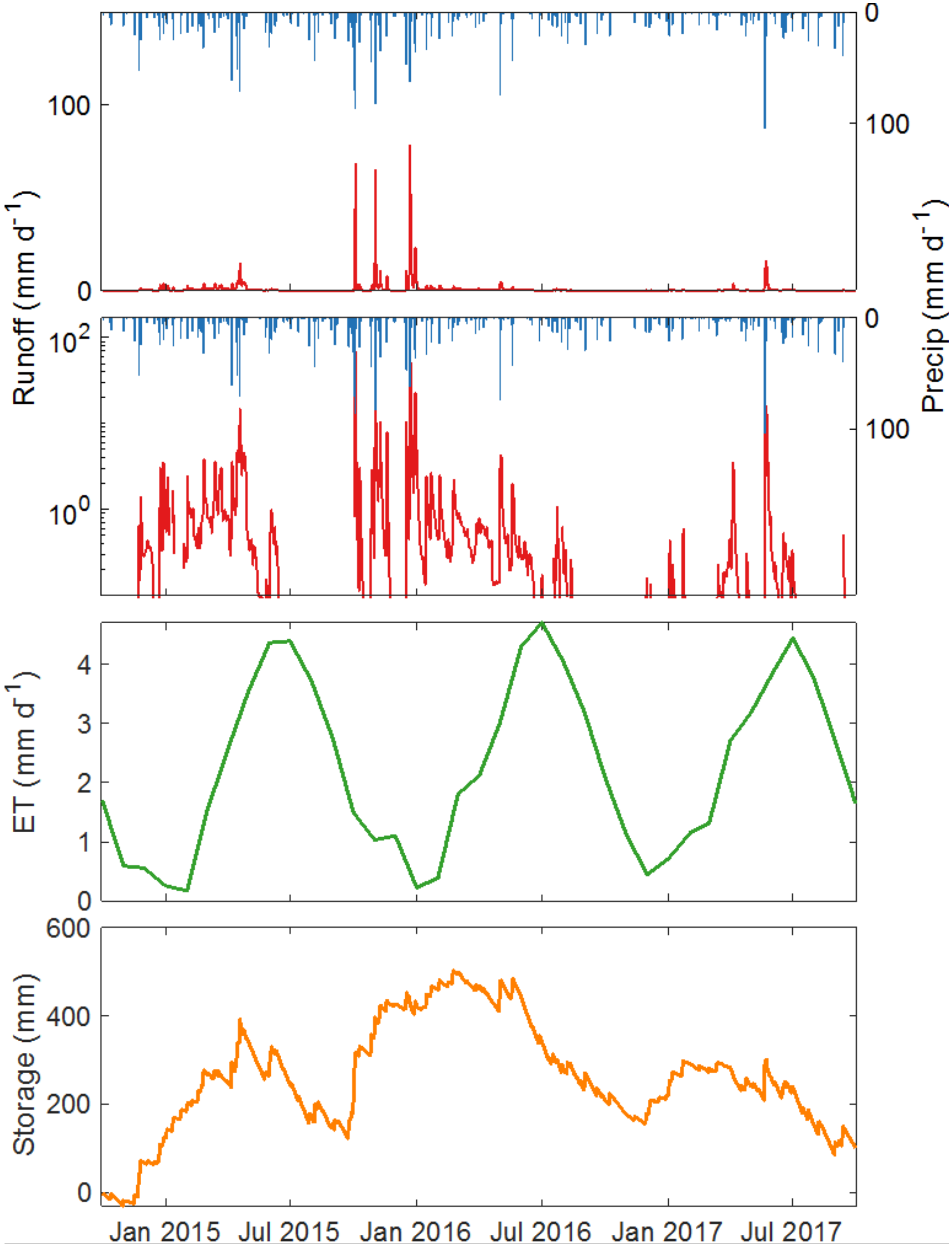

Runoff (mm d^{-1})
Precip (mm d^{-1})
0
100
10^2
10^0
ET (mm d^{-1})
0
1
2
3
4
Storage (mm)
0
200
400
600
Jan 2015
Jul 2015
Jan 2016
Jul 2016
Jan 2017
Jul 2017

Figure 7: Monthly water balance components for WS4 from October 2014 to September 2017, water years 2015-2017. First two panels present the same data but with linear and log axes. Evapotranspiration is an interpolation of monthly values for consistency with the other panels. Storage represents the daily residual of precipitation, runoff, and evapotranspiration (i.e., P-ET-Q).

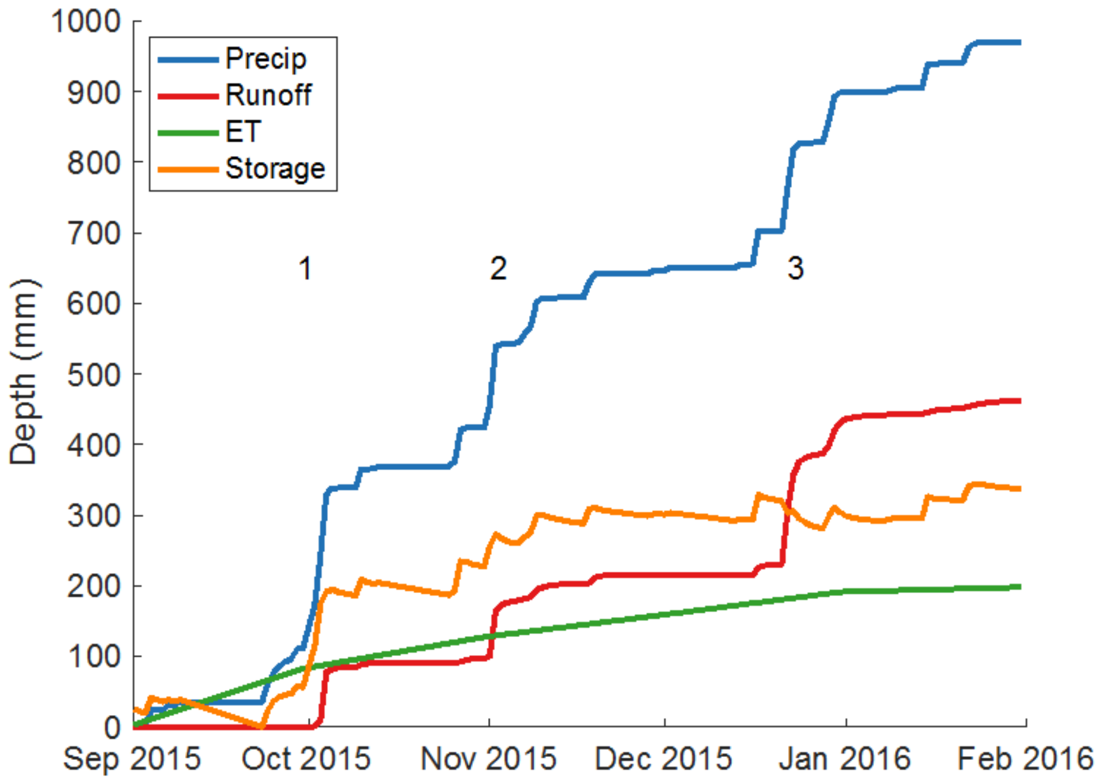

Figure 8: Cumulative daily water balance components in WS4 for the approximate dormant season in water year 2016, September 2015 to February 2016. Shaded areas highlight three specific storm cycles and their associated storage and runoff dynamics.

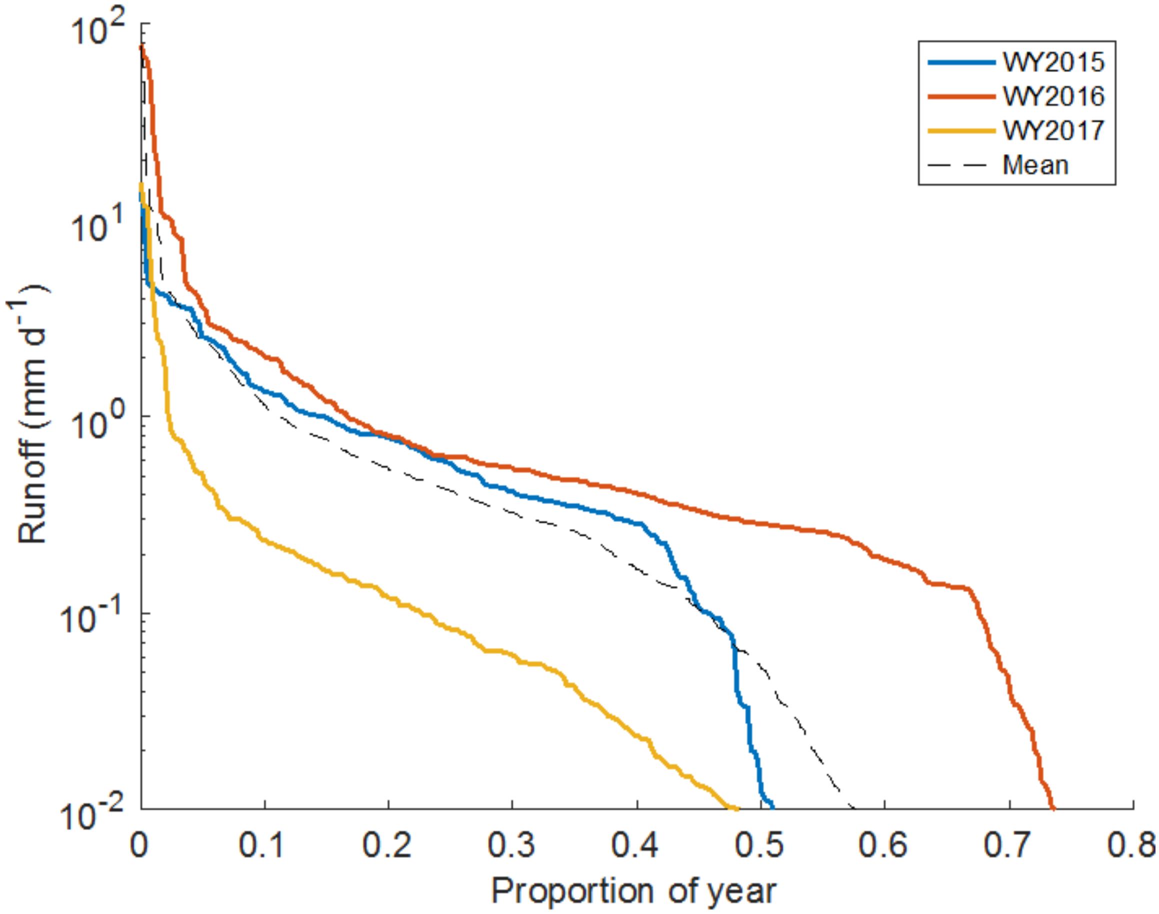

Figure 9: Flow duration curves for WS4 in water years 2015-2017 (solid lines) and for the 3-year period (dashed line). These indicate the proportion of the year where runoff in WS4 met or exceeded a given runoff.

2.4 Discussion

2.4.1 What are the long-term hydroclimatic conditions of the Southern Piedmont and what do they suggest about water or energy limitation at multiple time scales? – Seasonal and aseasonal hydroclimatic forcing lead to intra-annual switching between apparent water and energy limitation

The southeastern piedmont of the USA has a humid subtropical climate where precipitation (P) is greater than potential evapotranspiration (PET) on a mean annual basis. These two variables serve as surrogates for the fluxes of water (P) and energy

(PET) into the system that comprise the regional hydroclimate. This annual excess of water classifies the region as energy-limited, indicating that the region's energy inputs are insufficient to evaporate or transpire its water inputs. Our findings aligned with this general classification: long-term average P and PET were approximately 1200 mm and 800 mm, respectively, (Table 1, Figure 2) compared to 1120 mm of P and 809 mm of PET during our three-year study period (Table 1, Figure 3). This availability of water creates, in large part, the conditions that favor dense, productive mixed pine/hardwood forests in the region (Whittaker, 1970). At this time scale, the balance of P and PET is sufficient to characterize the limitation state of the system; however, here we refer to this type of limitation as *apparent* limitation in recognition of the reality that many internal processes and pools governing the usage of water and energy in the region and our study watershed (WS4) are not captured by these two variables. Indeed, at time scales shorter than annual we observed hydroclimatic conditions that switched from apparent energy limitation to apparent water limitation for substantial portions of the year.

Disaggregation of annual hydroclimatic conditions (i.e., P, PET, and their difference) to monthly revealed the variability subsumed in annual means that drives switching from one type of apparent limitation to the other within in the year. Further, the types of P and PET variability differed strongly: mean monthly P was relatively consistent through the year but differed from year to year (Figures 2a, 3a), while mean monthly PET exhibited a strong seasonal pattern and remained highly consistent interannually (Figures 2b, 3b). The combination of these aseasonal and seasonal modes of variability create conditions that are quasi-seasonal, with drier summers and wetter winters being generally true but with substantial year to year differences in the proportion of the year experiencing apparent water vs. energy limitation.

On average, mean monthly P was ~100 mm while mean monthly PET changed seasonally from a minimum of 7.5 mm in January to a maximum of 161 mm in July. As a result, the mean difference between P and PET switched from positive to negative depending on the season, with a maximum of 94 mm/month in January and a minimum of -38 mm/month in July (Figure 2). Further, these average differences change substantially from year to year (Figure 2c) due to high spread in precipitation relative to the magnitude of monthly precipitation (Figures 2a). January difference ranged between 3 and 180 mm/month while July difference ranged between -167 and 215 mm/month (Figure 2c), illustrating the potential for both dry winters and wet summers in the Southern Piedmont. However, it is broadly true that apparent water limitation persists through the period from later spring to early fall.

The growing season in this highly productive region occurs from April to September, during which transpiration and leaf area rapidly increase. Strong, seasonal increases in ET are dominated by these increases in transpiration. Stoy et al. (2006) illustrates that evapotranspiration in similar Southern Piedmont hardwood forests is primarily composed of transpiration that exhibits seasonal increases to account for seasonal increases in ET while evaporation remains much lower and relatively constant through the year, an observation that is also generally supported globally (Schlesinger & Jasechko, 2014). Additionally, they (Stoy et al., 2006) found that total growing season transpiration was relatively insensitive (<5% change) to climatic differences from year to year like growing season precipitation or relative humidity, indicating access to sufficient water to meet transpirative demand. However, our findings show that in an average year 60% of the growing season exhibited apparent water limitation and that 84% of study years (1950-2017) exhibited apparent water limitation for half or more of the growing season (Figure 3c). This counter-intuitive finding in an annually energy limited system indicates the potential importance of subsurface water storage subsidies that facilitate forest transpiration during the growing season not only between precipitation events within the growing season, but more importantly from the dormant season as has been described in theoretical terms (D'Odorico et al., 2010; Milly, 1994; Rodriguez-Iturbe et al., 1999) or with regards to regions with Mediterranean climates (Feng et al., 2019; Hahm, Rempe, et al., 2019). This seasonal transfer of water would be contingent on substantial seasonal dynamics in subsurface storage in order to adequately buffer growing season demand in excess of growing season precipitation. These dynamics form a central focus of this study.

2.4.2 How does integrated watershed storage vary at multiple time scales, and how does it reflect coupling to or buffering of hydroclimatic forcing? – Watershed storage varies seasonally, with high storage during the dormant season, suggesting its role in buffering stochastic precipitation and high growing season evapotranspiration

Integrated watershed storage in WS4 changed at both seasonal and event time scales, but seasonal changes predominate (Figures 3, 6). Although event-scale dynamics are observable as filling and/or draining of daily storage, rarely are the magnitudes of both similar. Rather, while PET was low in the dormant season, filling was generally greater than draining of storage and vice versa. Additionally, although the timing of storage filling differed due to wetter or drier fall/winter, in each year storage declined around the same time in late spring showing minimal response to precipitation inputs (Figure 6).

Over the entire water year storage increased and decreased by hundreds of millimeters, even in the relatively dry 2017. We observed a total storage range of ~500 mm and a mean annual range of ~280 mm across the three-year period. The annual range of storage corresponds to the seasonality of a region's response to hydroclimatic forcing. In the cool, humid climate of Scotland, Birkel et al. (2011) determined an annual storage range of ~50 mm. In contrast, in the Mediterranean climate of coastal California, Dralle et al. (2018) estimated annual storage range to be ~400 mm. Observed range of storage at the CCZO (Figures 3d, 6) suggest that despite evenly-distributed precipitation through the year, its storage seasonality is closer to that of Mediterranean climates than cooler humid climates like Scotland. In fact, as a proportion of precipitation (20-25%), the range we observe in storage is approximately equivalent to that observed in some Mediterranean regions (Dralle et al., 2018). This finding further aligns with observations of substantial seasonal change in deep groundwater levels in the region (Rasmussen & Mote, 2007; Rose & Peters, 2001) and a study of growing season changes in storage (Peters & Aulenbach, 2011), and our own observations of deep groundwater locally in the CCZO (Figure 6).

When considered in the context of apparent water limitation in the CCZO during the summer growing season (Figure 2c), the large seasonal changes in storage depth confirm that forest transpiration in the area was subsidized by water stored during the dormant season when transpiration is low. Although summer rains provide comparable depths on average to dormant season precipitation, hundreds of millimeters of transpiration during the growing season (Figure 2c) were balanced by hundreds of millimeters of drawdown of watershed storage (Figure 3d). Although this seasonal water subsidy is well-recognized in arid or Mediterranean climates where both precipitation/snowmelt and PET are seasonal and a least partially out of phase (Barnhart et al., 2016; J. R. Brooks et al., 2010; Hahm, Dralle, et al., 2019; Ryu et al., 2008), its comparable magnitude in warm, humid regions like the Southern Piedmont is poorly recognized to our knowledge. This seasonal filling and draining of watershed storage add inertia to moderate the regional hydrologic system. This inertia in turn facilitates the high transpirative demand and productivity of the predominant forests in a region with stochastic precipitation inputs and apparent water limitation during the growing season.

Because of our assumption that ET ≅ PET, any effect of uncertainty in ET on our calculation of S is likely to reflect an overestimation of ET, therefore increasing storage over time. We believe that our choice of ET estimation is relatively robust in this specific system, particularly given its simplicity, and is supported by the literature for this case (see discussion in section 2.2). Additionally, over the three study years we calculated a total increase in watershed storage, or residual in the water balance, of only 130 mm (Figure 3d) after 3359 mm of precipitation and 832 mm or runoff. To approximate closure of the water balance over a three-year period with total storage change of almost 600 mm further supports the utility of our assumption for this study. Although Nippgen et al. (2016) showed that year to year carryover storage is an underappreciated component of the water balance, and we do observe evidence of it here, they additionally observed that the effect persists for only the previous year, and the metric for determining that (relationship between precipitation and runoff ratio) does not appear to apply in this watershed during these years (Figure 3a,c). Nevertheless, we suggest that similar studies with access to direct measurements of ET could substantially resolve many of the relationships we observe from our parsimonious approach here.

Storage dynamics in the CCZO depict a relatively periodic hydrologic system with predominant seasonal variability (Figure 7c), a reflection of strong seasonality in PET and transpirative demand. It is intuitive that PET would induce seasonality in storage since it is comparable in magnitude to P (~25% less than; Figure 2) and on average exceeds P in magnitude for many months (Figure 2). However, it would then be reasonable to expect to observe comparable stochastic variability in storage in reflection of the stochastic P regime in the Southern Piedmont (Figures 3a, 7a). Our observed runoff dynamics illustrate why this is not observed. Although higher growing season PET relative to P does damp the effects of summer precipitation on storage, higher dormant season P relative to P generated as much runoff as it did storage increase in average and wet years (WYs 2015, 2016), and even in very dry WY 2017 it generated roughly half the amount of runoff as storage increase (Figure 3c,d). So, precipitation stochasticity is damped in the growing season by relatively higher PET and in the dormant season by partial partitioning into runoff, resulting in a predominant seasonality in watershed storage. However, this partitioning between runoff and storage does not occur in a consistent proportion. Rather, our findings point strongly to the manifestation of watershed storage in runoff dynamics and emphasize its crucial role in mediating the hydrologic cycle in the CCZO and Southern Piedmont.

2.4.3 What does the manifestation of storage dynamics in runoff suggest about the role of storage in mediating hydroclimatic forcing? – Runoff dynamics suggest threshold behavior in response to watershed storage, where higher runoff ratios, longer duration runoff, and less ephemeral flow are indicative of higher storage states regardless of immediate hydroclimatic forcing.

Storage adds inertia to the hydrologic system of the CCZO which facilitates steady growing-season transpirative demand even during apparent water limited conditions. Although runoff is dominated by event response (Figure 7a, Figure 9), it also presents a seasonal pattern in both magnitude and efficiency (i.e., runoff ratio). However, invoking the balance of P and PET alone is not sufficient to explain these seasonal patterns. At its peak, daily PET is on the order of 5 mm/d, while 24% of days with measurable P were greater than 10 mm/d and 12% were greater than 20 mm/d. Furthermore, of those days with P greater than 10 mm/d, 30% had no measurable runoff on that day or the next. This disconnect between inputs and runoff (Figure 4) emphasizes the role of watershed storage in mediating stochastic, aseasonal precipitation. We found that runoff response in WS4 occurred above a threshold (~200 mm) that displayed remarkable consistency across three years. Threshold behavior in runoff response with respect to storage, as opposed to precipitation intensity, magnitude, or API, is well recognized indirectly in the form of hillslope-scale dynamics (McGlynn & McDonnell, 2003a; Tromp-van Meerveld & McDonnell, 2006) or implications of point/hillslope-scale measurements at the watershed scale (McGlynn et al., 2004; Penna et al., 2011). However, direct relation of watershed storage to threshold behavior in runoff response has been more rare in empirical studies, in large part due to the complexity of integrated, heterogeneous hillslope processes at this scale (Spence, 2010). Some studies, though, have observed threshold-mediated relationships between runoff response and storage (Dralle et al., 2018; Hale et al., 2016; Sayama et al., 2011), and our study provides further indication of storage thresholds for runoff generation extending across multiple years, even with different precipitation magnitudes (Figures 3c,d, 5c). Storage depth manifests itself not only through threshold-mediation of runoff generation, though, but also in the variable efficiency of runoff generation (Figure 3c, 5c, 8) and observed flow regimes across different years (Figures 7a,b, 9). These findings emphasize the importance of interpreting runoff dynamics and flow regime in context of storage dynamics.

2.4.3.1 Runoff generation efficiency reflects seasonal changes in watershed storage

Watershed runoff generation efficiency can be succinctly described by the runoff ratio (RR), which has been tool of hydrology for over six decades (Hewlett & Hibbert, 1967). Although its specific formulation and name have varied since its introduction, it has remained some form of the ratio of runoff to precipitation (Blume et al., 2007). Runoff ratios are generally used to characterize either long-term (i.e., annual or greater) runoff generation efficiency (McNamara et al., 1998) or watershed quickflow response to discrete precipitation events (Detty & McGuire, 2010).

Over the three-year study period, the mean annual RR in WS4 was 0.22, which sits within a broad range of RRs regionally. A study of annual runoff ratios reported an average value of ~0.4 in the Southern Piedmont, placing the region at the global average reported in the same study (Dettinger & Diaz, 2000). Chang et al. (2014) in a study of spatial variability of annual runoff ratios across the contiguous United States observed annual values between 0.16 and 0.48 for the same region. A review of forest hydrology in the southeast of the United States (Jackson et al., 2004) reported annual runoff ratios in the Piedmont of 0.2 – 0.6 derived from coarse resolution measurements of hydroclimatic variables (Wolock & McCabe, 1999). Over 22 years, RRs ranging from 0.16 – 0.50 with a mean of 0.30 were observed in Panola Mountain Research Watershed, in the Southern Piedmont of Georgia ~250 km WSW of the CCZO (Peters & Aulenbach, 2011). In a regional study of hydrologic response in the Eastern United States, Woodruff & Hewlett (1970) observed runoff ratios of 0.16 – 0.4; however, they used only the “quickflow” component of runoff after a hydrograph separation rather than total runoff in their calculations, explaining the generally lower values and making them difficult to compare to numbers reported in this and other aforementioned studies. Our observation of a RR of 0.22 (Table 1) places WS4 at the low end of the observed range for the region, but this context more importantly illustrates how broad the range in RRs are within this region even at multi-annual time scales.

Disaggregation of the three-year mean RR in WS4 to annual values reveals its linkage to hydroclimatic forcing (i.e., the combination of P and PET). In general, studies across multiple hydroclimatic regimes have found greater runoff generation efficiency (i.e., higher RR) in regions with greater P relative to PET (Chang et al., 2014; Dettinger & Diaz, 2000; Wagener et al., 2007). This ratio is known as the wetness index (Figure 4), and have been positively correlated with higher RRs (Wagener et al., 2007). In WS4 we observed the same positive relationship. Over the three-year study period, WS4 received precipitation that was average (WY2015), relatively wet (WY2016, 117% of average), and relatively dry (WY2017, 67% of average). For these three years, runoff ratios ranged from 0.17, to 0.39, and 0.10, respectively (Table 1). These values lie within the range of RR reported from various studies in the region; however, their range is notable in that it is comparable in magnitude to ranges reported from sites across the region (see discussion above). Although the generally observed dependence of RRs on hydroclimatic forcing (i.e., wetness) across multiple regions holds, the spread of values from year to year highlights the limitations of using the RR as a characteristic watershed descriptor independent of interannual hydroclimatic variability. Annual runoff ratios illustrate the simple, intuitive relationship between precipitation and runoff at the annual time scale: as precipitation increased, runoff ratio also increased.

However, the linkage between hydroclimatology and RRs breaks down when annual runoff ratios are disaggregated into monthly ratios (Figure 4). Monthly runoff ratios ranged from 0% and 90% over this three-year period (Figure 3). This variability is remarkable alone, but especially when considering that some of the lowest runoff ratios (<5%) occurred during months where P exceeded PET (Figure 3a,b). In contrast, we observed multiple months when PET exceeded P but runoff ratios remained between 0.2 and 0.4, comparable to annual averages. The lowest runoff ratios were generally in the hottest months and highest runoff ratios in the coolest, the seasonal trend was often obscured and not entirely in phase from one year to the next. For example, the maximum monthly runoff ratios for each year were in March, December, and May for 2015, 2016, and 2017, respectively (Figure 3c). RR at the monthly time scale exhibited a stronger relationship to watershed storage (Figure 4c), emphasizing the interplay between watershed storage state and hydroclimatic forcing. A clear illustration of the mediating effects of storage are the months of October-December of 2016, when progressively increasing storage yielded increasing RRs and decreasing addition to storage in response to relatively similar precipitation events (Figure 8). Historically, API indices have been used to represent system memory; however, watershed storage as we present here reflects the underlying, internal hydrologic state that mediate generation mechanisms more directly (Nippgen et al., 2015).

The dynamics of runoff ratios and their connection to watershed storage at sub-annual time scales has been largely underappreciated, thus there is limited context for these findings. However, Yokoo et al. (2008) used a lumped, physically-based model to investigate water balance partitioning as a function of climate seasonality and catchment characteristics, finding that RR decreased with a decreasing wetness index. Additionally, they found that there was minimal connection to storage capacity, although they did not specifically investigate storage volumes. Past empirical studies have found minimal connection between hydroclimate and RRs at sub-annual time scales. For example, in relatively temperate, humid southeastern Australia, Wooldridge et al. (2001) found no correspondence between precipitation and RRs at monthly time scales; however, they did observe some dependence of RR on the phase of the ENSO oscillation, which they attributed to either seasonal changes in soil moisture or rainfall intensity. A study of decades of data from the nearby Coweeta Hydrologic Laboratory examined lag correlations between monthly precipitation and RR (Nippgen et al., 2016) determined that monthly runoff ratios were most strongly correlated with the previous month's precipitation, and remained significantly correlated to a lag of six months, strongly suggesting the importance of watershed storage. We found that in WS4 the highest runoff ratios were generally observed at higher storage values, above a rough storage threshold of 200 mm (Figure 3, Figure 5c). In a study of connections between runoff dynamics and bedrock permeability in 16 nested catchments in Luxembourg, Pfister et al. (2017) found a range in monthly RR between 0.1 and 0.8, suggesting that the substantial range we observed here could be prevalent in other regions; although they did not explicitly link these values to storage they did additionally observe similar seasonality in storage dynamics. Despite findings such as the modeling results from Yokoo et al. (2008) that point to direct linkages between hydroclimate and runoff dynamics, most other studies suggest and ours confirms the importance of watershed storage in mediating hydroclimatic inputs at this temporal scale and suggest that our observations are broadly applicable across other regions.

Decreasing temporal scales from multi-annual to monthly revealed a decoupling between hydroclimate and runoff that occurred at seasonal/monthly time scales. This indicates an emergent connection between integrated watershed storage and runoff that was stronger than the precipitation to runoff relationship. This dependency occurred at an approximate storage threshold (~200 mm), above which we observed a positive, albeit scattered relationship. Complexities in this relationship (Figure 5c) could reflect differences in how the precipitation fell (e.g. intensity) and how watershed storage was distributed internally, either vertically or spatially, and suggests the value of distributed measurements of internal watershed storage for future studies.

2.4.3.2 Flow regime changes interannually and seasonally in reflection of seasonal changes in storage.

Temporary streams (whether intermittent or ephemeral) likely comprise the majority of global stream network length (e.g., Hansen, 2001; Nadeau & Rains, 2007), and have been research foci within the hydrologic (Acuña et al., 2014; González-Ferreras & Barquín, 2017), geomorphic (Tooth, 2000), and ecologic (Datry et al., 2011; Meyer et al., 2007) communities for decades. However, relatively little is understood about their extent, dynamics, and related functioning in a watershed context, particularly in non-arid landscapes. Our study focuses on a single temporary stream system but emphasizes the importance of temporary streams in humid regions like the Southern Piedmont in a global understanding of watershed and stream network dynamics as they pertain to runoff generation, watershed storage, and ecohydrologic function. We determined that temporary streams in the Southern Piedmont can exhibit variable durations of flow interannually, and also switch between distinct flow regimes (i.e., intermittent or ephemeral), with seasonal switching between no flow in low storage times to either intermittent or ephemeral flow in higher storage times (Figure 7).

Current research on temporary streams has focused in part on the initial challenge of mapping their extent (S. E. Godsey & Kirchner, 2014; González-Ferreras &

Barquín, 2017; Jaeger et al., 2019; Zimmer & McGlynn, 2017b). WS4 is drained by a temporary stream, but that classification alone fails to capture the range of flow duration and flow regimes exhibited interannually within the watershed. Over the study period the number of days during each water year on which measurable flow occurred ranged between 48% and 73% (Figure 9); however, the dry (WY 2017) and average (WY 2015) years both exhibited roughly 50% flow days annually, despite 35% lower precipitation from annual average. In sharp contrast, WY 2017, with only 17% greater precipitation than annual average, exhibited 50% more flow days than the other two water years. This range in duration of stream flow is just one example of how variable a "temporary" stream can be, even in humid energy limited systems. Additionally, WS4 exhibited both intermittent and ephemeral flow regimes. WYs 2015 and 2016 were average and wet years (Figure 3a) and both exhibited intermittent flow (Figure 16b) while WY 2017 was a dry year (Figure 3a) and was ephemeral (Figure 16b). Intriguingly, WY 2015 had approximately the same flow duration as WY 2017 (50%) while exhibiting an intermittent flow regime more similar to WY 2016. These divergent similarities between water years create a framework for characterizing temporary streams based on both flow regime and flow duration, and clearly indicate the need to consider both in doing so.

Observing distinct flow regimes in the same watershed in different years is supported by regional context. In a lower relief but otherwise similar Southern Piedmont watershed, Zimmer & McGlynn (2017a) showed the role of regular, seasonal oscillations in watershed storage in inducing seasonality in runoff response despite aseasonal precipitation inputs. They inferred storage state classifications (i.e., high, transitional, and low) and connected them to switching from ephemeral flow (high ET/low storage) to intermittent flow (low ET/low storage) over the course of two water years. Intermittent, seasonal flow in the higher storage, “wet” season switched to ephemeral, storm-driven flow in the lower storage, “dry” season. In contrast, we observed no flow in WS4 during the low storage season, and during the wet season the flow regime switched between intermittent (WYs 2015 and 2016) and ephemeral (WY 2017) from one year to the next. This distinction between two systems that otherwise appear very similar could be due to differences in slope, where lower gradient headwaters such as the one studied in Zimmer & McGlynn (2017a, 2017b) potentially retain higher storage levels through the growing season and therefore are able to generate runoff during times that steeper watersheds like WS4 do not. But these differences primarily point to the value in expanding our studies of temporary streams in humid regions like the Southern Piedmont temporally, geographically, and to incorporate multiple watersheds into single studies to facilitate comparison within the region.

2.4.3.3 Summary of 2.4.3

We observed a range in runoff ratios in WS4 from 0% to 90%. We also observed flow durations from 50% to 70% of the water year and flow regimes switching between intermittent and ephemeral in different water years with complete drying during the growing season. These dynamics are not the readily apparent result of simple variability in precipitation and PET (Figures 3-5). Incorporating integrated watershed storage into this analysis suggests that the range in runoff ratios, flow duration, and distinct flow regimes (intermittent or ephemeral) are the manifestation of watershed storage state and highlight its complex role in mediating runoff dynamics.

2.5 Implications for Critical Zone hydrology and ecohydrology

A broadly-recognized challenge within current hydrologic research is to understand how critical zone (CZ) structure (ecologic, topographic, pedologic, geologic, etc.) controls storage and partitioning of precipitation into runoff and evapotranspiration (ET), and additionally how CZ hydrology feeds back to influence CZ structure (P. D. Brooks et al., 2015; Grant & Dietrich, 2017). The CCZO represents an ideal location to answer many of the questions that emerge from this challenge. In this study we explored hydroclimatic, storage, and runoff dynamics at monthly/seasonal time scales, and analyzed the mediating role that storage plays between runoff dynamics and hydroclimatic forcing. Potential implications of our study include: 1) how the subsurface structure of the CCZO, in conjunction with topography, creates three dimensional, spatiotemporal heterogeneity of storage and 2) how seasonal excess and deficit of storage interact to facilitate the ecohydrologic functioning of the Southern Piedmont but raise questions about the ecohydrologic future of the region.

2.5.1 How does subsurface critical zone structure organize storage and its connections to runoff three-dimensionally?

Both the relationship between storage and runoff (Figure 5c) and divergences between storage and deep groundwater levels (Figure 6) suggest internal 3D heterogeneity in storage within the subsurface CZ whose characterization could further resolve the connections between watershed storage and runoff. Separate, positive relationships exist between storage and runoff depending on the relative importance of stormflow and baseflow (Figure 5c). These two dynamics suggest slow draining of less transmissive storage pools generating baseflow, while high storage facilitates rapid flux through more transmissive storage pools generating stormflow in conjunction with, or instead of, filling those pools. Further illustrating these two runoff responses and suggesting distinct storage pools is slow draining of storage corresponding to low, constant runoff during inter-storm periods, while high magnitude precipitation events resulted in an increasing partitioning to runoff relative to storage as storage levels increased (Figure 8).

Similarly, divergences between deep groundwater and storage (Figure 6) reflect distinct storage pools in the subsurface CZ. Since storage is an integrated description of water in all storage pools within a watershed, and deep groundwater represents only one of these, divergence between the time series represent dynamics in other storage pools not reflected in deep groundwater. We observed this particularly in WY 2017 where winter increases in storage are not matched in deep groundwater (Figure 6). This disconnect suggests filling of a storage pool that precedes sufficient infiltration to deeper zones to be reflected in a rising water table. These could be shallower, perched water tables that drain laterally rather than vertically (e.g., Zimmer & McGlynn, 2017b) or unsaturated vadose zone water in smaller pores that fill preferentially before deeper infiltration (Selker et al., 1999).

Each of these observations clearly suggest internal heterogeneities in watershed storage possibly driven by or reflective of subsurface CZ structure. It has been well-documented that terrain structure can lead to lateral redistribution of water within watersheds such that distinct components of the watershed contribute preferentially to runoff at different times (e.g., Jencso et al., 2009; Nippgen et al., 2015). Similarly, our findings here suggest that the 3D spatial location of storage due to subsurface CZ structure at the CCZO likely plays a significant role in mediating runoff response potentially in addition to surface terrain structure.

Recent research into connections between subsurface CZ structure and hydrology (Rempe & Dietrich, 2018) or ecohydrology (Hahm, Rempe, et al., 2019) has focused on variability in CZ depth, and its potential to serve as a transport and storage zone for subsurface water. These studies focused specifically on the depth of "weathered bedrock," by which they mean regolith below the O-B soil horizons. Although such a focus is potentially more appropriate in certain regions than others (e.g., the relatively younger landscapes of California), there is substantial research pointing to the value of defining subsurface CZ structure not only in terms of depth but also in terms of hydraulic properties that vary between soil horizons and into the saprolite in landscapes ranging from high latitude to tropical (Elsenbeer, 2001; Gannon et al., 2014; Tetzlaff et al., 2014; Zimmer & McGlynn, 2017b). In studies across pedological chronosequences (Jefferson et al., 2010; Lohse & Dietrich, 2005), it has been suggested that older critical zones generally correspond to higher drainage densities and more responsive runoff generation due to development of relatively shallow clay-rich horizons from secondary weathering in the critical zone, despite increased weathering depths overall. Similarly, recent physically based modeling work predicated on the hydraulic structure observed in older critical zones (Harman & Cosans, 2019; Xiao et al., 2019) has highlighted the importance of understanding subsurface CZ structure in deeply weathered landscapes from a hydrologic perspective.

The Ultisols that characterize the CCZO exhibit clay-rich Bt horizons (Calabrese et al., 2018; Richter et al., 2019) with soil column residence times estimated at ~2 Ma of weathering (Bacon et al., 2012). In a similar Southern Piedmont landscape in North Carolina (Duke Forests, 270 km northeast), (Zimmer & McGlynn, 2017b) describe generally similar soil structure, also characterized as Ultisols. They observed both shallow perched water tables above these horizons corresponding to stormflow regardless of the presence or depth of deeper water tables. They additionally observed elevation of deeper water tables during higher storage times of year (largely aligned with the dormant season) that corresponded to baseflow during those times. These findings of seasonal response to stochastic precipitation likely corresponding to subsurface storage dynamics largely align with ours. Similar soil structure, climates, and land cover support these similarities with the CCZO; however, this site had several important differences to WS4 in the CCZO. Most importantly, the Duke Forest watershed exhibited lower relief and different underlying parent geology (finer-grained slate), both of which likely result in distinct soil profiles (Richter et al., 2019) that may have more continuous clay-rich B-horizons along lower-gradient hillslopes or lower conductivity saprolite due to finer-grained parent material. These differences are suggested by our observation of runoff response to precipitation only when a storage threshold was exceeded (Figures 3,5), which contrasts with the Duke Forest site where runoff was possible under any storage state. We believe that this context indicates the rich variability of subsurface CZ structure and associated hydrologic behaviors we find within this understudied region. Additionally, it implies that incorporating that subsurface CZ structure into our understanding of dynamic storage in the region is likely to substantially resolve our understanding of hydrologic dynamics regionally and with implications beyond the region.

2.5.2 Ecohydrologic functioning and future of the Southern Piedmont

Large-scale variation in vegetation composition has long been explained as a function of hydroclimate (Holdridge, 1947; Horton, 1933; Schymanski et al., 2009; Stephenson, 1990). Biomes (e.g., temperate forest, tropical rainforest) can be mapped into the space defined by water (mean annual precipitation) and energy (mean annual temperature) availability (Whittaker, 1970). The CCZO, and Southern Piedmont more broadly, falls on the transition between temperate forests (the current biome) and woodland/shrubland. Our study has emphasized the potential for water-limiting hydroclimatic conditions that can persist for time scales (months to seasons) greater than that of diel transpiration demand (Figure 2). In such cases, then, the applicability of the Whittaker framework is contingent on sufficient storage accumulated through the dormant season to subsidize insufficient growing season precipitation (e.g., Hahm, Rempe, et al., 2019). This suggest that storage characteristics (capacity and dynamics) are additional necessary variables for understanding the linkages between hydroclimatic conditions and regional ecohydrology. Study of the degree of agreement between current biomes and predicted biomes based on hydroclimate alone could help identify places or regions where subsurface storage more strongly affects ecohydrologic function, thereby either enhancing simple models like the Whittaker classification or supporting new conceptualizations of the links between the CZ and climate as expressed in vegetation. Additionally, the position of the CCZO so close to transitions between biomes points to the importance of fully understanding its ecohydrologic functioning in the face of potential climate trajectories.

In this region, systems can switch between water and energy limitation seasonally (Figure 2c) and exhibit strong threshold behavior in the relationships between storage and runoff (Figure 3c). Water limitation during the growing season is balanced by draining dynamic storage accumulated in the subsurface critical zone during the dormant season. Eagleson (1982) provided a framework for understanding ecohydrologic function in terms of distinct optimization strategies of humid (energy-limited) and arid (water-limited) systems: humid systems optimize energy usage by maximizing canopy coverage while arid systems minimize water stress by maximizing precipitation use in the form of soil storage. The Southern Piedmont presents components of both the humid strategy in the form of forests with dense canopies and the arid strategy in the form of threshold runoff response to subsurface water storage (Figure 3c). The co-location of characteristics of both water and energy limitation in the CCZO present an opportunity to expand our conceptual model of humid and arid zones beyond a binary classification of one or the other.

Understanding the role of the ecosystem in partitioning water between evapotranspiration (“green”) and runoff (“blue”) is a fundamental challenge of ecohydrology (D’Odorico et al., 2010) and directly relates to questions of critical zone structure in the form of soil pore-size distributions and rooting depths. Study of these two pathways in the water balance in regions where precipitation and transpiration demand are out of phase has yielded a conceptual model where transpiration draws from dormant-season precipitation held tightly in smaller soil pores that fill before larger pores while runoff is generated from subsequent precipitation that flows more rapidly through larger pores. Isotopic studies of these two subsurface pools have suggested that there is minimal mixing between these pools (J. R. Brooks et al., 2010). Although the majority of this work has been done in highly seasonal regions, a study in tropical Puerto Rico (Evaristo et al., 2016) and a global meta-analysis (Evaristo et al., 2015) that included temperate forests added evidence of separation between blue and green water across most biomes. However, Evaristo et al. (2015) found the least separation between the two pools in temperate biomes. Additionally, the grouping of temperate forests included a broad range of sites globally, only one of which was in the Southeastern United States

(North Carolina, likely the Coweeta Hydrologic Laboratory in the Appalachian Mountains) which notably exhibited some of the lowest separation of the group. This is explained as greater mixing between blue and green water in temperate forests relative to other sites (Evaristo et al., 2015); however, this explanation is not intuitive in the Southern Piedmont due to its deeply-weathered, high clay-content regolith. Two alternative, related hypotheses are that transpiration in the Southern Piedmont is drawn from a broad range of soil water 1) temporally, integrating from recent, growing-season precipitation to older precipitation stored from previous dormant-seasons and/or 2) vertically, accessing pore water across a much deeper soil profile than the ≤1 m depths samples in previous studies (J. R. Brooks et al., 2010; Evaristo et al., 2016). Although regional (Gao et al., 2014) and global (Fan et al., 2017) studies of potential root depths have suggested that humid climates likely have shallower rooting depths, our findings here of substantial loss of storage over the growing season imply the possibility that forests in the region may structure their root networks more similarly to plants in more arid zones. This implication again emphasizes the potential represented by the CCZO and other Southern Piedmont sites to refine our conceptual models of connections between climate, ecology, and CZ science.

The mean annual precipitation and temperature of the CCZO (1200mm and 16°C) lies on a hydroclimatic transition between temperate forests and woodland shrubland, and ~2°C less than the transition between temperate forests and tropical seasonal forest/savanna (Whittaker, 1970). Its proximity to biome transitions within this space raises the possibility of fundamental changes in biome and associated ecohydrolgic functioning of the Southern Piedmont within relatively near-term climate change scenarios. Such scenarios can be explored with regional projections of climate trajectories via the Multivariate Adaptive Constructed Analogs (MACA) (Abatzoglou & Brown, 2012) dataset, which is forced by global climate model data from the Coupled Model Intercomparison Project 5 (CMIP5) (Taylor et al., 2011). Over the time period 2019-2069, and under a "business-as-usual" emissions scenario (RCP 8.5), it is projected that mean annual temperature will increase by 2.75°C and mean annual precipitation by 86 mm in the CCZO region. These hydroclimatic conditions would shift the CCZO climate to one closer to that of coastal Texas, and move the CCZO into climatic conditions more favorable to woodland/shrubland. A transition to this biome could lead to a decrease in evapotranspiration of 10-30% (Donohue et al., 2007), increasing runoff and likely inducing long-term changes in subsurface water storage through the transition. Additionally, studies in the nearby Appalachian Mountains (Burt et al., 2018; Laseter et al., 2012) and across the eastern United States (Vose & Elliott, 2016) have illustrated a trend towards greater variability in precipitation even in the absence of changes in annual P: longer and more intense storms but longer and more severe droughts as well. Although our study illustrates the potential for dormant-season precipitation to subsidize growing-season evapotranspiration, studies have suggested that the degree of subsidy is limited by its potential maximum storage capacity (Hahm, Rempe, et al., 2019) or rooting depth (Porporato et al., 2002). This maximum capacity has been shown to be correlated to such characteristics of precipitation regimes as intervals between droughts, potentially due to co-evolution of climate, plants, and regolith (Gao et al., 2014). Both increasing temperatures or changing precipitation regimes could outstrip the capacity of storage zones in the CCZO to buffer stochastic precipitation inputs, creating the potential for storage limitation even with sufficient annual precipitation. This potential shift in biome provides further motivation for a deeper understanding of the interaction of ecohydrologic functioning of the Southern Piedmont with its hydroclimate and subsurface structure.

The Southern Piedmont of the United States is covered primarily in highly productive mixed pine-hardwood forests, in apparent reflection of its annual energy-limitation (Table 1) and in alignment with broadly-applicable models of biome distribution (e.g., Whittaker, 1970). However, our findings highlight the climatic conditions in the region that create conditions of apparent water limitation through the majority of the growing season despite precipitation distributed evenly throughout the year (Figure 2). These months of apparent growing season water limitation appear to be subsidized by substantial accumulation of dormant season precipitation in subsurface storage whose seasonal range is approximately 20-25% of total annual precipitation (Figure 3). This role of storage in maintaining energy limitation through months of apparent water limitation is primarily described in arid and semi-arid regions, and our observations of similar dynamics in this humid region implies that incorporating metrics of storage within the subsurface CZ (i.e., capacity and dynamics) could facilitate refinement of our conceptual models of the interactions between climate the climate system, geologic system, and ecosystem. Furthermore, our observations of apparent water limitation in this system, in conjunction with its position on or near transitions between biomes (Whittaker, 1970), implies that the region could be particularly vulnerable to broad shifts in biome and/or societally relevant shifts in water resource availability. Each of these implications further underscores the scientific and practical value of continued study in the region.

2.6 Conclusion

Utilizing a water balance approach from water years 2015-2017 in a headwater watershed in the Calhoun Critical Zone Observatory, in conjunction with 67 years of local precipitation and temperature data, we elucidated the role of watershed storage dynamics in mediating connections between precipitation, evapotranspiration, and runoff. Storage changes were a substantial portion of the water balance, and that its predominant, seasonal wet-up and dry-down buffered apparent water limitation during the majority of the growing season while setting threshold conditions for runoff generation in the dormant season. Our findings were as follows:

1. On average since 1950, the monthly balance between precipitation and evapotranspiration shifted from precipitation excess to evapotranspiration excess due to seasonal patterns in monthly evapotranspiration and aseasonal, stochastic precipitation patterns. This switch suggested apparent water limitation during those months, which included 60% of the growing season (roughly April-October) on average. Additionally, 84% of years since 1950 exhibited apparent water limitation for half or more of the growing season.
2. Integrated watershed storage exhibited primarily seasonal dynamics and ranged by 200-400 mm yr^{-1}, corresponding to 20-25% of annual precipitation. Seasonal wet-up of storage began after fall senescence (Nov-Jan) while dry-down began during spring leaf-out (April-May). The timing of dry-down corresponded to increasing transpirative demand and apparent water limitation in the region, indicating the importance water subsidy from the dormant season to facilitate elevated growing season demand.

3. Observations of nearby (<3 km) deep groundwater table in a 70 m well exhibited largely comparable timing and relative magnitude of seasonal fluctuations to watershed storage, with the water table rising by meters to within 2.5 meters of the surface during the dormant season and falling to 6.5 meters below the surface during the growing season. This general agreement was notably diverged from by delayed deep groundwater table rise relative to storage wet-up in two years, highlighting storage pools incorporated within integrated watershed storage that are not reflected in changes in the level of deeper saturated zones.
4. Runoff ratios ranged from 0-90% and flow regime from ephemeral to intermittent. These dynamics appeared to be manifestations of seasonal storage dynamics, with a generally positive relationship between runoff, runoff ratio, and storage values above a threshold value of 200 mm. Above this threshold the relationship was not a simple linear one, but rather appeared to differ depending on whether baseflow or stormflow was the predominant flow component.

These findings depict a system that experiences dramatic seasonal switching between apparent water and energy limitation, but whose deeply weathered subsurface accommodates storage accumulation through the dormant season to meet high transpirative demand during the growing season while facilitating runoff generation above a threshold storage. The range of storage change seasonally, nonlinear relationship with runoff, and discrete divergences from measured water tables all imply subsurface critical zone structure that partitions water into distinct pools with distinct dynamics and ultimate effluxes. Furthermore, highly productive forests with dense canopies dominating a region where substantial proportions of the growing season appear to be water limited point to the potential for research in this region to help expand our current conceptual models of the connection between climate and biome, and the potential for change under various climate trajectories. With an ongoing need to better understand complex critical zone structures and their feedbacks with terrestrial ecosystems at global scales (Fan et al., 2019), expanded study at the CCZO is likely to not only further our understanding of this under-studied region, but also to have implications of much broader relevance.

3. Watershed scale storage and runoff generation reflect hillslope hydrology and watershed structural heterogeneity

3.1 Introduction

Watersheds are by definition three dimensional structures. The shape and distribution of the hillslopes that comprise them, combined with the depth and stratification of their regolith, set the physical space that connects precipitation to runoff. Except in the case of a watershed comprised entirely of exposed bedrock or concrete, this connection is mediated by heterogeneous, dynamic, subsurface hydrologic storage within a watershed's regolith. Describing this dynamic heterogeneity, or its integrated effects on runoff observed at the watershed outlet, are central goals of hillslope and watershed hydrology. However, a holistic understanding of the linkages between hillslope and watershed scale subsurface storage, and their further connection to runoff generation, remains an ongoing challenge. To this end, we present an empirical study of integrated watershed hydrology (i.e., storage, runoff) and to measured hillslope scale subsurface hydrology in a watershed with deeply weathered regolith and complex terrain.

The three-dimensional structure of watersheds has been recognized for decades by the hydrologic community (Hewlett & Hibbert, 1963; Tsukamoto, 1963), and more recently interest has increased with the promotion of critical zone science (Brantley et al., 2007; P. D. Brooks et al., 2015; Grant & Dietrich, 2017). There is a rich literature relating hillslope hydrology to the topography (i.e., surficial structure) of watersheds and/or watershed runoff generation. With the development of the variable source area concept (Dunne & Black, 1970; Freeze, 1972; Hewlett & Hibbert, 1967), it was recognized that distinct parts of the watershed contributed more or less to runoff in dynamics ways, and that larger contributing area generally corresponded to greater local wetness. Although these earlier studies focused on the importance of large contributing area at the base of convergent hillslopes or in riparian areas, subsequent studies illustrated water tables dynamically extending into more distal hillslope locations in connection with runoff during large events (McDonnell, 1990; McGlynn & McDonnell, 2003a, 2003b; R. A. Woods & Rowe, 1996). Within these hillslopes, development of subsurface flow has been shown to exhibit threshold behavior where exceedance of certain hydrologic conditions leads to dramatic increases in hydrologic response (Penna et al., 2011; Sidle et al., 2000; Tromp-van Meerveld & McDonnell, 2006). By distributing hillslope scale measurements across topographic gradients in watersheds, it has been shown that watershed runoff relates positively to the proportion of the watershed connected via subsurface water tables to the stream, and that in steep watersheds with relatively shallow, homogeneous soils this connectivity can be interpolated continuously across the watershed using its topography (i.e., distribution of contributing area)(Jencso et al., 2009; Rinderer et al., 2014, 2019). Using topography as a surrogate for subsurface hydrology has been a tremendously useful tool due to its ease of measurement; however, it is most effective in mountainous watersheds where complex terrain and shallow, homogeneous soils make topography the dominant control on the heterogeneity of subsurface hydrology, and contributing area becomes a reliable proxy for the contributing volumes it represents (Nippgen et al., 2015). Empirical studies that distribute measurements throughout that structure are relatively rare (but see Zimmer & McGlynn, 2017, 2018), particularly with respect to incorporating depth and/or stratigraphic gradients within the regolith. In large part this is due to the fundamental challenge in measuring anything in the subsurface, including water tables or soil moisture, even at shallow depths. Although advances in near-surface geophysics are improving our ability to measure subsurface structure and hydrology (St. Clair et al., 2015; Hodges et al., 2019; Holbrook et al., 2014), we remain largely limited to point measurements, which can require significant labor to install and maintain.

One way of circumventing this difficulty is by integrating heterogenous subsurface hydrology into a metric of combined watershed storage. Although in some cases integrated storage has been calculated from distributed measurements of subsurface hydrology (McNamara et al., 2011) or from a combination of measurements and simulation (Seyfried et al., 2009), storage is largely inferred from indirect measurements such as hydrologic tracers (Soulsby et al., 2009), the watershed mass balance (Nippgen et al., 2016; Pfister et al., 2017), or analysis of hydrograph recessions (Kirchner, 2009). Few studies have coupled distributed measurements of subsurface hydrology with independent calculations of integrated storage, although several have related storage to smaller numbers of representative measurements (Dralle et al., 2018; Hale et al., 2016; Tetzlaff et al., 2014). In landscapes characterized by complex terrain and deep, stratified soils, however, it is likely insufficient to rely on few representative measurements. Instead, it can be valuable to directly measure subsurface heterogeneity across three dimensions and relate its dynamics to integrated watershed storage and runoff.

The Southern Piedmont of the United States extends from Maryland to Alabama and is characterized by highly-dissected headwaters and deeply weathered, stratified soils (Richter et al., 2019). Weathering fronts range up to 10s of meters in this region, but are additionally often characterized by relatively (i.e., <1 m) shallow, clay rich Bt horizons which have low hydraulic conductivity. The combination of complex headwater topography and soil stratigraphy make this region ideal to directly study three dimensional heterogeneity in subsurface hydrology and its linkages to integrated watershed storage and runoff generation. To do this, we address the following questions:

1. What are the relationships between deep groundwater, integrated watershed storage, and runoff dynamics?
2. When, how, and where does subsurface hydrology within watersheds correspond to runoff and/or storage dynamics?

3.2 Methods

3.2.1 Study Site: WS4 of the Calhoun Critical Zone Observatory

This study was conducted in the Calhoun Critical Zone Observatory (CCZO), part of the NSF-funded Critical Zone Observatory network. The CCZO is located in northern South Carolina, USA, in the Southern Piedmont region of the southeastern United States, which stretches from Maryland to Alabama between the Appalachian Mountains and the Atlantic coastal plain. The Southern Piedmont lies within a humid subtropical climate zone characterized by a hot, humid growing season lasting from approximately April through September (Stoy et al., 2006) and a mild dormant season for the remainder of the year. Land cover is predominantly a mixture of pines (*Pinus* spp.) and hardwoods such as oak (*Quercus* spp.) and hickory (*Carya* spp.). Average annual temperature at the CCZO is 15.8° C and average precipitation is ~1200 mm, distributed evenly through the year without a regular dry season and falling almost entirely as rain. The terrain of the CCZO is typical of the Southern Piedmont with upland, low-gradient interfluves joined to bottomland streams and rivers by highly dissected headwaters that switch seasonally between dry and 1st order; this terrain ranges from 110-190 m in elevation. The area is underlain by granite metamorphosed to granodiorite or metadiorite of the Wildcat Branch complex. Upland soils are primarily Ultisols of the Appling, Cecil, and Madison series. These soils generally consist of loamy

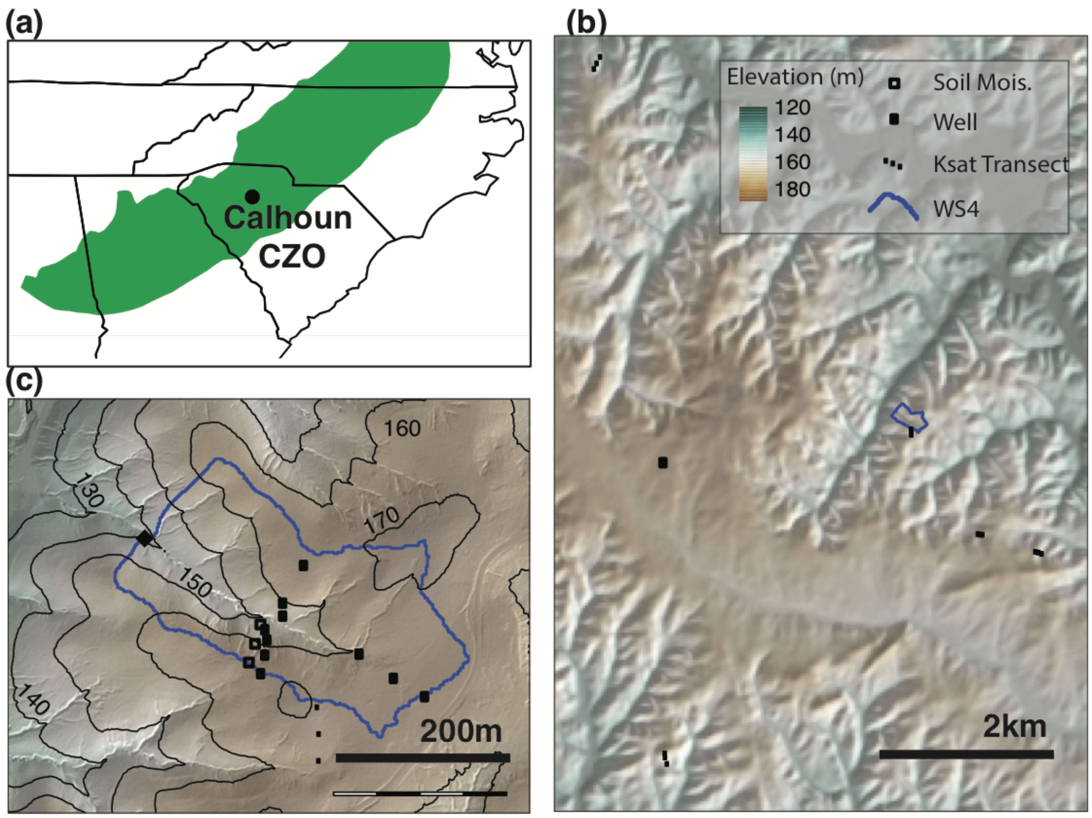

Figure 10: Site Map; (a) The Calhoun Critical Zone Observatory in upstate South Carolina, USA. (b) Area map of the CCZO including locations of soil hydraulic conductivity transects, precipitation gauge, deep groundwater well, and research watershed 4 (WS4). (c) Detail of WS4 indicating locations of weir, well nests, and soil moisture pits.

sands underlain by clay-rich argillic horizons over deeply weathered saprolite (Richter et al., 2000).

We focused this study on the intensively measured research watershed 4 (WS4), a 6.9 ha headwater with a total relief of 50 m (123-173m in elevation), and a mean slope of 19%. It is forested primarily with mixed hardwoods and few pines and underlain by Ultisols typical of the region. Soil depths were assessed via hand auguring (AMS; 2.25" auger diameter). Depth to argillic horizons ranged from 40-70 cm, and depth to refusal from 2-9 m. Generally, depth to argillic horizon increased and depth to refusal decreased moving down hillslopes from the ridge. This general pattern of deepening soils moving away from the stream has been additionally supported by geophysical monitoring in WS4 and adjacent watersheds (St. Clair et al., 2015). The stream draining WS4 dries completely in the summer growing season and flows ephemerally to intermittently during the dormant season from fall through early spring.

3.2.2 Surface and Subsurface Hydrologic Measurements

We monitored precipitation, discharge, and groundwater levels at 5-min frequency and temperature at hourly frequency for water year 2016 (October 2015 – September 2016) and the three months prior. Temperature was logged using a baffled temperature/relative humidity sensor (CS215-L, Campbell Scientific, ±0.4°C from 5°-40°C). Precipitation was measured using a tipping bucket rain gauge (TE525MM, Texas Instruments) with a 24.5 mm funnel, 0.1 mm per tip, and a nominal accuracy of 1% below 2.5 cm hr^{-1}. It was placed in a clearing <3 km from WS4 surrounded by a 45° cone without intercepting vegetation. We calculated discharge from stage continuously monitored (capacitance rods, TruTrack, ±1 mm) in a concrete stilling pool behind a 90° v-notch weir and the rating curve for a 90° v-notch weir (USBR, 2001). These were periodically verified by timing the filling of a container of known volume held below the weir notch. Groundwater levels were measured in 20 shallow wells within WS4 and one

Table 2: Physical characteristics of well nests. Depths are completion depths. Deep wells are screened below the completion depth of the corresponding shallow well. Catchment area calculated from MD∞ flow accumulation. Parenthetical designations under "transect" and "well nest" relate these descriptions to each measurement's unique name (e.g., T1W1shal being transect one, ridge well, shallow depth).

Transect (T_)	Well Nest (W_)	Hillslope position	Depth (m)		Contributing area (m^2)
			shal	deep	
1	1	ridge	0.28	3.84	25
	2	midslope	0.35	3.55	231
	3	toeslope	0.40	2.52	390
	4	riparian	0.70	2.18	360
2	1	ridge	0.40	4.40	76
	2	midslope	0.60	2.83	117
	3	toeslope	0.40	2.48	136
3	1	ridge	0.63	8.50	38
	2	midslope	0.44	2.43	285
	3	toeslope	0.92	2.33	263

Table 3: Physical characteristics of soil moisture pits. Depths are installation depths. Sensors installed in upslope pit wall lateral to predominant hillslope gradient. Parenthetical designation under "soil pit" relate these descriptions to each measurement's unique name (e.g., P1shal being ridge soil pit, shallow depth).

Soil Pit (P_)	Hillslope position	Depth (m)			Contributing area (m^2)
		shal	mid	deep	
1	ridge	0.15	0.45	1.0	40
2	midslope	0.15	0.50	1.0	174
3	toeslope	0.15	0.50	1.0	454

deep groundwater well (DW) on a relatively lower gradient, upland interfluve <3 km from WS4. These water levels were recorded with a mix of capacitance rods (TruTrack, ±1 mm) and pressure transducers (Solinst levelogger, ±5 mm) at 20- and 5-min frequency for the DW and WS4 wells, respectively. Pressure transducer water level measurements were corrected for atmospheric pressure changes using sensors located within WS4 and at DW (Solinst barologger, ± 0.05 kPa) at the same temporal frequency as water level sensors.

Wells were distributed to measure deep groundwater (DW), and more shallow subsurface water above and below clay-rich B-Horizons (shallow and deep wells, respectively). The DW is 15.25 cm in diameter, was completed at 70 m below the ground surface, and is cased to 16 m. Shallow groundwater wells were installed between the winter of 2014 and summer of 2015 using a 2.25” hand augur (AMS) and cased in solid or screened PVC with the same outer diameter as the bore hole. Wells were installed in a series of three transect running from ridge to geomorphic channel in WS4 which were chosen to encompass slope steepness and curvatures characteristic of WS4: steep and concave, moderate slope and planar, low slope and planar. We distributed a minimum of 3 measurement nests along each transect, and at each location installed a nest of two wells separated by ~1 m: one completed at the transition from A to B horizon (i.e., at the start of clay-rich argillic horizon) and one completed at refusal depth. Shallower wells were screened through their entire depth and deeper wells were solid above and screened below the B horizon to their completion depth. We sealed the upper 5 cm of each well with bentonite to prevent surface runoff entering the bore hole.

We estimated potential evapotranspiration (PET) using the Thornthwaite method (Thornthwaite, 1948) because it relies only on air temperature and we judged the limitations of this method to be minimized in this region. Although it has well-known limitations, including substantial underestimates in arid climates (Pereira & De Camargo, 1989) and high variability in accuracy across diverse climates (Vorosmarty et al., 1998), it is much more robust in humid climates similar to those in the NE United States in which it was developed (Thornthwaite, 1948), and specifically in uncultivated, deciduous forests (Vorosmarty et al., 1998). Further, results from this analysis yielded annual values consistent with those reported regionally from measurements based on latent heat flux (Novick et al., 2016). This method, and our subsequent assumption of energy-limitation (see section 3.2.3), captures water balance and storage dynamics and its parsimonious nature is both a strength and comparable to other simplifying methods in similar studies (Dralle et al., 2018; Pfister et al., 2017; Staudinger et al., 2017).

3.2.3 Water Balance Calculation of Storage

Our study period was July 1, 2015-September 30, 2016. This period was chosen to include a full water year (October 1, 2015-September 30, 2016) and sufficient time prior to its start to illustrate the dry conditions of late summer and early fall. We calculated changes in storage over the study period (July 2015 – September 2016) in WS4 as the residual of the watershed mass balance over time:

$$\text{(1)} \qquad \frac{dS_{tot}}{dt} = P_{tot} - Q_{tot} - ET$$

Change in storage (dS_{tot}) [L] over a time interval (dt) [T^{-1}] is the difference between total precipitation inputs (P_{tot}) [L T^{-1}], total surface and subsurface discharge (Q_{tot}) [L T^{-1}], and evapotranspiration (ET) [L T^{-1}]. S_{tot} is all storage within all potential storage compartments of the watershed and is indeterminate from the water balance alone due to the need for known initial conditions and more generally difficult to measure due to challenges with the lower watershed boundary condition. However, if we define S_{tot} as the sum of the initial storage in WS4 (S_0) and the cumulative storage relative to that value (S), we can rewrite equation 1 and integrate it to calculate S:

(2) $$S_{tot} = S + S_0 = \int_0^{\tau} (P_{tot} - Q_{tot} - ET)dt$$

S is the cumulative storage relative to the initial storage condition over the study period, τ. If we set the initial time to the period of the year that we assume to be the lowest storage state and integrate over at least a full year of average or wetter precipitation, we can further infer that the range of S represents the component of storage that varies through the year. In the Southern Piedmont, this time of year is the end of the growing season when streams have dried and groundwater has receded to its lowest level. This point is within weeks of the start of the USGS-defined water year (October 1), so we adopt this point as our t = 0 and set S = 0 at this time, though we provide data from several months prior to this point to illustrate the drying of the watershed through the summer (Figure 11).

Here we assume that precipitation is entirely rain and therefore that we can ignore seasonal storage of precipitation as snowpack, and additionally that discharge from the watershed is predominantly surface runoff. Further, we assume that the CCZO is an energy-limited system, such that ET ≅ PET. Based on these assumptions, and by focusing on cumulative storage rather than total storage, we rewrite equation 2 as:

(3) $$S = \int_0^{\tau} (P - Q - PET)dt$$

These assumptions allow us to use measured precipitation and discharge along with estimated PET to estimate cumulative storage, henceforth called simply storage, at daily frequency.

3.3. Results

3.3.1 Water Balance

Over the study period (July 1, 2015-October 1, 2016) precipitation totaled 1667 mm, with 1409 mm falling within water year 2016 (117% of annual average), while evapotranspiration was 1148 mm (822 mm in WY2016, 103% of annual average). Runoff was 554 mm, occurring entirely within water year 2016, and was 140% of the difference between long-term mean annual precipitation and evapotranspiration.

Although mean monthly precipitation in the region is approximately equivalent across all months at 100 mm, in water year 2016 October-December were the three wettest months with 56% of precipitation falling during that period. Runoff was concentrated in the fall through early summer, and 78% occurred during three large storm systems in October (Hurricane Joaquin), November, and December. Flow ceased following Hurricane Joaquin and the November storm system, while baseflow persisted after the December storm system through June 2016 (Figure 11). Monthly runoff ratios

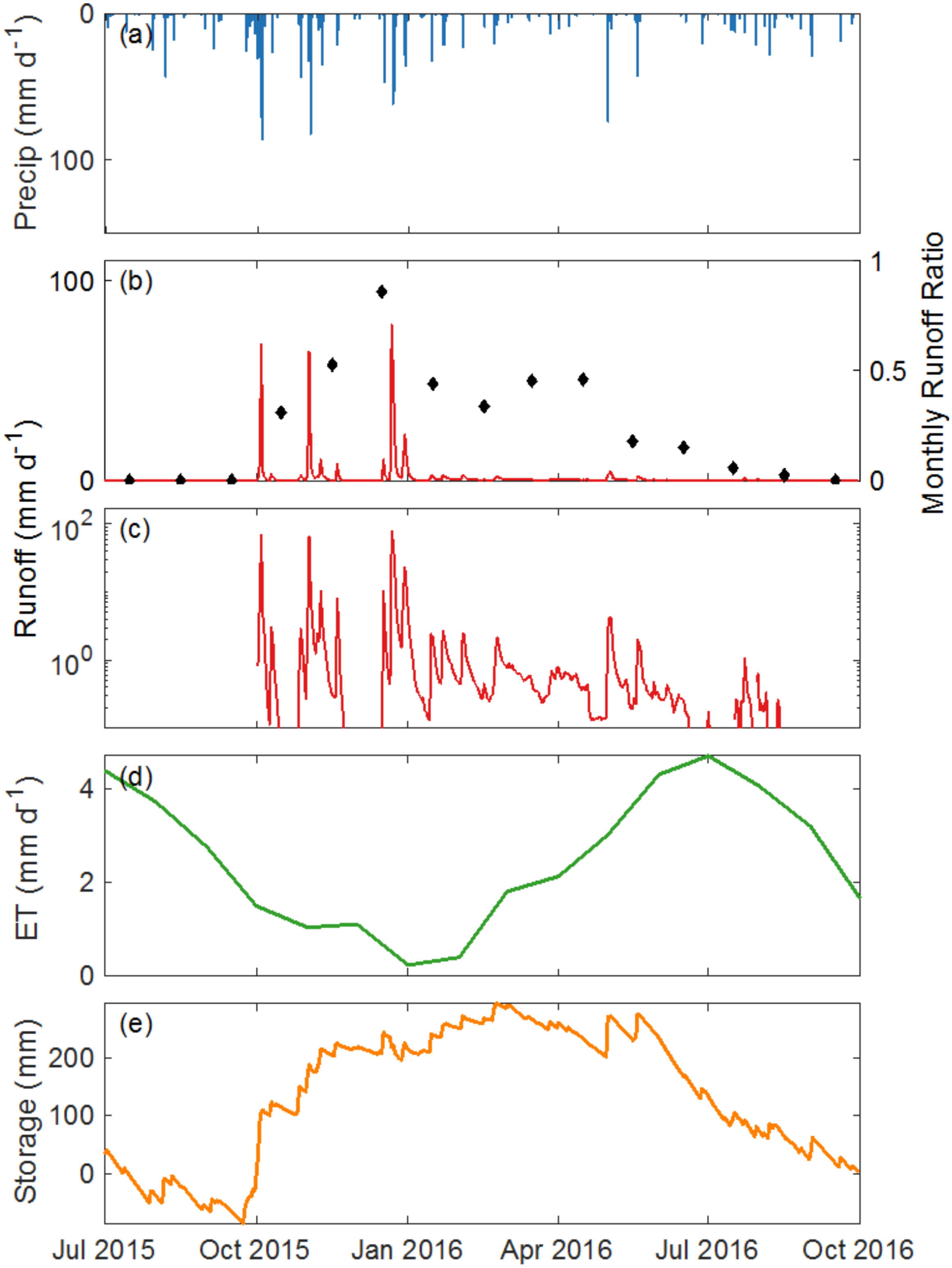

Precip (mm d^{-1})
(a)
0
100
(b)
100
0
1
0.5
0
Monthly Runoff Ratio
Runoff (mm d^{-1})
(c)
10^2
10^0
(d)
4
2
0
ET (mm d^{-1})
(e)
200
100
0
Storage (mm)
Jul 2015
Oct 2015
Jan 2016
Apr 2016
Jul 2016
Oct 2016

Figure 11: Water balance components for WS4 from water year 2016 and the three months preceding it. ET is estimated using a Thornthwaite approximation based on local temperature and is interpolated to daily from monthly. Storage is the cumulative sum of the daily residual of the other three components.

changed from 0 during the dry season to almost 0.9 in early winter (Figure 11). Storage calculated as a cumulative sum of the water balance residual exhibited primarily a seasonal wet up and dry down, with steeper increases in the fall corresponding to shorter, higher-magnitude precipitation inputs and slower decreases in the spring through summer corresponding to persistent, lower-magnitude baseflow runoff and evapotranspiration losses. Minimum storage was observed following the 2015 late summer dry down and was followed by an increase of 380 mm to its peak in March 2016; a range of 27% of annual precipitation and 69% of annual runoff. With the exception of a relatively low-magnitude runoff event in August 2016, runoff was confined to the period when storage exceeded 100 mm, roughly October 2015 – July 2016 (Figure 11).

3.3.2 Deep groundwater

The deep groundwater well (DW), located on a low-gradient interfluve within 3 km of WS4 (Figure 10), was judged to be representative of regional scale groundwater changes and was compared to integrated watershed storage calculated from the water balance to determine the extent to which the two exhibited similar dynamics (Figure 12). Annual ranges of the two were 4000 mm and 380 mm, respectively, with the order of magnitude difference between the two reflecting the porosity and unsaturated moisture content of the deep well's location. We found general correspondence between the two, with peaks occurring in late winter/early spring and lows in early fall. The relationship between the two was monotonic, positive, and significant (Spearman's ρ = 0.92, p << 0.05).

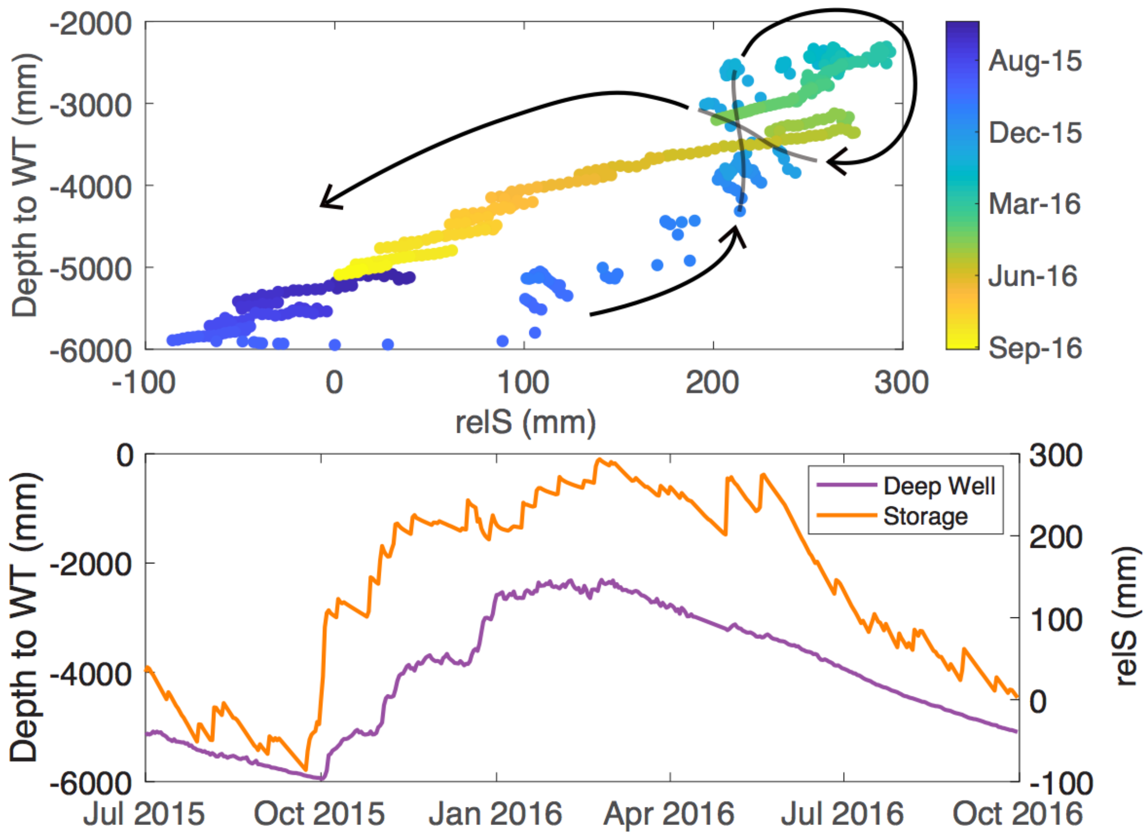

Figure 12: Storage and water table depth; (a) Cumulative storage calculated via water balance and water table in deep groundwater well over the study period. (b) Relationship between storage and water table depth with color depicting time. Arrows indicate general direction of hysteresis between the two.

However, we also observed bi-directional hysteresis between the two when their relationship was considered over time (Figure 12): counter-clockwise over lower storage and water table values and clockwise over higher storage and water table values. From their respective lows, increasing storage preceded increasing deep water table by approximately two weeks, an increase over the month of October that represented nearly one half of its total seasonal increase, compared to only about one fifth of the seasonal increase in the deep water table (Figure 12). However, in late December when both were near their peaks, an increase in deep water table was not coupled with an increase in storage. While both storage and deep water table were declining (March-October 2016) the correlation between the two strengthened (Spearman's ρ = 0.95), compared to wet up from October 2015-February 2016 (ρ = 0.86).

Correspondence between runoff and both deep water table level and storage was relatively poor (Figure 13). We observed runoff of comparable magnitude occurring across the entire 4 m range of the deep well measured water table over the study period, with no clear relationship between the two. There was a similar lack of relationship between storage and runoff with comparable runoff events observed across a ~200 mm range in storage; however, unlike the relationship with the deep water table, we did observe a clear storage threshold which delineated conditions favorable to runoff generation between October, 2015 and June, 2016 (Figures 11, 13). The lack of clearer runoff correspondence with either the deep well measured water table or storage, as well as hysteresis between the latter two, point strongly toward the value of measuring heterogeneous subsurface hydrology within WS4.

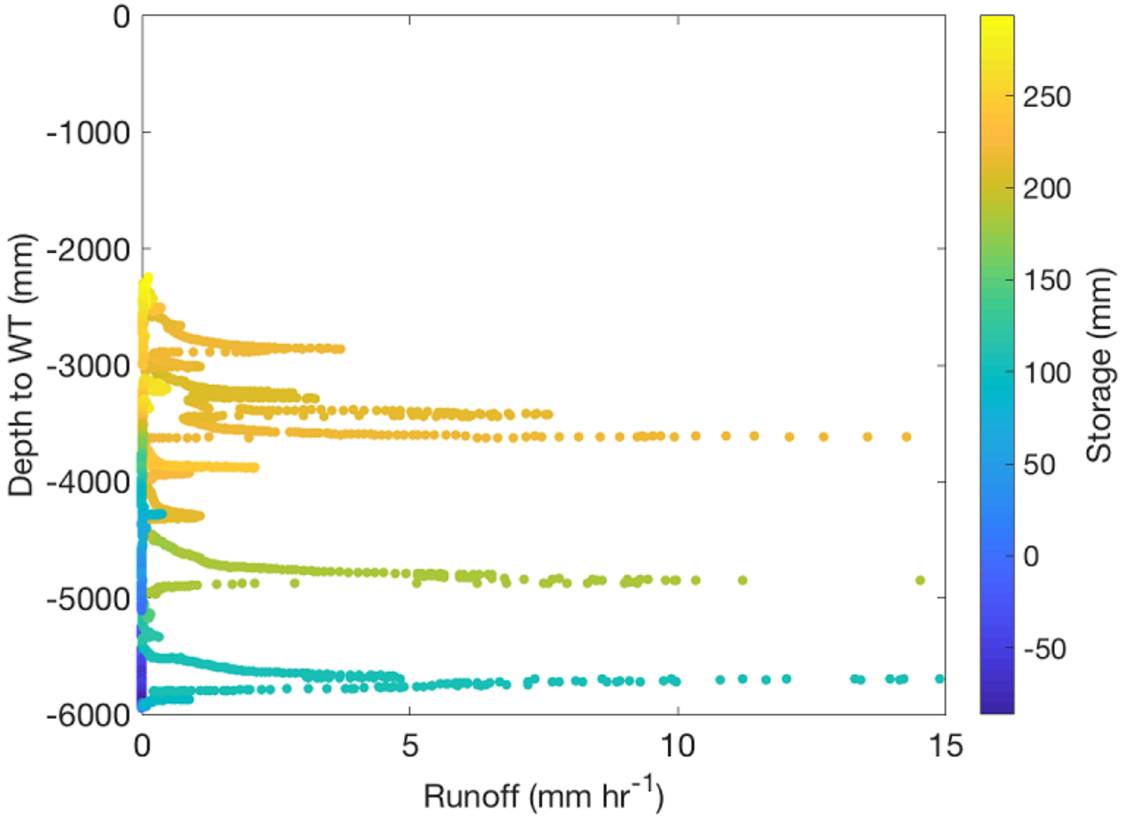

Figure 13: Relationship between depth to water table in deep groundwater well and runoff, color-weighted by cumulative storage calculated from water balance.

3.3.3 WS4 subsurface and terrain structure

We chose locations and depths for sensor installation in WS4 based on likely watershed structural influences on internal water storage heterogeneity. Potential structural influences were judged to be either pedologic (i.e., vertical position relative to soil strata displaying distinct hydraulic properties) or topographic (i.e., hillslope position and convergence). To that end we measured saturated hydraulic conductivity (Ksat) across a wide range of hillslopes within the larger CCZO and used these measurements in conjunction with soil profile observations, and topographic analysis of WS4 to distribute water table and soil moisture sensors within WS4.

Ksat was measured along five separate transects, each comprising a ridge, midslope, and toeslope vertical profile (Figures 10,14). The first three depths in each pit were approximately 15, 45, and 90 cm, chosen to characterize Ksat above, within, and below the clay-rich Bt horizon, and further depths ranged down to 370 cm if deeper hand-auguring was feasible. We found that Ksat decreased by 2-3 orders of magnitude between 15 and 45 cm. Moving down through the soil profile, Ksat generally remained within the same order of magnitude as at 45 cm. In approximately half of the soil profiles values increased by up to an order of magnitude below 100 cm (Figure 14). Although we observed ranges across orders of magnitude in the shallowest and deepest depths in these profiles, the general shape is consistent with a clay-rich Bt horizon typical of the prevalent Ultisols in the region, and therefore vertical distribution of hydrologic measurements in WS4 was delineated as above, within, and below the Bt horizon.

Based on observed Ksat, topography, and a general understanding of hydraulic characteristics of soils in the CCZO (e.g., Calabrese et al., 2018), we distributed shallow groundwater wells and soil moisture sensors across three gradients: above and below the Bt horizon, from ridge to toeslope, and on hillslopes that differ in terms of convergence (Figure 15) by auguring boreholes and digging soil pits.

We found that higher clay contents were encountered at fairly consistent depths from 40-70 cm (51 cm mean across all 23 boreholes and 3 soil pits). Refusal depth, meaning the depth where hand-auguring failed, varied widely, from almost 9 m at the very upper watershed divide to less than 2 m in some wells adjacent to the stream channel (3.5 m mean). Depth to refusal increased moving away from the stream, and depth to the clay-rich horizon increased moving towards the stream, although the latter was less consistent (Figure 15). Contributing area at each well site increased moving downslope along each transect by an order of magnitude. Transect 1 had the highest mean/maximum contributing area at 251/390 m^2 while transect 2 had the lowest at 110/136 m^2 (Table 2).

3.3.4 Soil moisture and shallow groundwater connections to runoff dynamics

Both soil moisture and groundwater dynamics were primarily responsive to seasonal wet and dry conditions, stochastic precipitation inputs, or some combination of each. Relationships between measurements of subsurface hydrology and runoff exhibited stronger threshold-behavior along gradients towards lower hillslope position, higher hillslope convergence, and greater depth.

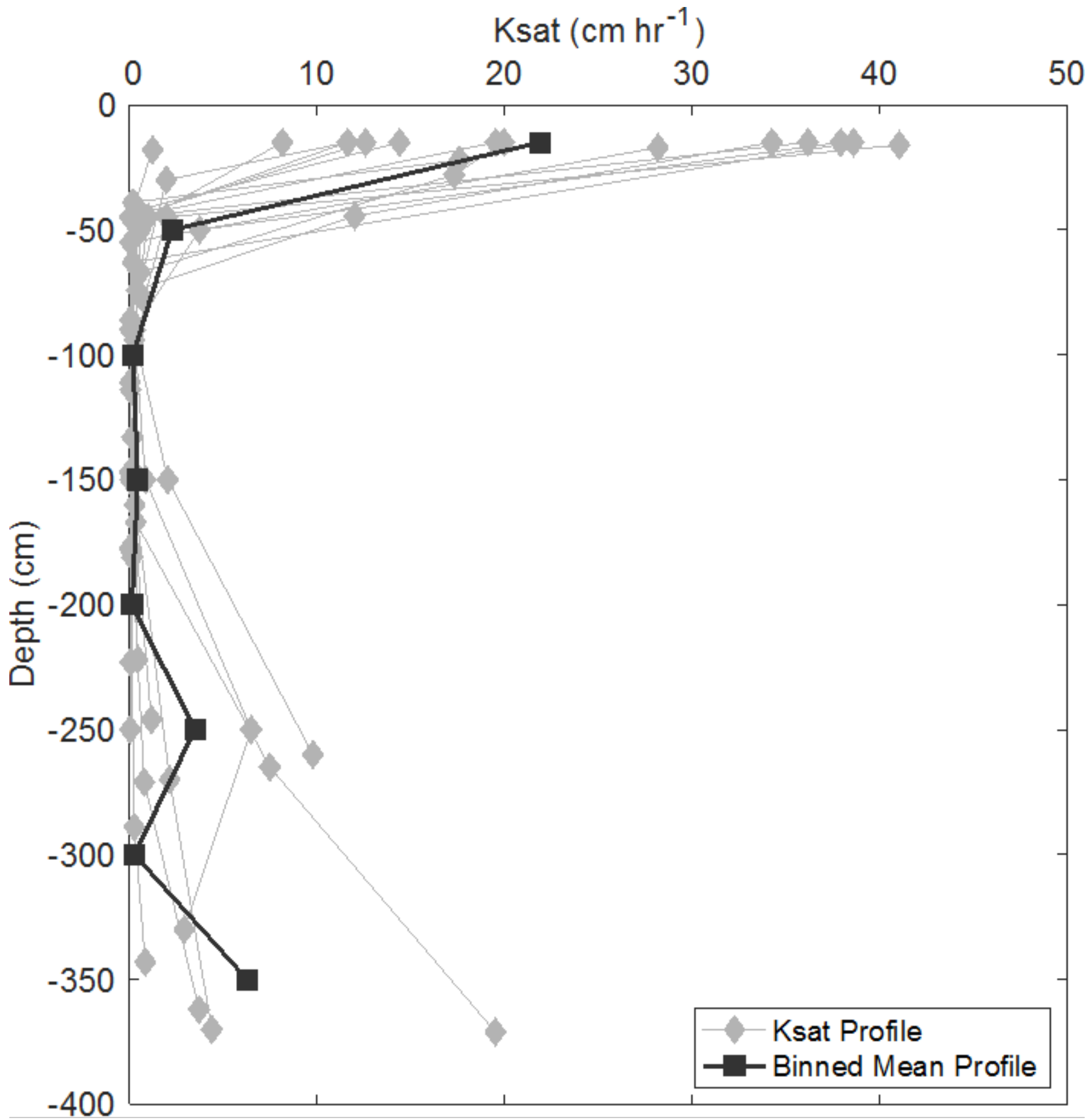

Figure 14: Depth profiles of saturated hydraulic conductivity (Ksat). Light grey profiles are each individual profile (15 total across five hillslope transects), while dark line is binned mean values.

3.3.4.1 Soil Moisture

Soil moisture at all hillslope and vertical positions exhibited seasonal wetting up and drying down coincident with the regional growing season: a rapid increase in fall and a slow decrease from spring through early summer. This consistent seasonal response across all positions was overlain by event-scale response that decreased with both depth (15 -> 50 -> 100 cm) and lower hillslope position (ridge -> midslope -> toeslope).

Soil moisture across all depths and through the seasonal wet up and dry down varied from 0.05 to 0.45 VWC (volumetric water content). Soil moisture content exhibited higher total range in magnitude in the shallow and mid depths. While soil moisture in these depths changed by 0.3-0.4 over the study period, deep positions changed by only ~0.15. This distinction was due less to higher moisture content during the wet season, but rather to substantially drier conditions in shallower soils during the dry season. At its lowest, deeper soil remained at approximately 0.2 VWC, while mid and shallow soils decreased below 0.1-0.05 VWC. Drier minimum soil moisture in shallower positions, however, was coupled with clear increases in response to precipitation events, a phenomenon which only occurred in deeper soil horizons at the ridge location (Figure 16).

Precipitation event time scale response occurred in shallow wells across the hillslope and through the entire depth range on the ridge, although the shallow position in the toeslope exhibited noticeably attenuated event response during the wet season relative to the midslope and ridge landscape positions. In shallow positions, event response ranged from all of the measured change in soil moisture during the dry season, to 60-75% during wetting up/drying down in early fall/early summer, to <15% during the peak wetness from late fall through spring. Event response generally decreased moving deeper in the soil profile and in a downslope direction.

Distinctions between the differential landscape positions and depths lead to characteristic relationships between soil moisture and runoff. Soil moisture in deeper or lower hillslope positions exhibited more threshold-driven relationships where moisture content increased to a point before runoff response was observed and subsequently did not vary or varied little as runoff changed. In contrast, shallower or higher hillslope positions showed a more responsive relationship where soil moisture and runoff covaried over a broader range. A range of responsiveness was observed moving from shallow to deep at the ridge location, and across shallow depths down the hillslope, while moving down the hillslope we observed increasingly threshold-driven relationships (Figure 16).

3.3.4.2 Shallow groundwater

In contrast to soil moisture measurements, shallow groundwater wells measure the dynamics of saturated water tables across their screened depth. Because they only indicate zones of saturation, their measurements are discontinuous through the study period and generally coincident with the seasonal wet up and dry down pattern (Figure 11). We measured water table development almost exclusively during the dormant and early growing season (October 2015 through June 2016). During this period, we observed

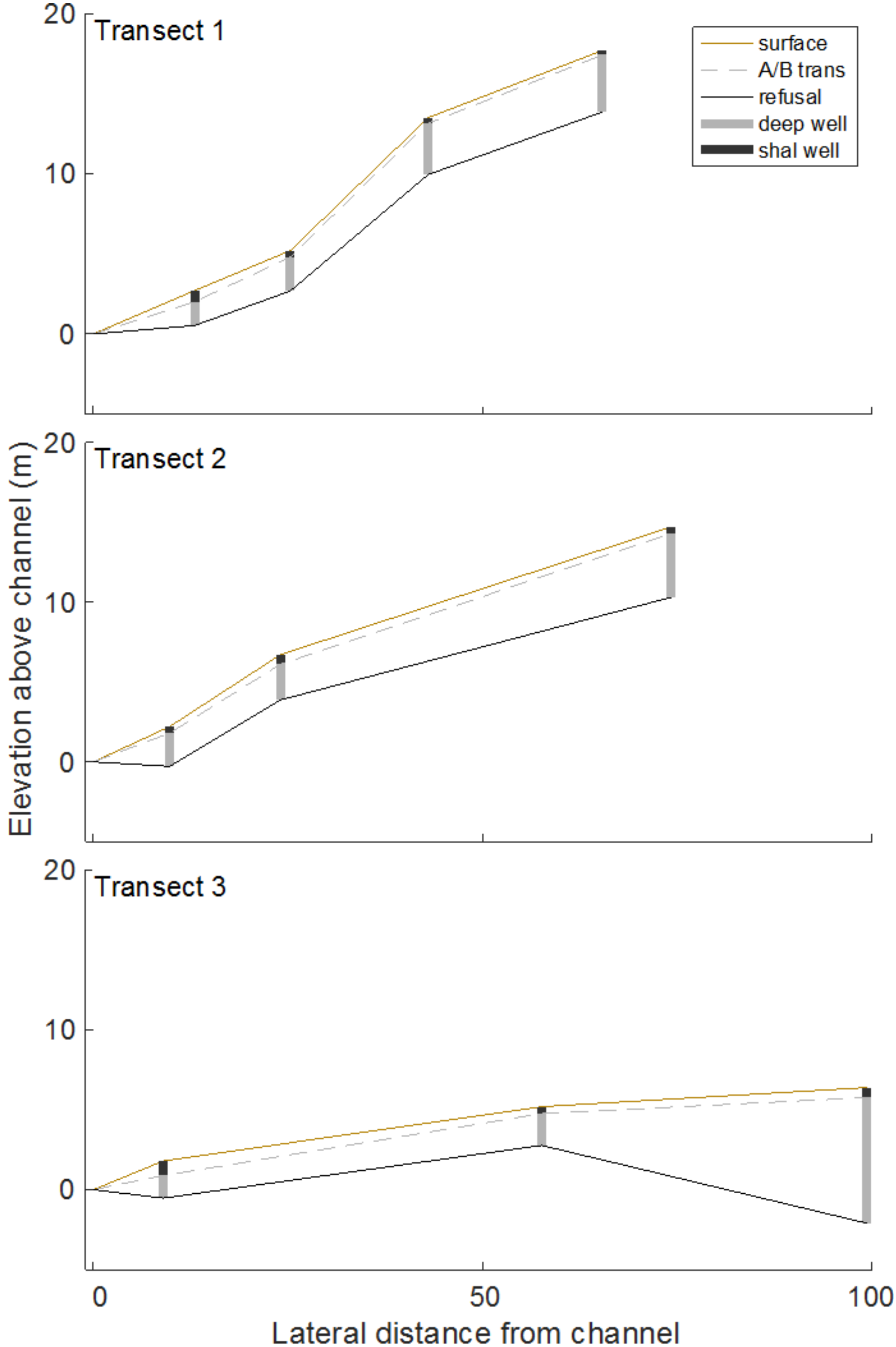

Transect 1
Transect 2
Transect 3
surface
A/B trans
refusal
deep well
shal well
Elevation above channel (m)
Lateral distance from channel
20
10
0
0
50
100

Figure 15: Lateral depth profiles of transects 1-3 in WS4. Vertical and horizontal scales are the same magnitude, with 0 in both directions set at the stream channel. Lateral lines indicate the ground surface (solid brown), the approximate A/B soil horizon transition (dashed, light grey), and refusal depth (solid, dark grey). Thicker, vertical lines indicate well nests. The dark grey portion is the screened interval for the wells designated "shallow" and the light grey for wells designated "deep."

water table development at all well depths and landscape positions that we instrumented. Distinct depths and positions differed in how continuous and variable their water tables were in similar ways to our observations of soil moisture, where deeper wells at lower hillslope positions on more convergent hillslopes exhibited more seasonally consistent water tables, and vice versa.

Shallow wells (completed above the B horizon) exhibited some level of water table for 16% of the study period, and 26% of the wet period (October 2015-June 2016). Deep wells exhibited a water table for 38% of the study period and 58% of the wet period. Perched shallow water tables (i.e., with no saturated zone measured between shallow and deep water tables) were common across all landscape positions, although in approximately one third of the well nest locations elevated deep water tables obscured our ability to distinguish between the two (Figures 17-19).

In general, shallow water tables rose and fell across their entire depth on the time scale of individual events, while deep wells did the same seasonally. This distinction between deep and shallow wells was further evident in their relationships with runoff, where deep wells exhibited more threshold-driven and shallow wells more responsive relationships with runoff (Figures 17-19). In this case, we describe these relationships as threshold driven when we observe an abrupt increase in runoff only after significant increases in water table elevation. In contrast, more responsive relationships exhibit concomitant changes in both runoff and water table elevation in response to precipitation. However, we observed multiple cases where this general classification did not hold. For example, the deep water table in the ridge position of transect 3 rose and fell through its entire depth range over the course of multiple storm events from the late winter to spring, drying completely between most storms (Figure 19). The water table measured in the shallow well in the lowest hillslope position of transect 1 similarly diverges from the broader classification: its water table persisted through the entire wet season (Figure 17).

Similarly, neither hillslope convergence nor position provided a single metric that facilitated the classification of measured water table responses into seasonal or event-scale. Rather, we observed that position along all three gradients formed a more complete picture of which positions exhibited primarily which response. For example, the midslope and toeslope water tables in transect 1 were seasonal (Figure 17), unlike wells at similar positions in transects 2 and 3 (Figures 18,19). However, when considering all three gradients (well depth, transect convergence, and hillslope position), we found that greater depth, convergence, or lower hillslope position all contribute to a stronger seasonal well response and relatively less reactivity to recent precipitation.

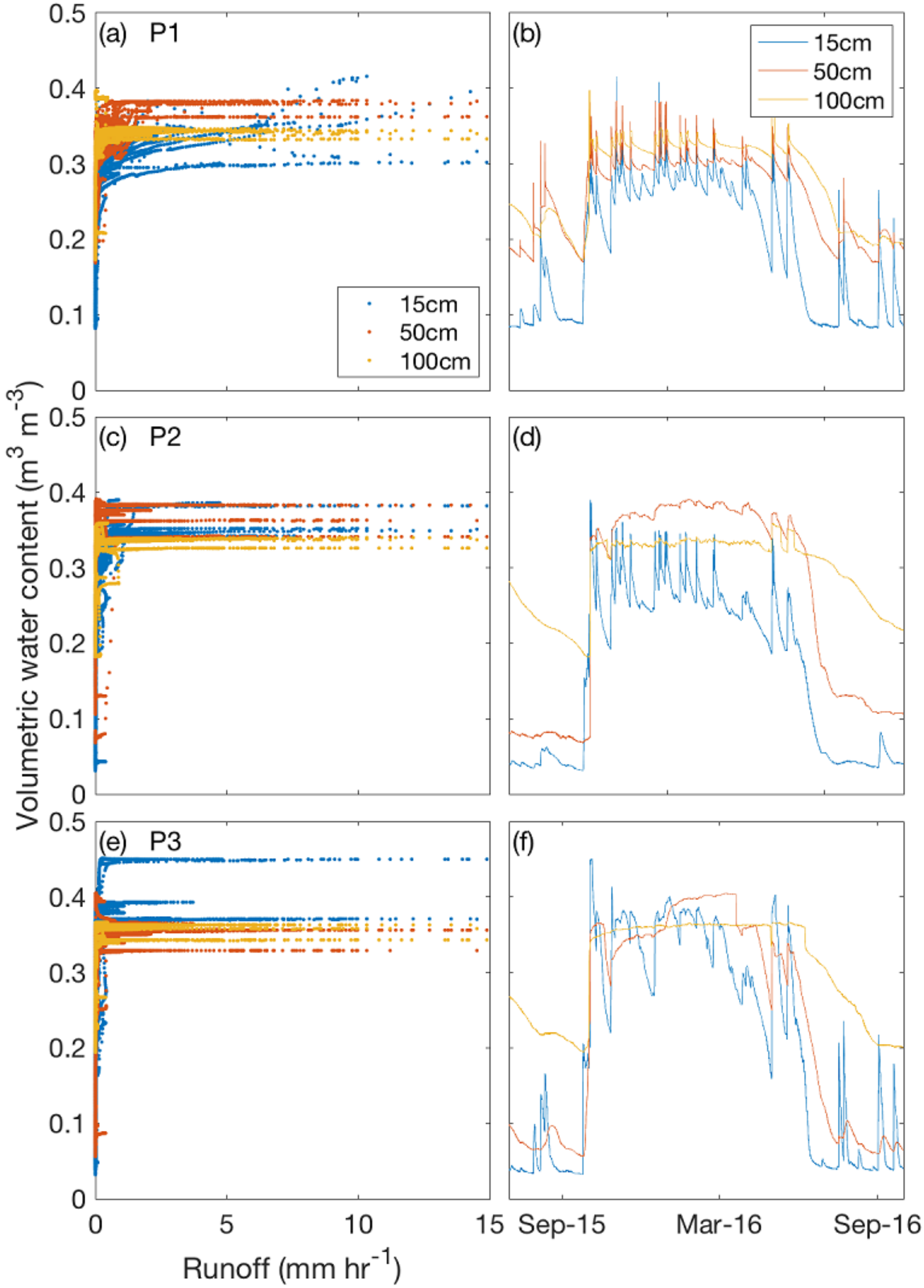
(a) P1
(b)
(c) P2
(d)
(e) P3
(f)
15cm
50cm
100cm
Volumetric water content (m^3 m^{-3})
Runoff (mm hr^{-1})
Sep-15
Mar-16
Sep-16
0
0.1
0.2
0.3
0.4
0.5
5
10
15

Figure 16: Hourly runoff and soil moisture; (a, c, e) Relationship between hourly runoff and soil moisture for each of three soil pits. (b, d, f) Time series of soil moisture sensors within each soil pit. P1, P2, and P3 are located at the ridge, midslope, and toeslope adjacent to well nest transect 1. Soil moisture was measured using TDR sensors, which integrate ~7.5 cm radius around installation depth. Each pit contained three sensors installed at 15, 50, and 100 cm above, within, and below the Bt horizon, respectively.

3.4 Discussion

3.4.1 Water tables and soil moisture display primarily either event- or seasonal-scale dynamics

3.4.1.1 Subsurface hydrologic dynamics correspond to longitudinal, lateral, and vertical watershed structural gradients, suggesting an underlying relationship with contributing volume.

The hydrogeomorphic relationship between increasing wetness and higher upslope area can be traced back at least forty to fifty years (e.g., Anderson & Burt, 1978; Beven & Kirkby, 1979; Dunne & Black, 1970; Freeze, 1972, and others). Contributing area combines longitudinal (distance upslope) and lateral (convergence of hillslope) gradients to provide a topographic proxy for the relative potential for concentration of water at a point in a watershed. It has remained an invaluable tool allowing hillslope and watershed hydrologists to draw connections between more easily quantified watershed topography and either sparsely measured or unmeasured subsurface hydrology. It's effectiveness in explaining internal watershed subsurface hydrology is maximized in mountainous watersheds where contributing area has a broad and heterogeneous distribution across a watershed and where soils are often relatively shallow and homogenous. In these cases, we implicitly describe contributing volume with an assumption of approximately uniform depth and contributing area becomes a singular, 2-D surrogate for subsurface hydrology occurring in three dimensions through the soil profile (Jencso et al., 2009; Rinderer et al., 2014, 2019). The CCZO and the Southern

Piedmont region do exhibit heterogeneous hillslope topography conducive to delineating differences in hillslopes (Figures 10,15); however, deeply weathered and stratified soils differentiate it from much of the mountain hydrology research over the last decades and motivated the addition of the depth dimension to our study (Figure 15). While in mountainous terrain around the world it is often sufficient to use contributing area as a surrogate for subsurface hydrology, our study emphasizes the importance of explicit observation of subsurface hydrology across a depth gradient in landscapes where that common simplifying assumption is invalid.

Based on 29 water level and soil moisture sensors distributed throughout WS4, we identified a broad range of primary subsurface hydrologic responses that varied between wetting up/drying down in response to precipitation events or seasonal changes in evapotranspiration (Figures 16-19). These sensors were distributed across the watershed with the goal of capturing the range of gradients in soil structure (Figures 14,15), hillslope position, and topographic convergence (Figure 14). Although each of these gradients did generally relate to differences in hydrologic response, we did not identify any that could serve as a singular metric that fully captured heterogeneity in hydrologic response. However, despite challenges in quantifying the combinations of each gradient

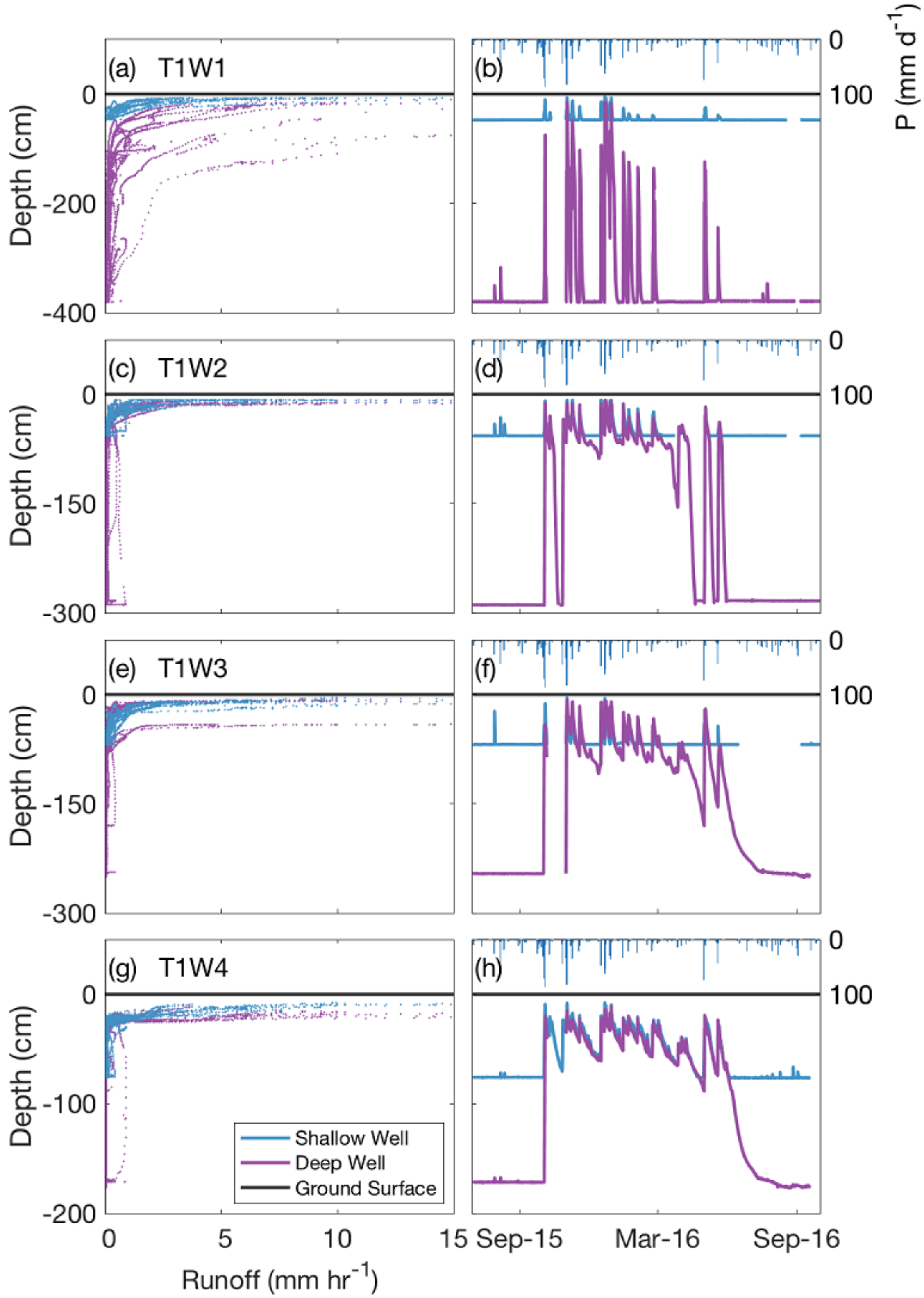

(a) T1W1
(b)
(c) T1W2
(d)
(e) T1W3
(f)
(g) T1W4
(h)
Depth (cm)
0
-200
-400
-150
-300
-100
-200
P (mm d^{-1})
0
100
Shallow Well
Deep Well
Ground Surface
0
5
10
15
Sep-15
Mar-16
Sep-16
Runoff (mm hr^{-1})

Figure 17: Hourly runoff and shallow/deep water table along transect 1; (a, c, e, g) Relationship between hourly runoff and shallow/deep water table for each of four well nests along transect 1. W1, W2, W3, W4 are located at the ridge, midslope, toeslope, and riparian hillslope positions. (b, d, f, h) Time series of these same well nests. Horizontal blue/purple lines represent completion depth of shallow/deep wells.

that related to hydrologic response, it became clear that each exerted some fractional influence on hydrologic response, and their combination better explained our observations. We found that measurements taken deeper in the soil column, lower on the hillslope, and along transects with more convergent terrain tended to exhibit primarily seasonal hydrologic response while their opposing locations, shallow, planar, and upslope exhibited more event driven response. The latter two gradients more generally describe lateral and longitudinal redistribution of water, and in combination represent the contributing area of a location. With respect to volume of water present at a location in a watershed, a higher contributing area would generally mean that 1) more water flows through that location than others and 2) the hydrologic response that location would be more attenuated as water from a wider range of distances flows through it. Both of these points are true to an even greater extent with the incorporation of depth. We propose that the incorporation of subsurface hydrologic measurements across vertical as well as lateral and longitudinal gradients provides an enhanced means of generally characterizing the underlying gradient being indirectly measured: contributing volume.

Of each gradient that we distributed our sensor network across, changes in depth generally led to the most substantial changes in seasonal- vs. event- response (Figures 16-19): the most clearly distinguishable classification amongst the 20 wells and 9 soil moisture sensors were between shallow and deeper. Shallow water table and soil moisture was almost entirely event-associated, and most seasonally-associated measurements were deep. Although there are multiple possible explanations for this observation, including differences in soil hydraulic properties with depth (Figure 14), we believe the simplest explanation is geometric. As the size of hillslopes increases to 100s of m^2 (Tables 2,3), relatively small changes in depth correspond to larger changes in contributing volume, and therefore a clearer transition between event- and seasonally-associated response. Further, this higher marginal change of contributing volume with changes in depth readily explains why deep ridge wells are primarily event-driven despite being deeper than any other hillslope positions: their greater depth is counterbalanced by contributing areas an order of magnitude lower than other hillslope positions (Tables 2,3, Figures 17b,18b,19b).

Incorporating measurement depth, hillslope position, and hillslope convergence (i.e., vertical, longitudinal, and lateral gradients respectively) facilitated a more complete understanding of the distinct dynamics of subsurface hydrology across WS4. This combination of three watershed structural gradients is necessarily qualitative because we lack continuous measurements of the lower boundary depth beyond our well-completion depths to accurately calculate an approximate contributing volume for each point, and furthermore it must be seen as a conservative proxy for contributing volume due to unmeasured groundwater dynamics occurring below refusal depth that likely have some influence on downslope measurements. However, we believe there remains substantial opportunity in this region and specifically the CCZO to advance our robust understanding of subsurface hydrology as it relates to watershed topography by incorporating 3-D soil structure and the concept of contributing volume. Further study could build on and feed back to regionally-relevant research on formation of soil stratigraphy as a function of moisture states (Calabrese et al., 2018), connections between geomorphology and pedology (Richter et al., 2019), and hillslope hydrology studies in lower-gradient Southern Piedmont watersheds (Zimmer & McGlynn, 2017b, 2018). We believe that drawing connections between these disparate fields and field sites are crucial to generalizing the work herein to deeply-weathered landscapes more broadly and in doing so contribute to watershed hydrology understanding more globally.

3.4.1.2 Individual water table and soil moisture locations generally correspond to either runoff or storage.

Subsurface hydrology measured during this study varied primarily either on event- or seasonal-scales in relation to its landscape position and depth. Additionally these distinct event- and seasonal-scale dynamics can be related to measured watershed runoff and integrated watershed storage. Because measured runoff and calculated

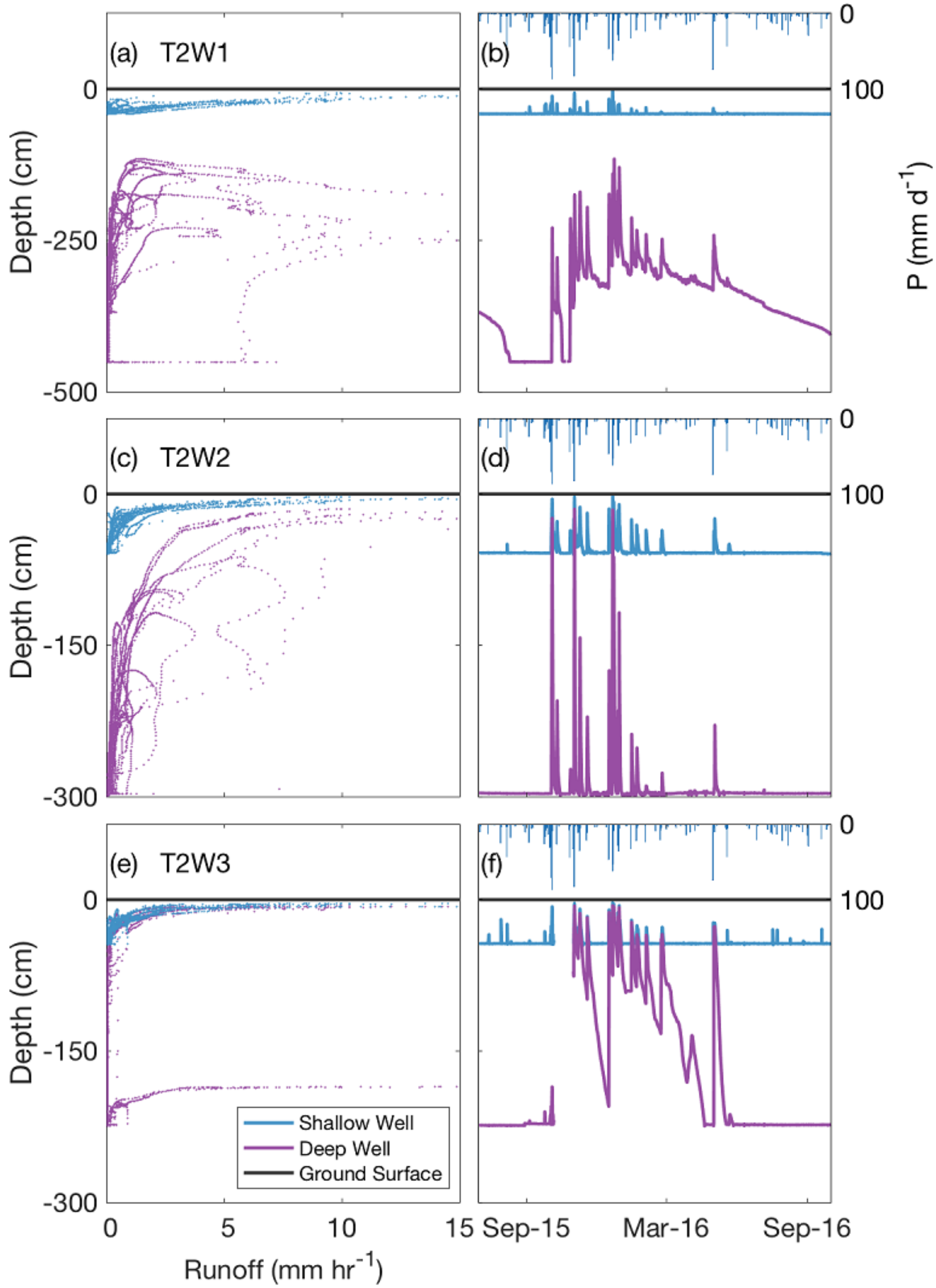

(a) T2W1
(b)
(c) T2W2
(d)
(e) T2W3
(f)
Depth (cm)
0
-250
-500
0
-150
-300
P (mm d^{-1})
100
Shallow Well
Deep Well
Ground Surface
0
5
10
15
Runoff (mm hr^{-1})
Sep-15
Mar-16
Sep-16

Figure 18: Hourly runoff and shallow/deep water table along transect 2; (a, c, e) Relationship between hourly runoff and shallow/deep water table for each of four well nests along transect 2. W1, W2, W3 are located at the ridge, midslope, and toeslope hillslope positions. (b, d, f) Time series of these same well nests. Horizontal blue/purple lines represent completion depth of shallow/deep wells.

storage exhibit a similar dichotomy, we can draw stronger connections between specific measured hydrologic pools and either runoff or storage (Figures 20,21).

Integrated watershed storage was better represented by locations with higher contributing volume. In addition to the correspondence between groundwater measured in the deep groundwater well (Figure 12), we observed that many WS4 wells, including deeper depths located lowest on the hillslope in all three transects and midslope deep wells in the more convergent transect 1, also exhibited strong overlap in timing and relative magnitude of wet up and dry down (Figure 21). These relationships suggest which pools comprise and reflect integrated watershed storage, and additionally highlight the limitations of considering only one location or type of measurement in watershed studies attempting to understand runoff in terms of internal watershed dynamics.

We determined, based on comparison of their time series, that integrated watershed storage corresponded most strongly but in order of decreasing strength, to the DW, deeper soil moisture, shallow soil moisture, and the deep wells in our well nests, approximately in that order (Figure 21). We observed rapidly increasing values of water table elevations and soil moisture prior to runoff beginning in fall 2015, followed by persistence through the wet season, and then more gradual dry down through early summer (Figure 21). More than half of the total range of these storage-related sites occurred during seasonal wet up and dry down, and similar to storage (Figure 13), each of these pools displayed a more threshold-driven relationship with runoff (Figures 16-19). Although the deep groundwater site represents the strongest single correlation to storage (Spearman's ρ = 0.93, p << 0), counterclockwise hysteresis between the two at low values indicates rapidly wetting components of watershed storage not reflected in deep groundwater, while clockwise hysteresis at higher values suggest hydrologic dynamics poorly captured by integrated watershed storage (Figure 12). While the former suggests the rapid increase in soil moisture observed at wet up (Figure 16), the latter suggest short-duration storage that mostly bypasses longer-term storage as it rapidly drains to runoff, therefore being poorly captured by watershed storage integrated at daily or longer time steps (Figure 11). As evidenced by the deep groundwater well, none of the sites we identify as more storage-linked could serve as a singular proxy for storage, but rather it represents a dynamic combination of measured and unmeasured locations and depths.

In contrast, lower contributing volume sites (generally shallower wells or deeper wells on planar hillslopes, or higher up the hillslope) wet up almost entirely in response to immediate precipitation and in conjunction with runoff peaks, followed by a rapid, complete dry down unless interrupted by a subsequent precipitation event (e.g., Figure 17b). Although wetting of these sites does represent an increase in storage and can be observed in integrated watershed storage, their dynamics are far less evident and

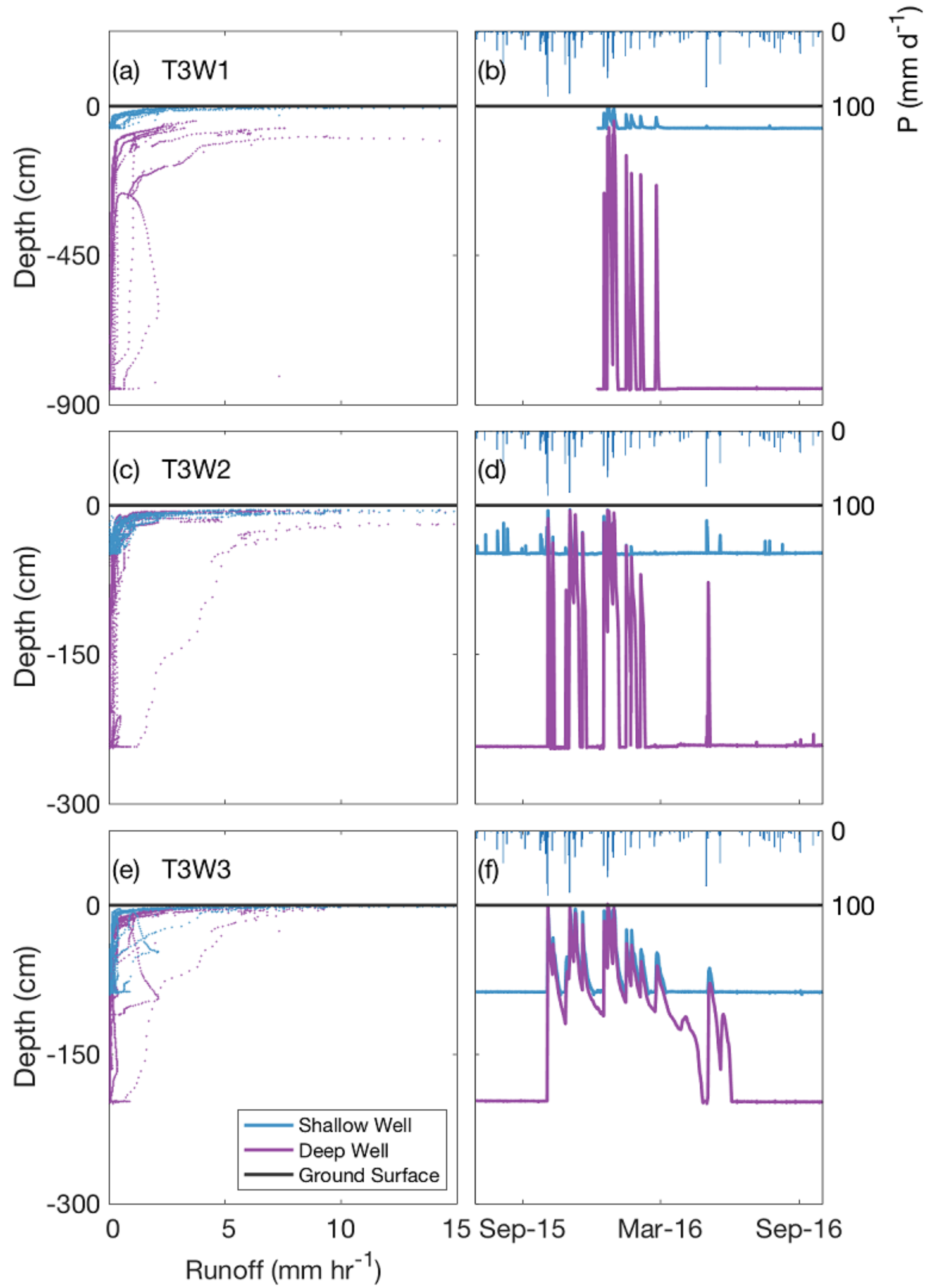

(a) T3W1
(b)
(c) T3W2
(d)
(e) T3W3
(f)
Depth (cm)
0
-450
-900
-150
-300
P (mm d-1)
0
100
Shallow Well
Deep Well
Ground Surface
0
5
10
15
Sep-15
Mar-16
Sep-16
Runoff (mm hr-1)

Figure 19: Hourly runoff and shallow/deep water table along transect 3; (a, c, e) Relationship between hourly runoff and shallow/deep water table for each of four well nests along transect 3. W1, W2, W3 are located at the ridge, midslope, and toeslope hillslope positions. (b, d, f) Time series of these same well nests. Horizontal blue/purple lines represent completion depth of shallow/deep wells.

represent a smaller component of its change through the year. This minimal response in integrated watershed storage to increases in water level at sites with lower contributing volume can be understood by considering the magnitude of increases in storage at event time scales. After the initial wet-up period in 2015 (late September-early October) through the start of the growing season in March, 12 discrete increases in storage that occurred over 1-3 days can be observed (Figure 12). These increases averaged 42 mm with none less than 10 mm or greater than 100 mm. In terms of the shallow soil horizon with an average porosity of 0.4, that 42 mm rise in storage would be ~10 cm, only capturing about one quarter of the event-scale rise of most of the shallow wells. This lack of correspondence between these lower contributing volume sites and storage emphasizes their primary linkage to runoff: when these sites increase they initiate fluxes so effectively that their dynamics are hardly observed in integrated storage.

3.4.1.3 An evolving understanding of storage heterogeneity and runoff generation with deeply-weathered, vertically-stratified landscapes

Our extensive subsurface hydrologic sensor network revealed spatially distinct dynamics that related to three-dimensional landscape gradients (Figures 12, 16-19). Further, we observed that hydrologic dynamics corresponded more strongly to either integrated watershed storage (Figures 11e,21) or measured runoff (Figures 11b,20), allowing us to classify measurement positions into storage-associated or runoff-associated and connect those linkages to landscape position (Figure 14). More storage-linked positions represented a larger contributing volume (i.e., combination of hillslope position, hillslope convergence, and depth) and vice versa. From this dichotomy in subsurface hydrologic dynamics and their relationships to watershed-scale hydrology we developed a conceptual model (Figure 22) in which seasonal wetting up of storage-linked positions creates threshold conditions for runoff while subsequent, event-driven wetting up of runoff-linked positions drive larger fluxes through the watershed into the stream.

Beginning in early fall, storage is at a minimum, there is no runoff, and the water table is below measured depth, and likely even below the level of the dry streambed (Figure 22a). With high-magnitude precipitation arriving in late September followed by Hurricane Joaquin in early October, storage began to increase rapidly without runoff response (Figure 22b), corresponding to measured soil moisture increases across all depths and hillslope positions (Figure 16) followed by the deeper water table rising to saturate positions lower on the hillslope (Figure 22b). Once these threshold conditions were reached, runoff was initiated as both shallow, perched flowpaths were activated higher on the hillslope and the deeper water table rose to intersect with the more transmissive, shallow soil horizons lower on the hillslope (Figure 22c). Following drying of runoff-linked positions the water table returned to the state (Figure 22b) that preceded runoff generation. This conceptual model (Figure 21) describes the dynamic hillslope hydrology of a generalized hillslope and how it varies along its length and through its depth. A watershed, then, is composed of this general hillslope response that is then weighted by the convergence of each individual hillslope, resulting in an accumulation of hillslope responses whose range is generally reflected in differences between transects 1 and 2, for example (Figures 17,18).

This conceptual model ties threshold-mediation of runoff generation (Dralle et al., 2018; Jencso et al., 2009; McGlynn et al., 2004; Penna et al., 2011; Sayama et al., 2011; Tromp-van Meerveld & McDonnell, 2006), to runoff generation by transmissivity feedback (K. H. Bishop, 1991; Kendall et al., 1999) and perched interflow at the transition to lower-conductivity soil horizons (Elsenbeer, 2001; S. Godsey et al., 2004; Zimmer & McGlynn, 2017b). Similar to Zimmer & McGlynn (2017) in the Duke Forest site of the North Carolina Piedmont, we observed and extended the concept of hillslope-stream connectivity beyond the higher gradient, shallow soiled landscapes in which it was initially identified (e.g., Jencso et al., 2009; McGlynn & McDonnell, 2003). Intriguing differences between Duke Forest and the CCZO point to the importance of broader research in this and similar regions around the world and highlight the hydrologic, geomorphic, geologic, and pedologic differences between these extensive regions and those that have received the most research attention to date. Despite the differences

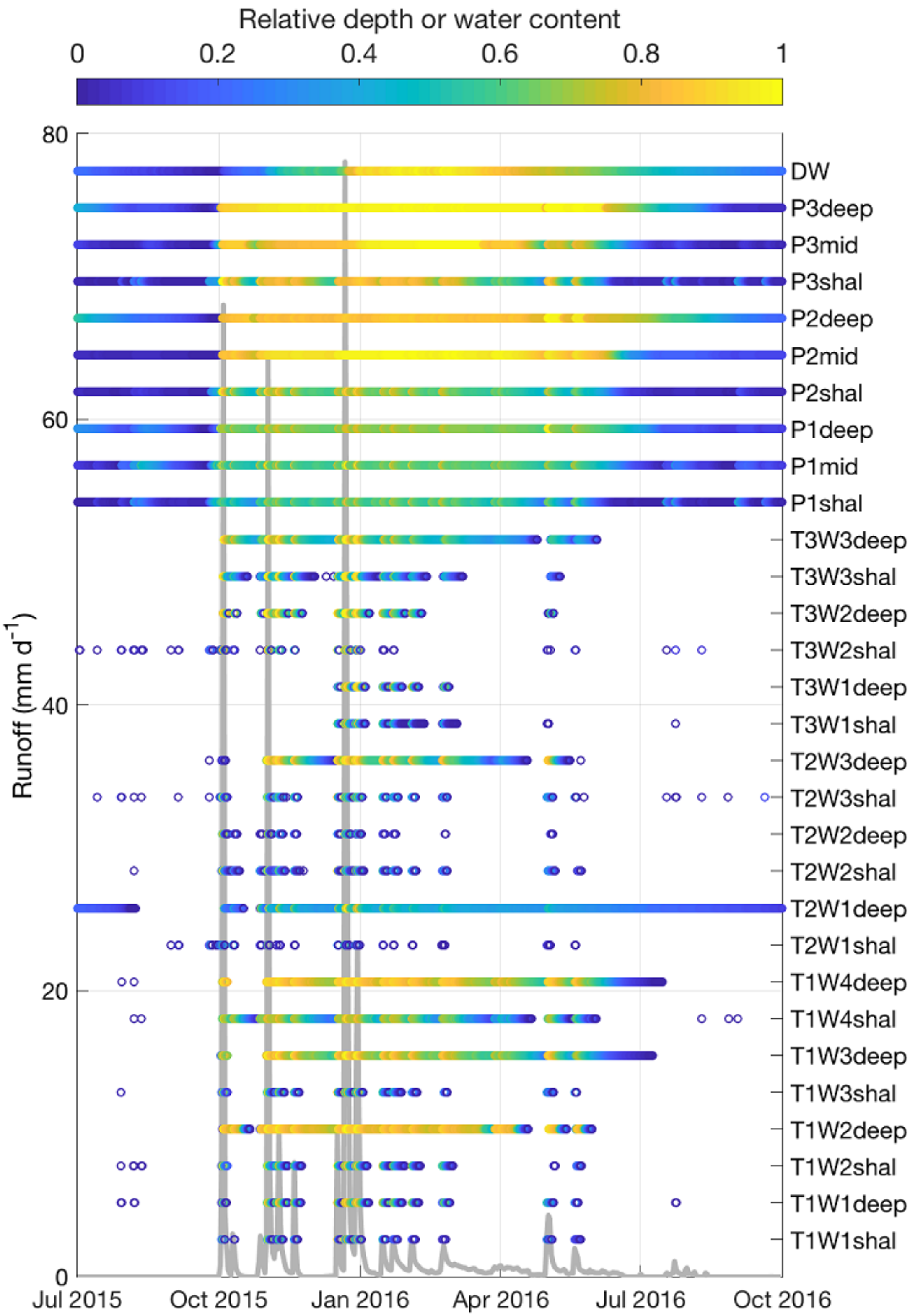
Relative depth or water content
0
0.2
0.4
0.6
0.8
1
Runoff (mm d^{-1})
80
60
40
20
0
DW
P3deep
P3mid
P3shal
P2deep
P2mid
P2shal
P1deep
P1mid
P1shal
T3W3deep
T3W3shal
T3W2deep
T3W2shal
T3W1deep
T3W1shal
T2W3deep
T2W3shal
T2W2deep
T2W2shal
T2W1deep
T2W1shal
T1W4deep
T1W4shal
T1W3deep
T1W3shal
T1W2deep
T1W2shal
T1W1deep
T1W1shal
Jul 2015
Oct 2015
Jan 2016
Apr 2016
Jul 2016
Oct 2016

Figure 20: Continuity of each subsurface hydrologic measurement through the study period weighted by its relative value. No point indicates a dry well; note that soil moisture and deep groundwater well (DW) do not fully dry. Light grey background is daily runoff for WS4. Refer to Tables 2,3 for site naming schemes.

between the Duke Forest and CCZO Piedmont sites, however, the importance of hydrologic connectivity that extends laterally and longitudinally into hillslopes and vertically through soil strata is emphasized. Although the language of hydrologic connectivity has been used to describe multiple concepts that span temporal and spatial scales (Covino, 2017), here we refer to the definition advanced by Jencso et al. (2009) and others which simply describes watershed components as connected if they have a continuous water table that extends to the stream. This definition is useful due to its simplicity: it is readily confirmed empirically, and does not require assumptions about particle velocities through soil horizons characterized by heterogeneous flowpaths and preferential flow (Sidle et al., 2001). Recent work (Klaus & Jackson, 2018) has questioned this characterization based on a definition of hydrologic connectivity rooted in particle transport (Bracken & Croke, 2007) and presents the mathematical likelihood that most water entering the stream via interflow is from relatively lower on the hillslope; indeed, the predominance of riparian water in streamwater (e.g., K. Bishop et al., 2004; McGlynn et al., 2004) as opposed to hillslope contributions is well-recognized. However, streamflow being composed primarily of water from proximal watershed locations excludes neither the hydraulic effects of continuous saturation extending above near-stream locations into hillslopes nor the rapid transport of hillslope water through

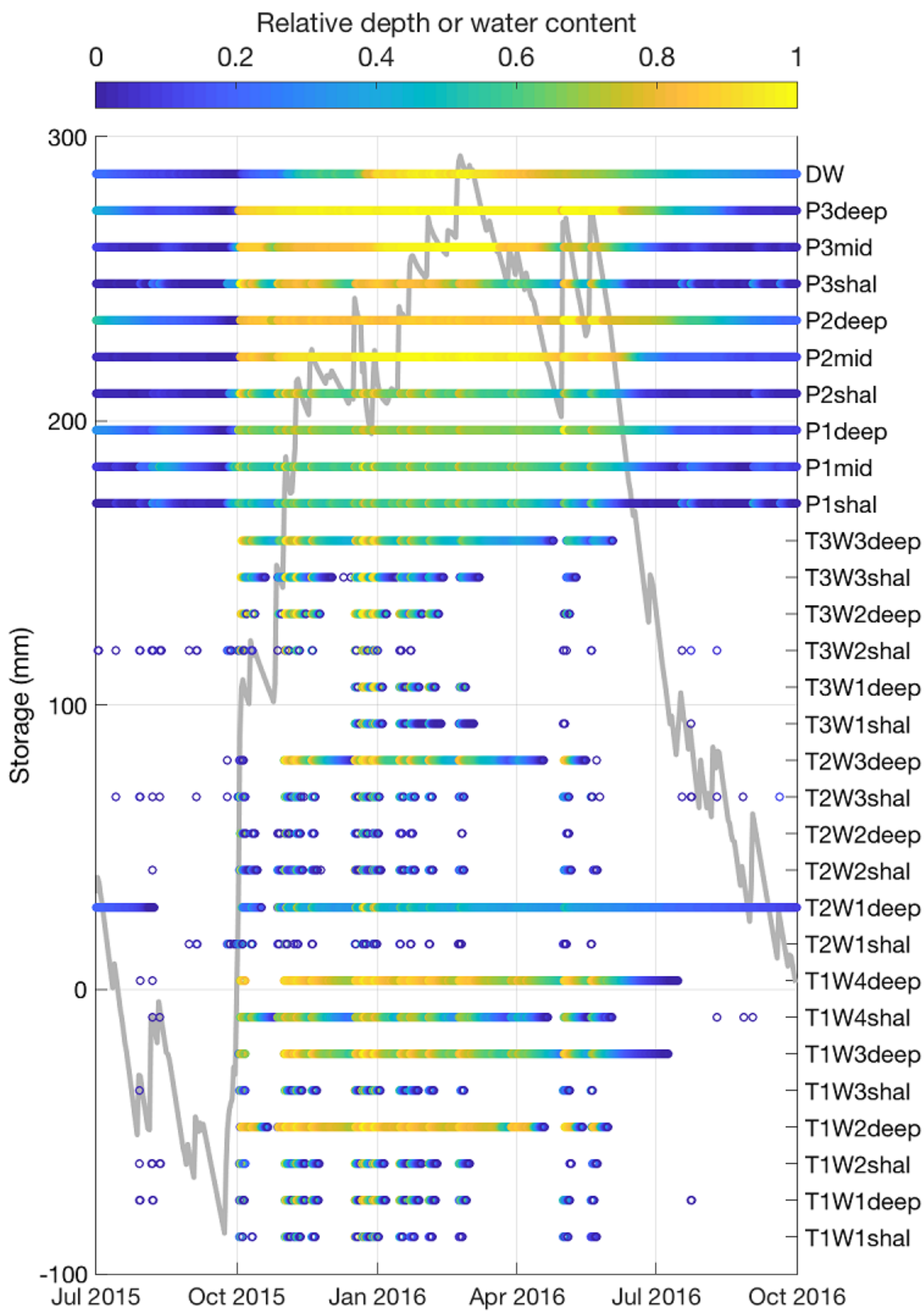

Relative depth or water content
0
0.2
0.4
0.6
0.8
1
Storage (mm)
300
200
100
0
-100
Jul 2015
Oct 2015
Jan 2016
Apr 2016
Jul 2016
Oct 2016
DW
P3deep
P3mid
P3shal
P2deep
P2mid
P2shal
P1deep
P1mid
P1shal
T3W3deep
T3W3shal
T3W2deep
T3W2shal
T3W1deep
T3W1shal
T2W3deep
T2W3shal
T2W2deep
T2W2shal
T2W1deep
T2W1shal
T1W4deep
T1W4shal
T1W3deep
T1W3shal
T1W2deep
T1W2shal
T1W1deep
T1W1shal

Figure 21: Continuity of each subsurface hydrologic measurement through the study period weighted by its relative value. No point indicates a dry well; note that soil moisture and deep groundwater well (DW) do not fully dry. Light grey background is cumulative storage for WS4 calculated via the water balance. Refer to Tables 2,3 for site naming schemes.

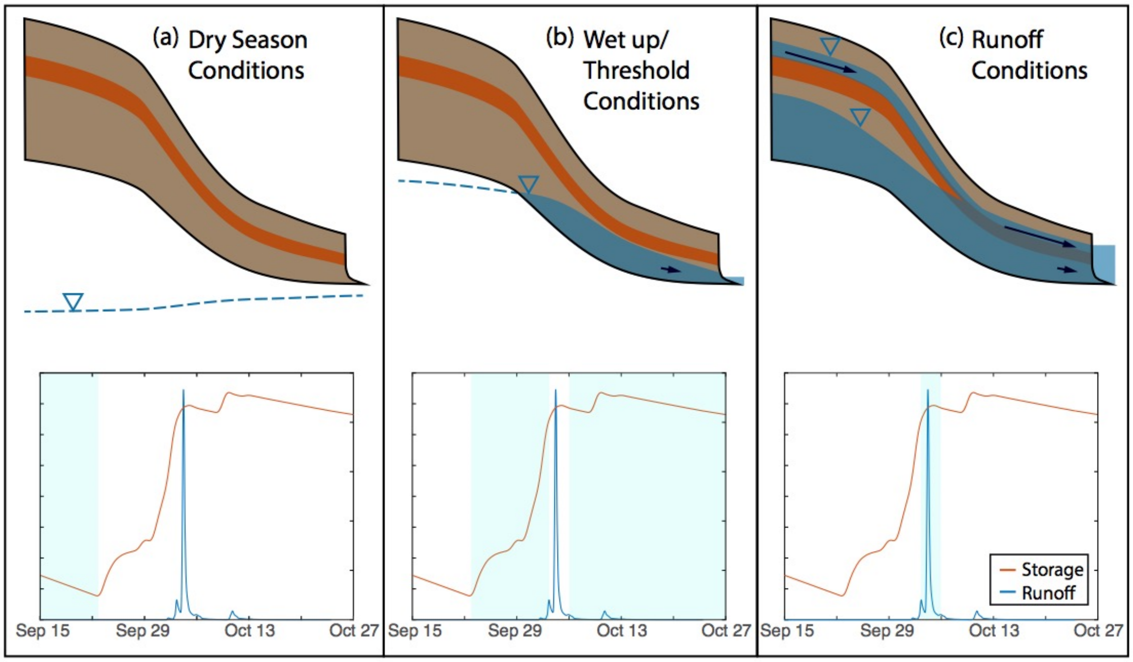

Figure 22: Conceptual model of storage and runoff conditions through the transition from dry to wet season in early fall. Each panel depicts water table development (blue shading) and relative magnitude and depth of lateral flow (black arrows) in a simplified lateral hillslope profile from ridge to stream. Profile depicts an argillic Bt horizon (orange) between a sandy A and C horizon. C horizon transitions to less-weathered saprolite at lower boundary of the hillslope, corresponding to refusal depth we encountered in the field with a hand augur. Time series show cumulative storage and runoff for WS4 over approximately six weeks in early fall of 2015.

heterogeneous flowpaths. Here, we observed nearly the full range of runoff behavior in WS4 while water tables in near-stream locations varied relatively little relative to their annual range (e.g., Figure 17h). Concurrently, upslope water tables (e.g., Figure 17b), indicated that connected, perched hillslope water tables drive fluxes through near-stream locations, via either rapid interflow or hydraulic displacement, or likely both.

We found that substantial subsurface hydrologic heterogeneity can be organized by both its dynamic similarity to either storage or runoff, and additionally by its landscape position. These observations led to a conceptual model that allows us to interpret storage and runoff dynamics in the context of distinct landscape positions and their variable hydrologic response and contributions to runoff, highlighting the organized heterogeneity encapsulated within watershed systems.

3.5 Conclusion

We intensively instrumented a structurally complex headwater watershed to explore how internal watershed heterogeneity and deeper groundwater relate to runoff and integrated watershed storage. Our findings are summarized as follows:

1. Deep groundwater and integrated storage have a positive, statistically significant relationship and both largely exhibit a seasonal wet up and dry down with minimal observable event-scale changes. However, distinct hysteresis depending on magnitudes of each point to conditions where their correspondence breaks down: specifically the rapid early dormant season rise of storage not seen in deep groundwater and increases in deep groundwater not seen in storage due to rapid runoff generation immediately drawing storage down (Figures 11,12).
2. In contrast to both storage and deep groundwater, runoff in WS4 exhibited primarily event-associated dynamics. Although runoff only occurred seasonally, its greatest changes were rapid increases and decreases in

response to storm events. There was no direct correspondence between runoff and deep groundwater; runoff events occurred throughout the 4 meter range of the deep groundwater table over our study period. Similarly, runoff occurred across a range of storage values; however, only when storage was above a threshold of ~100 mm, indicating the connection between the two as storage setting conditions for runoff to be generated (Figures 11,13).

3. Our internal watershed measurements revealed dynamics that generally corresponded more or less strongly to either the seasonal pattern observed in integrated watershed storage or event-scale response of runoff (Figures 20, 21).
4. Further, although no single landscape gradient we distributed sensors across (slope length, convergence, or depth) was sufficient to explain which positions were seasonal- vs event-associated, the combination of the three generally was: deeper positions, lower on the hillslope, with a more convergent hillslope generally displayed more seasonal dynamics, and vice versa. The combination of these three can be succinctly described as contributing volume. Positions with more contributing volume displayed a seasonal pattern and those with less a more event-scale pattern. (Tables 2,3; Figures 16-19).
5. Points 3 and 4 allow us to broadly classify the watershed into positions more related to storage or runoff. These distinct, sequential dynamics reflect complex runoff generation mechanisms dependent on storage thresholds and connectivity three-dimensionally through the watershed (Figure 22).

Despite the substantial heterogeneity observed across WS4s complex 3-D structure, our study yielded findings allowing us to organize that complexity in ways that will help advance our larger understanding of hydrology but also points to substantial further opportunities to expand our understanding of these still relatively novel systems.

4. Connectivity between intermittent headwaters and higher order streams mediated by dynamic storage in legacy anthropogenic sediments deposited on floodplains.

4.1 Introduction

4.1.1 Hydrologic connectivity across mountain fronts and alluvial fans in arid and semi-arid zones.

Stream networks and the watersheds that contain them can span a wide range of geomorphic forms that modify hydrologic processes occurring within the network. This may manifest as gradual, continuous change in channel morphology moving downstream through a network (Wondzell, 2011), or a sharp transition in geomorphic setting such as when smaller streams join larger streams or rivers and enter lower-gradient valleys. One specific case, commonly observed in arid and semi-arid environments, is flow over a divergent alluvial fan either at the outlet of a watershed or upon exiting a mountain range (i.e., at its “mountain front”)(J. L. Wilson & Guan, 2004). At these points some combination of lower slope angle, flow divergence, more porous sediments, and available pore space shifts the stream water balance more towards infiltration than runoff generation and the stream will begin to lose water (Herron & Wilson, 2001). These points are often key landscape positions for recharging groundwater (Mountain Front Recharge, MFR) in arid regions, and hence have been subject of substantial study (Markovich et al., 2019; Meixner et al., 2016); however, the fate of the surface flow moving through, into, and potentially back out of these systems has been relatively less studied (Covino & McGlynn, 2007; S. W. Woods et al., 2006).

But, the timing and magnitude of these exchanges between surface and subsurface water have substantial implications for downstream hydrology and biogeochemistry (Covino & McGlynn, 2007; Herron & Wilson, 2001). Substantial exchange can attenuate hydrologic fluxes by decreasing flow velocity or facilitate return flow by saturating downslope sediments. Because these depositional zones can modify hydrologic connectivity moving through a stream network, and because they occur at predictable locations within the network (i.e., at clear geomorphic transitions between higher-gradient watersheds and broader valleys) they can be identified readily from topography and their potential behavior predicted a priori (Bowen et al., 2014).

Though many humid regions, such as the Southern Piedmont of the United States, also display the geomorphic transitions similar to those in arid and semi-arid environments, the potential for MFR-like features or processes in such regions remains underappreciated and understudied. One potential reason is the understanding that a MFR zone must have unsaturated water storage capacity (Herron & Wilson, 2001; Puigdefabregas et al., 1998), otherwise surface runoff would continue as surface runoff over saturated sediments. Although the extent to which humid subtropical regions vary in moisture state remains underappreciated, it is nevertheless true that water tables in these regions are generally higher and sediment is more saturated. However, human modifications of sediment fluxes in the region may have created conditions favorable to greater unsaturated sediment abundance thus leading to hydrological processes similar to arid and semi-arid systems in a humid, energy-limited region like the Southern Piedmont.

4.1.2 Legacy sediments in the Southern Piedmont

Human activities are strong drivers of geomorphic change across global landscapes (Hooke, 2000). Anthropogenic impacts on watersheds and river systems are particularly ubiquitous, as geomorphic change in these areas may reflect relatively distal activities such as logging or farming within watershed headwaters or uplands as well as more direct modifications to the river corridor (Walter & Merritts, 2008), with impacts propagating great distances upstream or downstream (Wohl, 2019). An increasingly recognized facet of manmade geomorphic change is distribution of legacy sediments through bottomlands relatively close to their origin (James, 2013; Wade et al., 2020). The Southern Piedmont, with an estimated 17 cm of soil erosion across the entire region (Trimble, 1975), presents an opportunity to study the lasting effects of these anthropogenically-derived features.

From the late 18th to the early 20th century, intensive agriculture in the Southern Piedmont accelerated upland erosion and bottomland deposition, altering the geomorphology and pedology of both and creating settings for modified hydrologic and biogeochemical processes. Valleys and floodplains receiving legacy sediments generally see their streams become disconnected from their floodplains, with the former accelerating incision and the latter becoming a terrace. Of the 17 cm loss of upland soil, it is likely that the vast majority remains stored in valleys down gradient of its initial erosion (Jackson et al., 2005). Although research in systems characterized by legacy sediment deposition has accelerated in a number of fields, the hydrologic legacy of these sediments remains largely unexplored. The Southern Piedmont represents a unique opportunity to leverage anthropogenic legacies to observe these processes. To that end we address the following questions:

1. What differences or similarities in flow characteristics emerge as one moves up in scale from headwaters to higher order streams?
2. Can these similarities or dissimilarities be related to surface-subsurface storage processes occurring in legacy sediments deposited on the original floodplain separating headwaters from higher-order streams?
3. How prevalent are these types of landform in the larger watershed?

4.2 Methods

4.2.1 Study Site: nested watersheds within the Calhoun Critical Zone Observatory

This study was conducted in the Calhoun Critical Zone Observatory (CCZO), part of the NSF-funded Critical Zone Observatory network. The CCZO is located in northern South Carolina, USA, in the Southern Piedmont physiographic region of the southeastern United States (Figure 23). The CCZO lies within a humid subtropical climate zone characterized by a hot, humid growing season lasting from approximately April through September (Stoy et al., 2006) and a mild dormant season for the remainder of the year. Average annual temperature is 15.8° C and average precipitation is ~1200 mm, distributed evenly through the year without a regular dry season, and falling almost entirely as rain. Land cover is predominantly a mixture of pines (*Pinus* spp.) and hardwoods such as oak (*Quercus* spp.) and hickory (*Carya* spp.); these forests are a mix of old-field succession and pine stands planted for timber production. The terrain of the CCZO is typical of the Southern Piedmont with upland, low-gradient interfluves joined to bottomland streams and rivers by highly dissected headwaters that switch seasonally between dry and 1st order. These landforms range between 110 and 190 m in elevation.

The area is underlain by granite metamorphosed to granodiorite or metadiorite of the Wildcat Branch complex. Upland soils are primarily Ultisols of the Appling, Cecil, and Madison series. These soils generally consist of loamy sands underlain by clay-rich argillic horizons over deeply weathered saprolite (Richter et al., 2000). Bottomland soils are Fluvent Entisols with an incipient A-horizon within legacy sediment deposits on top of pre-legacy soils with a defined Ab horizon and occasional Bwb horizons. The entire profile is predominantly sand-fraction, though the legacy sediments exhibit slightly finer-grained sand (Wade et al., 2020).

Study watersheds were a 322 ha third order watershed (Holcombe's Branch, HLCM) and a 6.9 ha, zero to first order headwater (Watershed 4, WS4) nested within the former. Holcomb's Branch consists of a main stem, second order stream fed by a series of higher-gradient headwaters with narrow valleys whose outlets are separated from the main stem by floodplains that range between 10 and 80 m in width. Elevation ranges from 120 m along the main stem to 195 m along the watershed divide. Mean watershed slope is 8.5°, with slopes of 4° along the main stem and up to 35° on the steepest hillslopes in headwaters. Legacy alluvial fan sediment deposition along the floodplain of ~1.5 m (Wade et al., 2020) at the outlets of headwater tributaries has in many cases buried surface channels connecting headwaters to the main stem, including at the outlet of WS4 (Figure 24). WS4 ranges in elevation between 123 m and 173 m, with a mean slope of 19%. Connecting it to deposited legacy sediments along the main stem in HLCM, WS4 exhibits evidence of substantial pre-succession and ongoing erosion in the form of a deeply incised main channel and side channels (0.5-2m) that propagate almost to the watershed divide, visible erosion pillars on hillslopes (1-5 cm), and shallow hillslope gullies disconnected from the main channel (Figure 23).

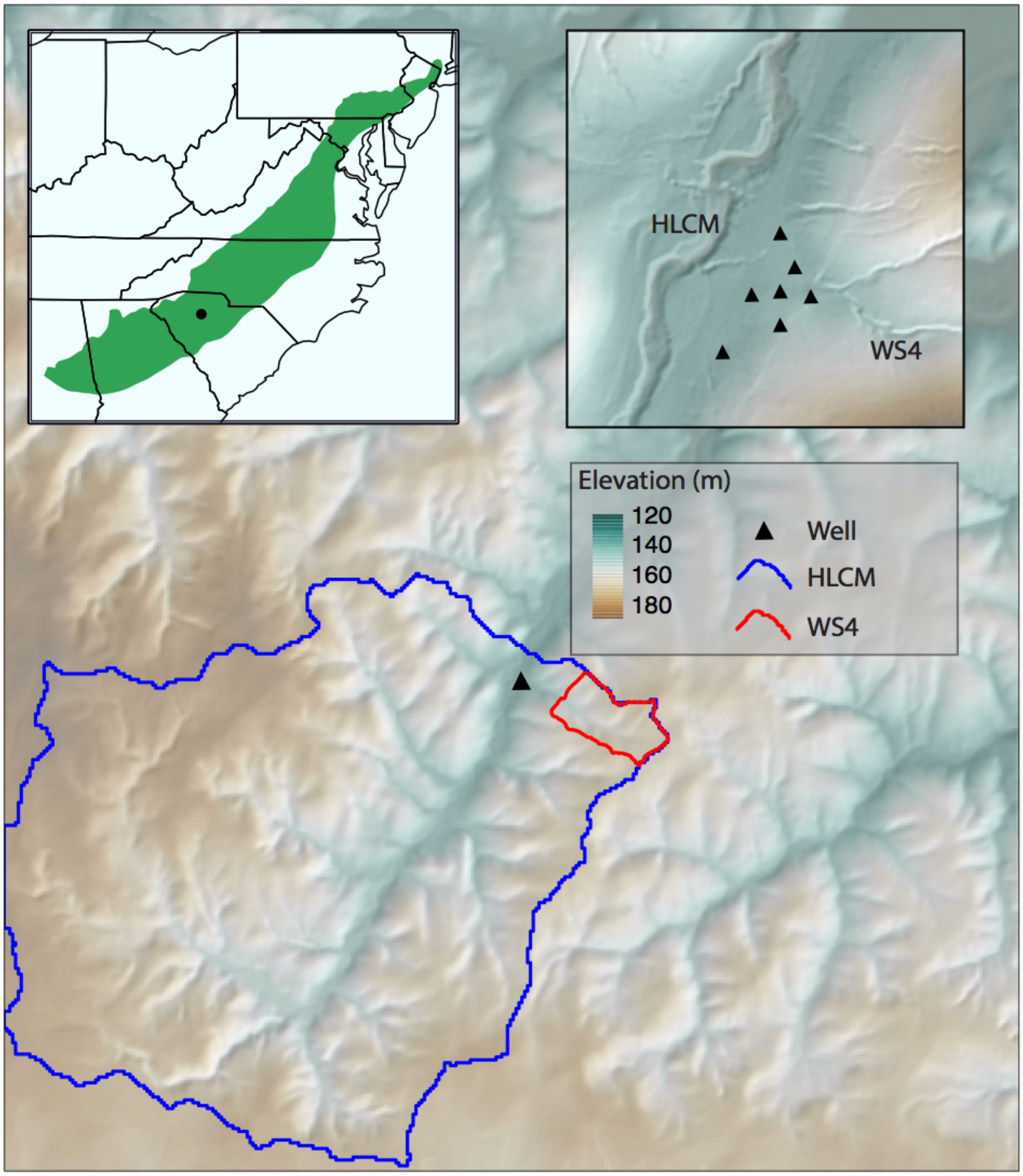

Figure 23: Site Map; Regional setting within Piedmont region of the southeastern USA (upper left), overall Holcombe's Branch watershed (main panel), and detail of alluvial fan at the outlet of watershed 4 with well installation locations (upper right).

Table 4: Physical and flow characteristics of watershed 4 (WS4) and Holcombe's Branch (HLCM) for water years (WY) 2016, 2017.

		WS4	HLCM
Watershed Area (ha)		6.9	322
Slope (°) Mean/Std Dev		11/5.8	8.3/5.5
Precipitation (mm)	WY 2016	1409	
	WY 2017	791	
Runoff (mm)	WY 2016	554	603
	WY 2017	78	219
Runoff Ratio (Q/P)	WY 2016	0.39	0.43
	WY 2017	0.10	0.28
	Total	0.29	0.37
Richards- Baker Index (ΣdQ/ΣQ)	WY 2016	1.03	0.77
	WY 2017	0.89	0.16
	Total	0.97	0.61

4.2.2 Hydrologic measurements and flow characteristics

Data were collected from July 1, 2015 through September 30, 2017, incorporating water years 2016, 2017 and the preceding summer dry down. Hydrologic measurements consisted of precipitation and temperature for the CCZO, and runoff in both WS4 and HLCM. Additionally, we measured water table in seven shallow groundwater wells distributed through the floodplain separating WS4 from the second order stream directly downstream of it in HLCM.

Precipitation was measured using a tipping bucket rain gauge (TE525MM, Texas Instruments) with a 24.5 mm funnel, 0.1 mm per tip, and a nominal accuracy of 1% below 2.5 cm hr^{-1}. Temperature was measured with a shielded thermistor (CS215, Campbell Scientific) with a nominal accuracy of ±0.4°C from 5°C to 40°C.

Stage in WS4 was measured at 5 min frequency (WT-VO capacitance rod, TruTrack, ±1 mm) in a concrete stilling pool with a 90° v-notch weir. Runoff was calculated using the rating curve for a 90° v-notch weir (USBR, 2001) and periodically validated with manual measurements. In-channel stage was measured (SR50A-L sonic depth sensor, Campbell Scientific, ±1 cm) at 5 min frequency in HLCM within a free-flowing reach at the downstream end of floodplain at the outlet to WS4 (Figure 23). We calculated runoff using a rating curve developed from manual discharge measurements co-located with stage measurements and spanning the majority of observed flow conditions.

Wells were distributed across the area of the floodplain at the natural outlet of WS4 ~80 m downstream of the weir (Figure 23) using a 2.25 inches hand augur (AMS) with the goal of fully capturing the dynamics of the shallow water table in the legacy sediments deposited at its outlet. They ranged in depth from 0.8 to 2.3 m, with their completion depth limited by a layer of gravel/cobble and/or less weathered saprolite unconducive to hand auguring (Wade et al., 2020). Wells were cased in screened PVC with the same outer diameter as the bore hole and the upper 5 cm of the bore hole on the exterior of the PVC was sealed with bentonite to prevent surface runoff from flowing into the bore hole.

Flow characteristics were described using runoff ratios (monthly, annual, study period) and the Richards-Baker index (RBI) (Baker et al., 2004). The former is the ratio of runoff to precipitation over a given time period; values closer to one indicate a watershed that produces more runoff relative to P. The latter calculates the total magnitude in change of a flow variable, q, (i.e., runoff, discharge) over a time period, t, and normalizes it to the sum of that variable over the same time.

(1) $RBI = \sum_t |dq| / \sum_t q$

Large values of RBI represent a flashy stream and low values a stream more dominated by baseflow.

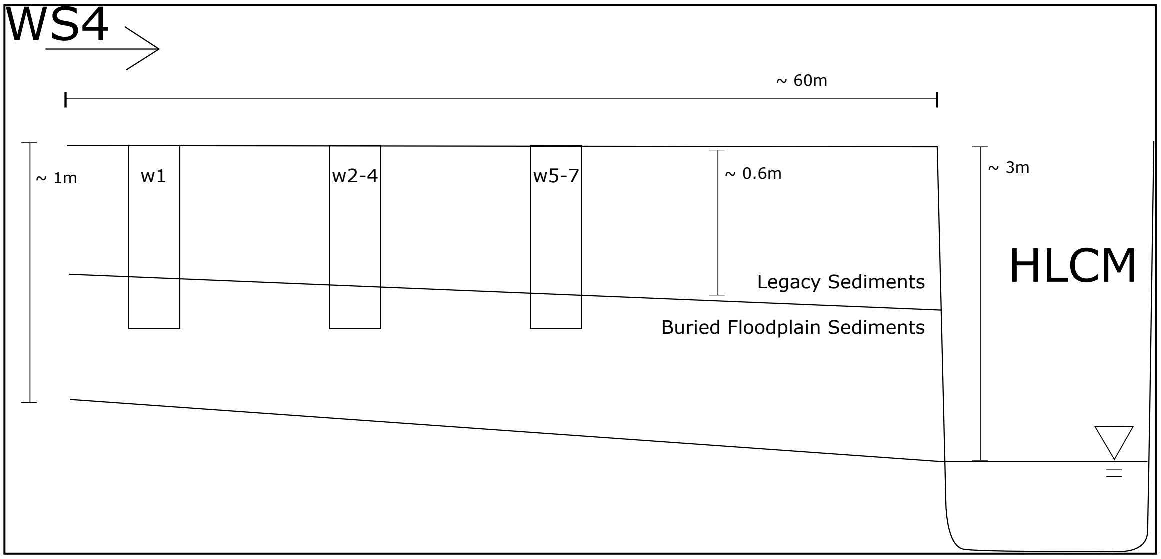

Figure 24: General well installation within legacy sediments on alluvial fan between WS4 and HLCM. Depth of legacy sediments from Wade et al. (2020).

4.2.3 Estimation of legacy sediment pore volume

Our network of wells was used to estimate storage volume and dynamics in the legacy sediments at the outlet of WS4. The volume of interest was simplified as a triangular prism with its face (A) being the surface of the sediments, and edge length the depth of the sediments (z_s). We delineated the area of the triangular faces with the well locations (i.e., with vertices at wells 1,5, and 7), and used the mean completion depth of all seven wells as depth. The product of area and depth yielded the total volume of the sediments (V_t), which included soil, water, and gas. Porosity (ϕ) is the ratio of void volume (V_v) to total volume. We approximated porosity using the mean bulk density of the sediments in Holcombe's Branch from a prior study (Wade et al., 2020) and the consistent density of mineral soil grains. The product of porosity and total volume is the void volume, which could consist of either water or air (ϕ * V_t).

Mean water table elevation from all seven wells (h) was calculated to define the dynamic upper bound of the water stored in legacy sediments. It was assumed that soil pores were distributed evenly through the depth profile, and therefore the volume of water (V_w) or volume of air (V_a) could be calculated as a function of time from porosity, area, and water table elevation, according to

$$(2) \quad V_w = \phi A h; V_a = \phi A(z_s - h) = V_t - V_w$$

We make several simplifying assumptions in generating this estimate; however, we believe that they are minor in effect or have a known direction of bias which can be accounted for in further analyses.

First, by simplifying the shape of the sediment volume to a triangular prism (confining its boundary to the area enclosed by our well network), we substantially underestimate the potential volume stored in these sediments by not including the portion from the line created by wells 5-7 to Holcombe's Branch. However, we believe that that the further assumptions necessary to extrapolate into this area (e.g., how to account for longitudinal as well as lateral dispersion) would be likely to lead to additional uncertainties whose direction may be less clearly known. By confining our estimate to the volume we directly measured we have high confidence in the accuracy within that volume and provide a conservative estimate of its function. In knowing that it is a strongly conservative estimate of overall storage in legacy sediments, we are better able to frame our findings relative to potential error.

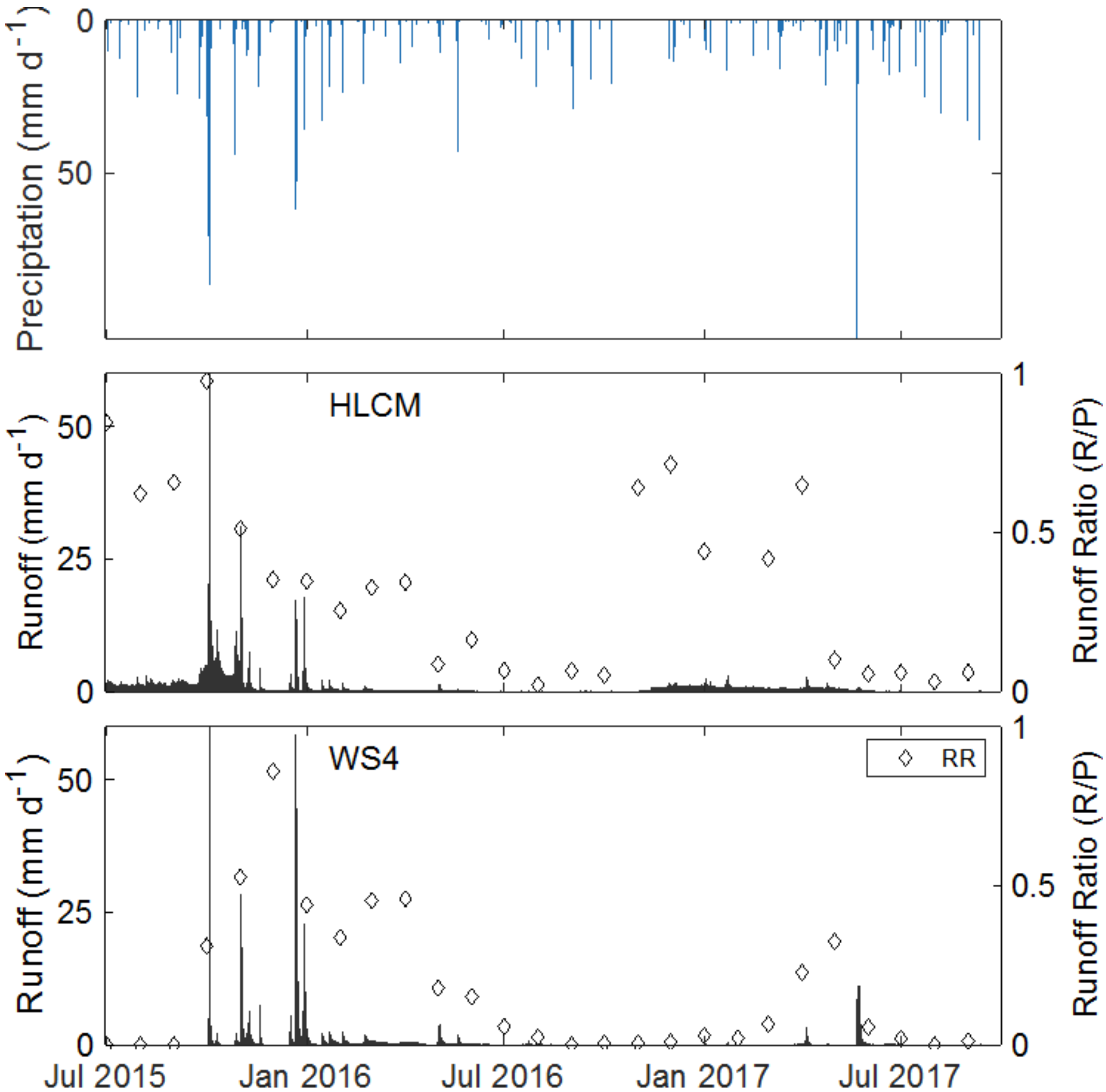

Figure 25: Precipitation and runoff for HLCM and WS4 ; Precipitation (top), monthly runoff ratio, and runoff for HLCM (middle) and WS4 (bottom). Runoff ratio calculated from summed runoff and precipitation numbers for each calendar month.

Second, we assume that bulk density serves as a reasonable proxy for porosity in these sediments. This assumption is potentially problematic because of the difference between porosity and effective porosity: total void space vs void space that can drain freely. This assumption is most likely to be problematic in older soils with higher clay content, that have high porosity but small pore sizes and high capillary forces that limit the proportion of those pores which can drain freely. These legacy sediments, though, are predominantly sand fraction (78% compared to 8% clay fraction) (Wade et al., 2020). In such soils, porosity is approximately equivalent to effective porosity due to larger pore spaces and lower capillary forces.

4.3 Results

4.3.1 Flow characteristics of watershed 4 and Holcombe's Branch

Watershed 4 (WS4) and Holcombe's Branch (HLCM) exhibited distinct flow behavior that was dependent on the annual precipitation regime or the timing and magnitude of specific storm events. Our study period spanned water years (WY, October 1 – September 30) 2016 and 2017, which were generally wet and dry, respectively (Table 4). The CCZO received 1409 mm of precipitation in water year 2016 (WY2016) and only 791 mm in water year 2017 (WY2017), 117% and 66% of long-term regional average, respectively. During WY2016, high precipitation yielded 554 and 603 mm of runoff for WS4 and HLCM, respectively, a difference within 10%; however, the much drier conditions in WY 2017 led to an 86% decrease in WS4 runoff compared to only a 63% decrease in HLCM. This difference was reflected in their respective annual runoff ratios, as well, where runoff ratios in WS4 dropped from 0.39 to 0.10 compared to a much smaller decrease in HLCM (0.43 – 0.28).

The Richards-Baker Index (RBI) (Baker et al., 2004) was used to characterize the flashiness of each watershed (Table 4). Over the whole study period, HLCM had a lower RBI (0.61 compared to 0.97 for WS40, but more interestingly it had a substantial difference in RBI between WY2016 and WY2017: 0.77 vs. 0.16. These numbers

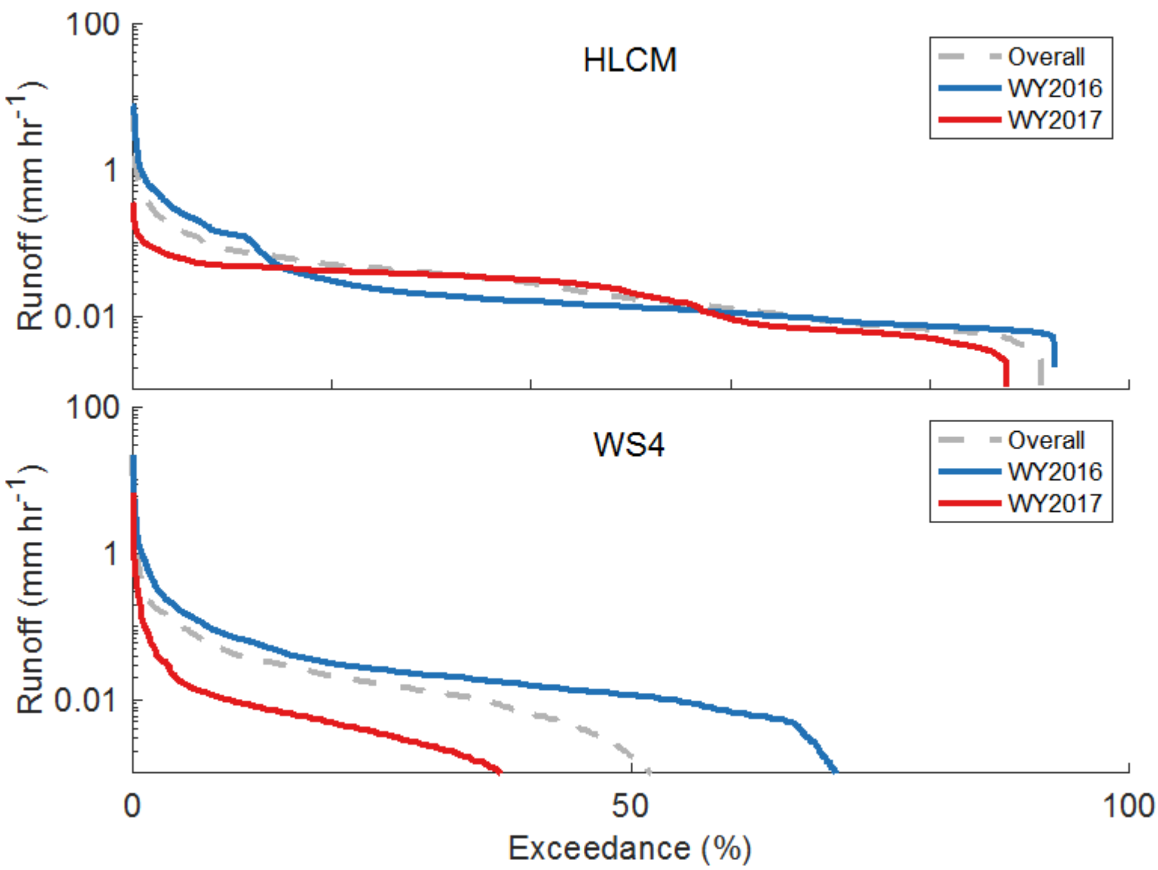

Figure 26: Flow duration curves ; Flow duration curves for HLCM (top) and WS4 (bottom). Curves shown for individual water years and combined for both water years together. Exceedance is the percent of the time period at that runoff value or higher.

indicated that while HLCM experienced high changes in flow relative to total amount in WY2016, during WY2017 it exhibited low changes in flow relative to total.

Runoff generation in both watersheds (Figure 25) was dominated by a few, high magnitude precipitation events. Hurricane Joaquin in October 2015 was followed by large frontal systems in November and December 2015. These three storm systems generated approximately 50% (HLCM) and 68% (WS4) of measured runoff over the entire time period. Additionally, a seasonal pattern was evident in both watersheds, with most runoff occurring late fall through late spring.

Despite these similarities, responses between watersheds differed strongly in both flow duration and baseflow. HLCM flowed almost perennially and exhibited higher, more persistent baseflow while WS4 flowed on average only half of the year and only exhibited baseflow in the winter and spring of 2016 following the wet end to 2015 (Figure 25). Over the study period more runoff flowed from HLCM (Table 4), but this difference in baseflow and flow duration is balanced in part by higher peak flows in WS4 in both WY2016 and WY2017

Taken together, flow characteristics indicate watersheds that in some ways are quite similar, but that differ in important and consistent ways. HLCM, with its steadier runoff magnitude from year to year, lower RBI, and more substantial baseflow appears to draw runoff from sources that flow across more diverse spatial and temporal scales than those that comprise flow in headwaters like WS4.

4.3.2 Hydrologic dynamics in legacy sediments between Holcombe's Branch and watershed 4.

Over the course of the study period, flow from WS4 was frequently observed to propagate over the sediments at its outlet between 20 and 40 m (~33%-66% of the distance to HLCM) before fully infiltrating. However, only during the high magnitude events in October-December 2015 (Figure 25) did we observe a continuous surface flow connection from the outlet of WS4 to HLCM across legacy sediment deposits.

Water table measured in our well network within those sediments revealed a coherent, but highly dynamic wet up and dry down response in both years, primarily from late fall through early spring when ET is at a minimum (Figure 27). All wells displayed largely the same dynamics, although water table responses differed year to year. In each well we observed increases in water table of a meter or more over single days,

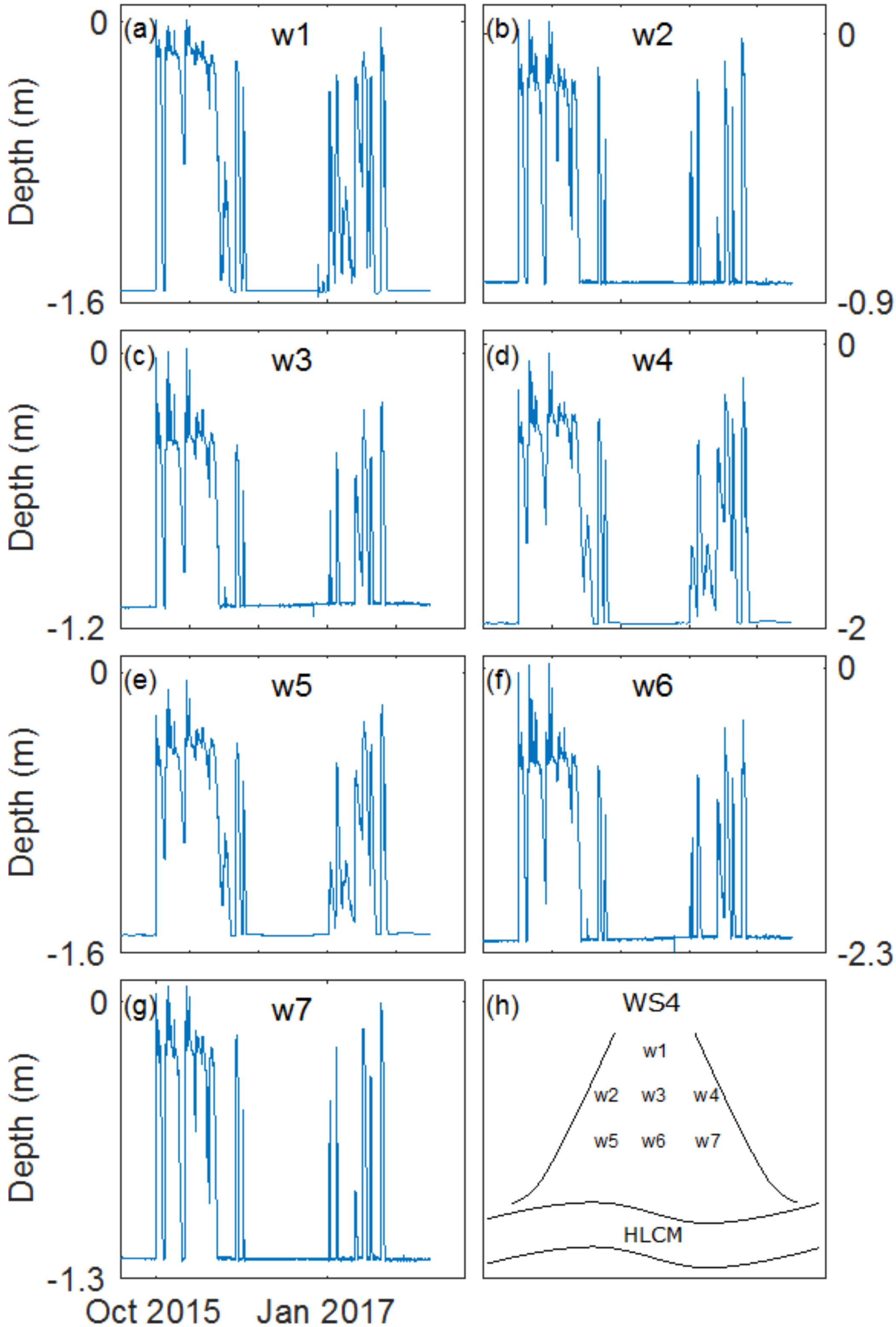

(a) w1
(b) w2
(c) w3
(d) w4
(e) w5
(f) w6
(g) w7
(h) WS4
Depth (m)
0
-1.6
-0.9
-1.2
-2
-2.3
-1.3
Oct 2015
Jan 2017
w1
w2 w3 w4
w5 w6 w7
HLCM

Figure 27: Flood plain wells; (a-g) Flood plain wells over the study period. 0 is the ground surface. Horizontal lines are completion depth for that well and indicate no water present. (h) Plan view schematic (not to scale) of the distribution and numbering of wells.

while dry down over the same depth range occurred over 1-2 weeks. The latter time scale was more typical of water table response during WY2016, when after an initial wet up in October the water table stayed more persistently elevated through March. In contrast, during WY 2017 the water table wet up and dried down fully multiple times. This distinction is similar to the contrast between runoff in WY2016 and WY2017 in WS4 (Figure 25). Indeed, storage (a linear function of water table level, Equation 2) and discharge from WS4 are positively and significantly related (Spearman's ρ = 0.70 and p << 0.05) (Figure 28, inset).

Potential storage volume in the legacy sediments at the outlet of WS4 (i.e., V_v) was 921 m^3 based on ϕ = 0.46 and V_t = 1960 m^3. This potential storage volume changes from V_w to V_a as the water table decreases. Because they are derived from it, both exhibited the same dynamics as the water table (V_a inversely); however, units of volume facilitate comparison to volumetric fluxes from WS4. We found that available storage volume (i.e., V_a) exceeded daily WS4 discharge for 97% of the study period. Only during the three large storm events in October-December 2015 and additionally a short, high-intensity storm in May 2017 was it exceeded (Figure 28).

During these events the water table was at or within centimeters of the ground surface (Figure 26), during which runoff in HLCM peaked rapidly (Figure 25). We found a significant and positive relationship between these two (Spearman's ρ = 0.14 and p << 0.05), however, the low correlation reflected a poorly defined relationship between water table depth and runoff at most water table depths. The predominant feature of this relationship was a strong threshold response in HLCM runoff when the water table was within approximately 20 cm of the surface (Figure 29).

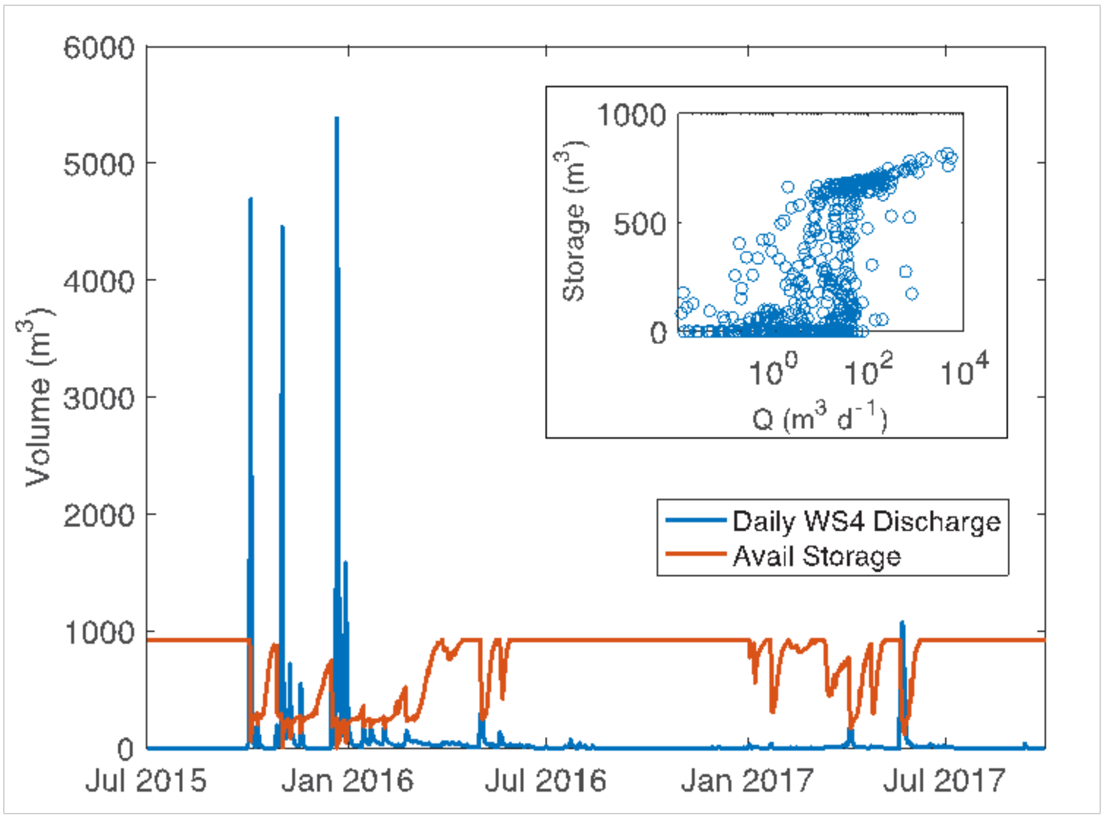

Figure 28: Volume over time for both WS4 discharge and air volume (i.e., legacy sediment storage not filled by water and therefore available) in legacy sediments. Discharge presented in units of m^3 d^{-1} to allow both to be on the same axis. Horizontal portion of orange line indicates legacy sediments have no measured saturation and therefore available volume is equal to total volume, ~920 m^3.

4.4 Discussion

4.4.1 Infiltration of runoff from headwaters into legacy sediments at their outlets mediates connectivity across scale in humid, low-relief landscapes

Mountain front recharge (MFR) refers to the increased loss of water from the stream channel to the subsurface at the transition from confined, high-gradient mountain streams to lower-gradient alluvial features between valley bottoms and mountain ranges. This process has been almost exclusively been studied in arid (Herron & Wilson, 2001) and semi-arid, mountainous environments (Covino & McGlynn, 2007), where it can represent a dominant component of groundwater recharge (Markovich et al., 2019). Conditions requisite for MFR are commonly presented as some combination of change in slope, change in convergence, temporally sparse or spatially heterogeneous precipitation, and sediments with high infiltration and storage capacity, a number of which are directly invoked to explain why MFR is a phenomenon of arid, mountainous landscapes (Herron & Wilson, 2001). However, here we present an example of MFR type recharge and discharge in a depositional fan in the humid subtropical, low-relief Southern Piedmont of the United States.

The transition from WS4 across legacy sediments to HLCM represents a change to a lower-slope, divergent alluvial fan with sediments whose hydraulic properties (Wade et al., 2020) are conducive to infiltration. In short, this site provides the same shift of geomorphic and pedologic conditions towards those more conducive to infiltration than overland flow that have been observed in multiple studies confined to more arid landscapes (Covino & McGlynn, 2007; Herron & Wilson, 2001; Puigdefabregas et al., 1998; S. W. Woods et al., 2006). Further, we observed the crucial hydrologic condition that there is sufficient subsurface storage volume (Figures 5,6) to influence hydrologic connectivity between headwaters and the higher order HLCM stream.

Although it is most frequently addressed at large scales in the context of deep aquifer recharge (Markovich et al., 2019), MFR has been shown to occur through shallow, rapid flowpaths (Covino & McGlynn, 2007; S. W. Woods et al., 2006) where recharge functions to both buffer downstream waters from flashy mountain runoff but also ultimately serves as a runoff source for streams and rivers lower in the valley. Similarly, legacy sediments between WS4 and HLCM store and slowly release runoff from WS4 as baseflow, but also when saturated they rapidly transmit runoff from WS4 as they become a saturated source area (Figure 29). This shifting between attenuating and facilitating flashy storm flow is a function of the hydrologic state of the sediments, and creates the conditions for the remarkable variability in flow regime as captured by RBI in HLCM: from flashy and storm-driven in WY2016 when threshold wetness is achieved to persistent and baseflow-dominant in WY2017 when storage remains low and surface flow from WS4 is almost completely buffered and released slowly as baseflow (Figures 3,4).

These dynamics in which hydrologic storage in legacy sediment both attenuates and amplifies headwater runoff as a function of storage state point to ample opportunity to further refine our process understanding of MFR in these landscapes and to expand our spatial scope to identify where and to what extent these processes (for a related example see Zimmer & McGlynn, 2017) generally thought to be confined to arid and semi-arid regions are far more relevant and ubiquitous than previously understood.

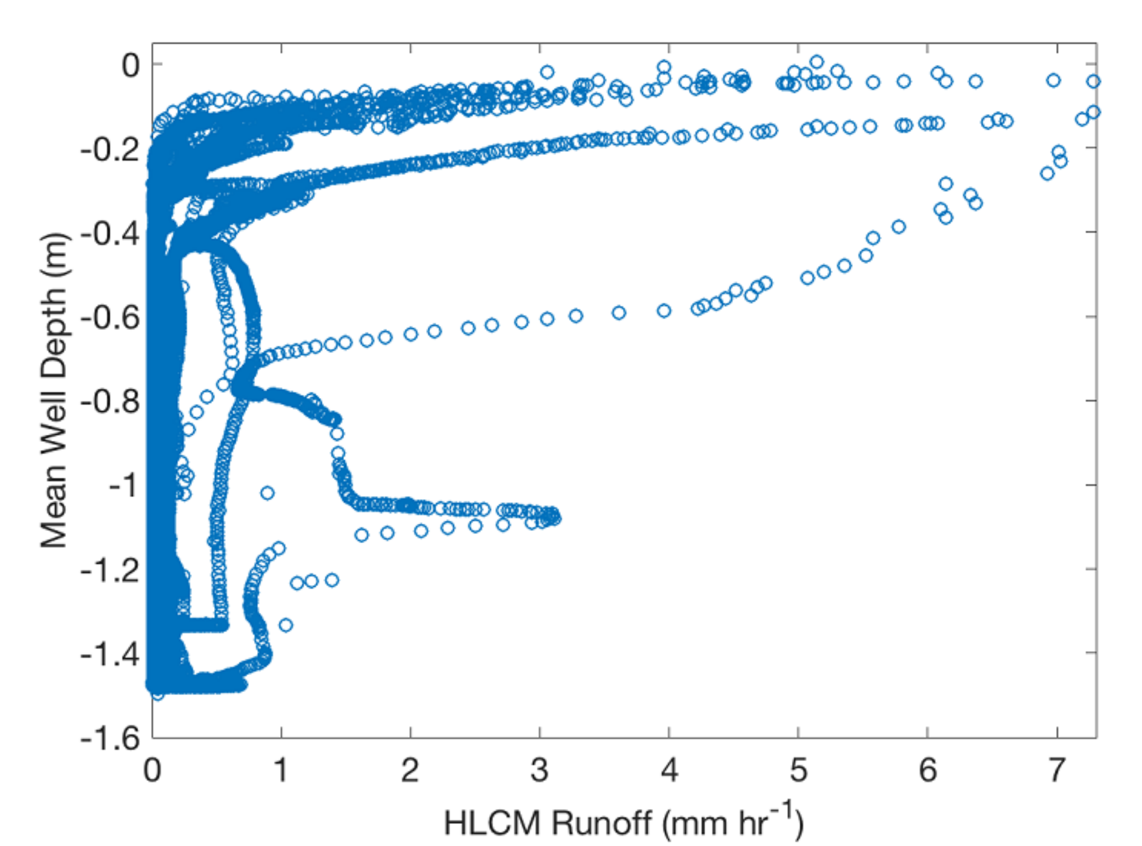

Figure 29: Mean flood plain well depth versus runoff in HLCM.

4.4.2 Implications for hydrologic functioning in the Southern Piedmont

Here we observed the mediation of connectivity between a headwater and higher order stream were by storage dynamics in sediments deposited on the floodplain that separates them (Figures 28, 29). We believe that these observations are representative of a phenomenon that is likely very common across the Southern Piedmont or other regions with similar landscapes, especially those with legacies of anthropogenic change.

HLCM consists primarily of a single main stem fed by multiple, steeper subwatersheds on the same order as WS4 (Figures 1,8). Each of these watersheds

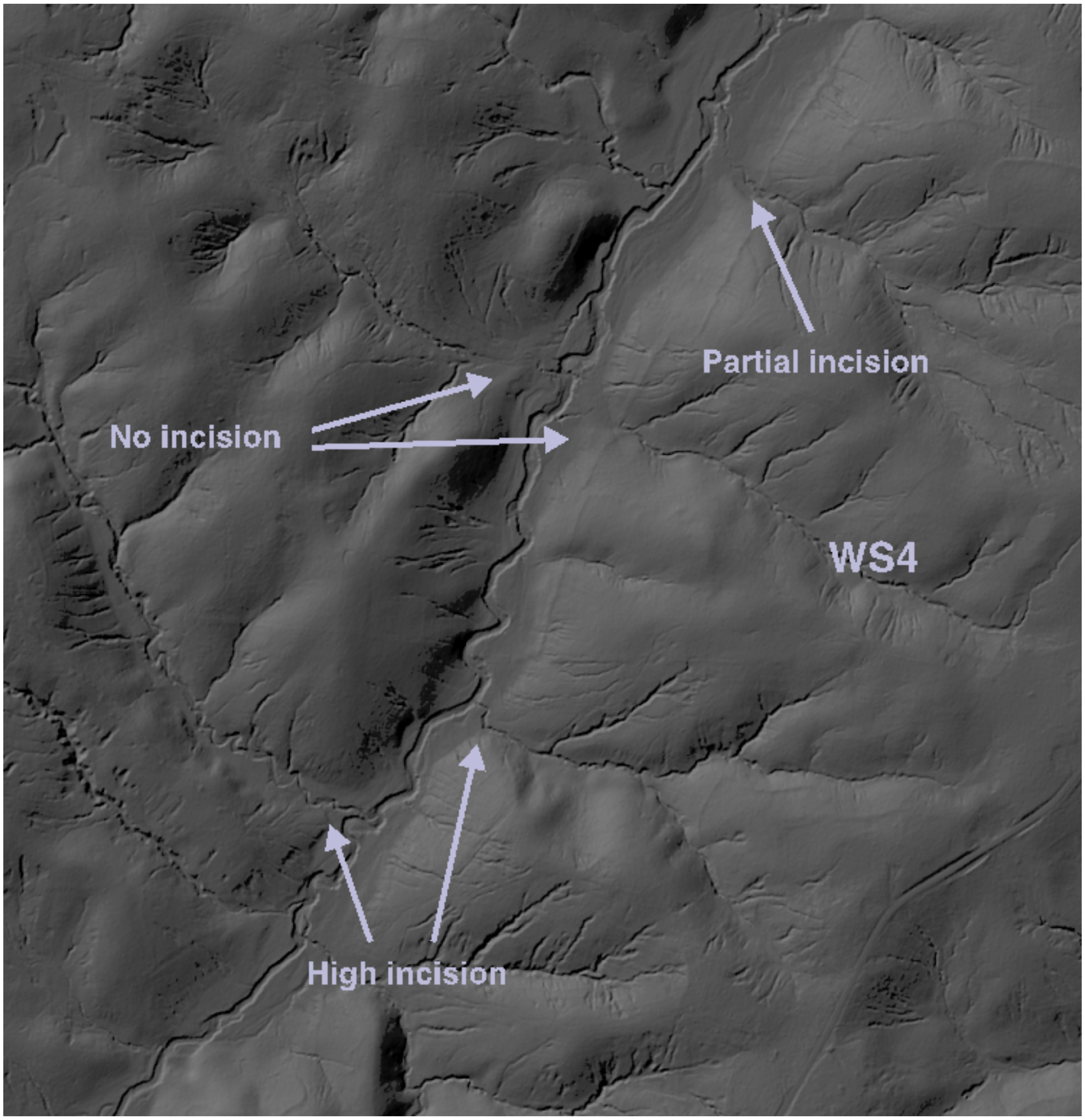

Figure 30: Location of WS4 floodplain sediments and four other examples of different levels of a defined surface channel across them.

drains to HLCM over or through similar legacy sediments to those observed at the outlet of WS4. In many cases we observe a similar lack of a defined surface channel to the legacy sediment deposits below WS4, or occasionally a relatively shallow channel just barely incised into the sediments. In other cases, we observe a clear, deep, active channel cutting through legacy sediments (Figure 30). Although it is likely that the hydrologic connection of the headwater streams contributing to HLCM via defined surface channels are less attenuated, it is important to note that even in cases where there is continuous surface flow across porous legacy sediments, the majority of surface flow is likely still being lost to infiltration as a function of water table elevation in the depositional fans that are present in all headwater to valley transitions. Although these deposits make up only ~3% of HLCM's watershed area (Wade et al., 2020), their near ubiquitous position in between the HLCM main stem and its headwaters suggests that they are the dominant landform controlling connections between headwater components (~90%) and the main stem of HLCM watershed.

It has been well known since at least Trimble's (1975) quantification of erosion loss from the Piedmont Plateau that this region is one of the most heavily eroded in the USA. With the ubiquity of this geomorphic change, and the large proportion of this eroded sediment that can remain stored in local bottomlands (Trimble, 1981), it is likely that the hydrologic processes associated with legacy sediments that we observed in HLCM are the norm rather than the exception around the region. The characteristics of connectivity (Figures 6,7) and flow regime (Figures 3,4) we observed here in HLCM and their likely widespread relevance suggests the possibility of defining a "Rural Stream Syndrome," analogous to the "Urban Stream Syndrome" (Walsh et al., 2005) commonly leveraged in stream ecology to describe streams displaying flashier hydrographs, elevated nutrients and/or contaminants, and geomorphic changes. With ubiquitous legacy sediments stored within stream networks, our findings of strong attenuation of flashy headwater runoff up to a threshold where legacy sediments become a source of rapid runoff generation could be a ubiquitous characteristic of streams in rural areas with a history of agriculture followed by forest succession and regrowth, with implications across the region and to other regions with similar legacies.

4.5 Conclusion

We utilized hydrologic measurements across watershed scales from an intermittent headwater (WS4) to the third-order watershed that contains it (HLCM) to understand how flow characteristics change across that transition. Additionally, we intensively monitored water table dynamics in anthropogenic legacy sediments deposited over the flood plain positioned between WS4's outlet and the main stem in HLCM with the goal of understanding how this and similar landforms mediate hydrologic connectivity between headwaters and higher order streams.

We found flow characteristics (runoff ratio, Richards-Baker Index) differed between WS4 and HLCM, suggesting the latter is more attenuated and baseflow-dominated. However, HLCM displayed a complete shift from WY2016 to WY2017 from a flashy stream (though still less so than WS4) to an almost entirely baseflow-derived stream. A generally more baseflow-dominant stream would suggest a role of storage in adjacent sediments, or contributions from deeper groundwater, playing a role in slowly releasing flow, but shifts in flow regime from flashy to baseflow-dominated suggest some more complex hydrology emergent in HLCM not present in WS4.

Similar to alluvial fans in mountain valleys in arid and semi-arid regions, the legacy sediments at the outlet of WS4 exhibit surface flow over a third to a half of the distance to HLCM before it fully infiltrates, with the exception of very high magnitude precipitation events. Driven by that infiltration, we found a highly dynamic water table that wet up and dried down more than 1 m over a day to days in response to inputs from WS4. Based on a geometric simplification and estimates of porosity we calculated total storage and used measured water table to generate water storage and available storage time series for the legacy sediments. Available storage in the alluvial fan was ~900 m^3 when dry, and this estimate was likely quite conservative because we constrained our estimates to the part of the legacy sediments covered by our well network. Despite this, we found this available storage to exceed daily discharge from WS4 for 97% of the study period, suggesting that the majority of the year runoff from WS4 is temporarily stored in legacy sediments and more slowly released to HLCM, driving baseflow. However, when legacy sediments were full or mostly so, they became source areas capable of transmitting saturation excess flow rapidly from WS4 to Holcomb. These times corresponded to the largest flow events we recorded in Holcomb.

This threshold-mediated switching between functions helps create conditions in higher order streams where flow regimes can switch types from year to year: generating massive runoff events or exhibiting almost no annual variability. This intensive field study did not extend beyond the connection between WS4 and HLCM; however, we have observed multiple other subwatersheds of HLCM that exhibit similar outlet landforms. More generally, the erosion of upland soils followed by deposition in adjacent bottomlands as legacy sediments is recognized to be spatially extensive across the Southern Piedmont. Given that and the underappreciated hydrologic processes we observed here, it is likely possible to start constraining characteristic functioning of streams in rural areas with similar legacies in the Southern Piedmont or elsewhere.

5. Conclusions

This dissertation was built on an intensive empirical field campaign bringing classic tools and methods of the hydrologic sciences to a system (the Southern Piedmont) that is both poorly studied and represents the types of deeper, more stratified, lower-relief systems that have been such a blind spot for hydrology. In doing so we observed remarkable seasonality in the hydrologic system despite ample, evenly distributed precipitation. We also identified distinct parts of the landscape which correspond more strongly to runoff generation or storage threshold setting. Finally, attenuation of hydrographs moving to higher stream orders was framed in terms of connectivity through anthropogenic legacy sediments deposited on top of the now-inactive floodplain between WS4 and HLCM.

Major conclusions from this dissertation, organized by chapter, are as follows:

1. At sub-annual time scales, the balance of precipitation and evapotranspiration at the CCZO reveals a system that experiences apparent water limitation through a substantial portion of the growing season, even as highly productive deciduous forests grow. This seeming contradiction is clarified by annual range in storage of hundreds of millimeters, representing a subsidy of water from the dormant season to the growing season. This substantial range in storage has a clear connection to runoff, where storage sets a threshold for runoff generation and further facilitates distinct flow regimes between years as a function of annual storage. These findings challenge common assumptions about water availability and seasonality in humid energy limited systems and clearly indicate the dominant role the forests play in the hydrologic system of the region.

2. Runoff and integrated watershed storage display changes corresponding primarily either to precipitation events or seasonal wet up and dry down, respectively. Similarly, most point measurements of subsurface hydrology (groundwater, soil moisture) fell into one category or the other, allowing point measurements to be classified as more similar to runoff or storage. Landscape scale gradients (hillslope length, convergence, and depth) that point measurements were distributed along in combination suggest an underlying representation of contributing volume; intuitively, points with higher contributing volume are more similar to storage and vice versa. This leads to a sequential wetting up to generate runoff where deeper positions lower on hillslopes wet up first and mostly remain so, setting threshold conditions for runoff generation. During large runoff events, both deeper positions higher on the hillslope, and shallower positions rapidly wet up and drive runoff either via transmissivity feedback as deeper water connects vertically to shallower water or shallow perched interflow along Bt horizons. This chapter both builds on previous studies of hillslope hydrology by incorporating depth and vertical connectivity into our understanding of runoff generation and illustrates the diversity of hydrologic functioning even within the Southern Piedmont, where perched flow at the CCZO does not occur without sufficient storage and runoff is much more strongly connected to deeper water rising into shallower layers.
3. Flow characteristics become more attenuated moving to higher stream orders. Although this finding is typical of any stream network, in this case we observed the loss of WS4 runoff to subsurface flow as it left the outlet and

flowed across anthropogenic legacy sediments deposited over a century ago from accelerated erosion. Infiltration of surface flow from WS4 into these sediments corresponded to an extremely dynamic water table, suggesting that surface flow was being converted to slower subsurface flow before moving to HLCM. Based on a conservative geometric approximation of the sediment's volume and an estimate of porosity, we found that the sediment had sufficient available pore storage for WS4s runoff for 97% of the two year study period. This indicated that these legacy sediments primarily serve as a buffer on flashy runoff from WS4. However, as these sediments get close to saturation, they become very effective at transmitting surface flow via saturation excess overland flow, negating the buffering effect. These findings present two novel findings. Observation of alluvial sediments serving as a buffer of surface flow is broadly understood to be characteristic of arid or semi-arid regions on large alluvial fans or at mountain fronts. Although on a smaller scale, here we show how easily the same geomorphic conditions can be found in this humid region. Additionally, we believe this is the first direct study of the hydrologic effects of legacy sediment deposition in the Southern Piedmont, one which also illustrates the somewhat novel finding of an anthropogenic effect on a stream attenuating rather than amplifying runoff dynamics.

References

Abatzoglou, J. T., & Brown, T. J. (2012). A comparison of statistical downscaling methods suited for wildfire applications. *International Journal of Climatology*, *32*(5), 772–780. https://doi.org/10.1002/joc.2312

Acuña, V., Datry, T., Marshall, J., Barceló, D., Dahm, C. N., Ginebreda, A., et al. (2014). Why Should We Care About Temporary Waterways? *Science*, *343*(6175), 1080 LP – 1081. https://doi.org/10.1126/science.1246666

Adusumilli, S., Borsa, A. A., Fish, M. A., McMillan, H. K., & Silverii, F. (2019). A decade of terrestrial water storage changes across the contiguous United States from GPS and GRACE. *Geophysical Research Letters*, *0*(ja). https://doi.org/10.1029/2019GL085370

Anderson, M. G., & Burt, T. P. (1978). The role of topography in controlling throughflow generation. *Earth Surface Processes*, *3*(4), 331–344. https://doi.org/10.1002/esp.3290030402

Bacon, A. R., Richter, D. deB., Bierman, P. R., & Rood, D. H. (2012). Coupling meteoric 10Be with pedogenic losses of 9Be to improve soil residence time estimates on an ancient North American interfluve. *Geology*, *40*(9), 847–850. https://doi.org/10.1130/G33449.1

Baker, D. B., Richards, R. P., Loftus, T. T., & Kramer, J. W. (2004). A NEW FLASHINESS INDEX: CHARACTERISTICS AND APPLICATIONS TO MIDWESTERN RIVERS AND STREAMS. *JAWRA Journal of the American Water Resources Association*, *40*(2), 503–522. https://doi.org/10.1111/j.1752-1688.2004.tb01046.x

Barnhart, T. B., Molotch, N. P., Livneh, B., Harpold, A. A., Knowles, J. F., & Schneider, D. (2016). Snowmelt rate dictates streamflow. *Geophysical Research Letters*, *43*(15), 8006–8016. https://doi.org/10.1002/2016GL069690

Betson, R. P. (1964). What is watershed runoff? *Journal of Geophysical Research (1896-1977)*, *69*(8), 1541–1552. https://doi.org/10.1029/JZ069i008p01541

Beven, K., & Germann, P. (1982). Macropores and water flow in soils. *Water Resources Research*, *18*(5), 1311–1325. https://doi.org/10.1029/WR018i005p01311

Beven, K. J., & Kirkby, M. J. (1979). A physically based, variable contributing area model of basin hydrology/Un modèle à base physique de zone d'appel variable de l'hydrologie du bassin versant. *Hydrological Sciences Journal*, *24*(1), 43–69.

Birkel, C., Soulsby, C., & Tetzlaff, D. (2011). Modelling catchment-scale water storage dynamics: reconciling dynamic storage with tracer-inferred passive storage. *Hydrological Processes*, *25*(25), 3924–3936. https://doi.org/10.1002/hyp.8201

Bishop, K., Seibert, J., Köhler, S., & Laudon, H. (2004). Resolving the Double Paradox of rapidly mobilized old water with highly variable responses in runoff chemistry. *Hydrological Processes*, *18*(1), 185–189. https://doi.org/10.1002/hyp.5209

Bishop, K. H. (1991). Episodic increases in stream acidity, catchment flow pathways and hydrograph separation. *Ph. D. Thesis, Univ. of Cambridge*.

Blume, T., Zehe, E., & Bronstert, A. (2007). Rainfall—runoff response, event-based runoff coefficients and hydrograph separation. *Hydrological Sciences Journal*, *52*(5), 843–862. https://doi.org/10.1623/hysj.52.5.843

Bowen, E. E., Hamada, Y., & O'Connor, B. L. (2014). Mapping Mountain Front Recharge Areas in Arid Watersheds Based on a Digital Elevation Model and Land Cover Types. *Journal of Water Resource and Protection*. https://doi.org/10.4236/jwarp.2014.68072

Bracken, L. J., & Croke, J. (2007). The concept of hydrological connectivity and its contribution to understanding runoff-dominated geomorphic systems. *Hydrological Processes*, *21*(13), 1749–1763. https://doi.org/10.1002/hyp.6313

Brantley, S. L., Goldhaber, M. B., & Ragnarsdottir, K. V. (2007). Crossing Disciplines and Scales to Understand the Critical Zone. *Elements*, *3*(5), 307–314. https://doi.org/10.2113/gselements.3.5.307

Brooks, J. R., Barnard, H. R., Coulombe, R., & McDonnell, J. J. (2010). Ecohydrologic separation of water between trees and streams in a Mediterranean climate. *Nature Geoscience*, *3*(2), 100–104. https://doi.org/10.1038/ngeo722

Brooks, P. D., Chorover, J., Fan, Y., Godsey, S. E., Maxwell, R. M., McNamara, J. P., & Tague, C. (2015). Hydrological partitioning in the critical zone: Recent advances and opportunities for developing transferable understanding of water cycle dynamics. *Water Resources Research*, n/a--

n/a. https://doi.org/10.1002/2015WR017039

Burt, T. P., Ford Miniat, C., Laseter, S. H., & Swank, W. T. (2018). Changing patterns of daily precipitation totals at the Coweeta Hydrologic Laboratory, North Carolina, USA. *International Journal of Climatology*, *38*(1), 94–104. https://doi.org/10.1002/joc.5163

Buttle, J. M. (2016). Dynamic storage: a potential metric of inter-basin differences in storage properties. *Hydrological Processes*, *30*(24), 4644–4653. https://doi.org/10.1002/hyp.10931

Buttle, J. M., & McDonald, D. J. (2002). Coupled vertical and lateral preferential flow on a forested slope. *Water Resources Research*, *38*(5), 11–18.

Calabrese, S., Richter, D. D., & Porporato, A. (2018). The Formation of Clay-Enriched Horizons by Lessivage. *Geophysical Research Letters*, *45*(15), 7588–7595. https://doi.org/10.1029/2018GL078778

Chang, H., Johnson, G., Hinkley, T., & Jung, I.-W. (2014). Spatial analysis of annual runoff ratios and their variability across the contiguous U.S. *Journal of Hydrology*, *511*, 387–402. https://doi.org/https://doi.org/10.1016/j.jhydrol.2014.01.066

St. Clair, J., Moon, S., Holbrook, W. S., Perron, J. T., Riebe, C. S., Martel, S. J., et al. (2015). Geophysical imaging reveals topographic stress control of bedrock weathering. *Science*, *350*(6260), 534 LP – 538. https://doi.org/10.1126/science.aab2210

Cochand, M., Christe, P., Ornstein, P., & Hunkeler, D. (2019). Groundwater Storage in High Alpine Catchments and its Contribution to Streamflow. *Water Resources Research*, *0*(ja). https://doi.org/10.1029/2018WR022989

Covino, T. P. (2017). Hydrologic connectivity as a framework for understanding biogeochemical flux through watersheds and along fluvial networks. *Geomorphology*, *277*, 133–144. https://doi.org/https://doi.org/10.1016/j.geomorph.2016.09.030

Covino, T. P., & McGlynn, B. L. (2007). Stream gains and losses across a mountain-to-valley transition: Impacts on watershed hydrology and stream water chemistry. *Water Resources Research*, *43*(10), n/a--n/a. https://doi.org/10.1029/2006WR005544

D'Odorico, P., Laio, F., Porporato, A., Ridolfi, L., Rinaldo, A., & Rodriguez-Iturbe, I. (2010). Ecohydrology of Terrestrial Ecosystems. *BioScience*, *60*(11), 898–907. https://doi.org/10.1525/bio.2010.60.11.6

Datry, T., Arscott, D. B., & Sabater, S. (2011). Recent perspectives on temporary river ecology. *Aquatic Sciences*, *73*(4), 453. https://doi.org/10.1007/s00027-011-0236-1

Dettinger, M. D., & Diaz, H. F. (2000). Global characteristics of stream flow seasonality and variability. *Journal of Hydrometeorology*, *1*(4), 289–310.

Detty, J. M., & McGuire, K. J. (2010). Topographic controls on shallow groundwater dynamics: implications of hydrologic connectivity between hillslopes and riparian zones in a till mantled catchment. *Hydrological Processes*, *24*(16), 2222–2236.

Donohue, R. J., Roderick, M. L., & McVicar, T. R. (2007). On the importance of including vegetation dynamics in Budyko's hydrological model. *Hydrol. Earth Syst. Sci.*, *11*(2), 983–995. https://doi.org/10.5194/hess-11-983-2007

Dralle, D. N., Hahm, W. J., Rempe, D. M., Karst, N. J., Thompson, S. E., & Dietrich, W. E. (2018). Quantification of the seasonal hillslope water storage that does not drive streamflow. *Hydrological Processes*, *32*(13), 1978–1992. https://doi.org/10.1002/hyp.11627

Dunne, T., & Black, R. D. (1970). Partial Area Contributions to Storm Runoff in a Small New England Watershed. *Water Resources Research*, *6*(5), 1296–1311. https://doi.org/10.1029/WR006i005p01296

Eagleson, P. S. (1982). Ecological optimality in water-limited natural soil-vegetation systems: 1. Theory and hypothesis. *Water Resources Research*, *18*(2), 325–340. https://doi.org/10.1029/WR018i002p00325

Elsenbeer, H. (2001). Hydrologic flowpaths in tropical rainforest soilscapes—a review. *Hydrological Processes*, *15*(10), 1751–1759. https://doi.org/10.1002/hyp.237

Evaristo, J., Jasechko, S., & McDonnell, J. J. (2015). Global separation of plant transpiration from groundwater and streamflow. *Nature*, *525*, 91. Retrieved from https://doi.org/10.1038/nature14983

Evaristo, J., McDonnell, J. J., Scholl, M. A., Bruijnzeel, L. A., & Chun, K. P. (2016). Insights into plant water uptake from xylem-water isotope measurements in two tropical catchments with contrasting moisture conditions. *Hydrological Processes*, *30*(18), 3210–3227. https://doi.org/10.1002/hyp.10841

Fan, Y., Miguez-Macho, G., Jobbágy, E. G., Jackson, R. B., & Otero-Casal, C. (2017). Hydrologic regulation of plant rooting depth. *Proceedings of the*

National Academy of Sciences, *114*(40), 10572 LP – 10577. https://doi.org/10.1073/pnas.1712381114

Fan, Y., Clark, M., Lawrence, D. M., Swenson, S., Band, L. E., Brantley, S. L., et al. (2019). Hillslope Hydrology in Global Change Research and Earth System Modeling. *Water Resources Research*, *0*(0). https://doi.org/10.1029/2018WR023903

Fedora, M. A., & Beschta, R. L. (1989). Storm runoff simulation using an antecedent precipitation index (API) model. *Journal of Hydrology*, *112*(1–2), 121–133.

Feng, X., Thompson, S. E., Woods, R. A., & Porporato, A. (2019). Quantifying Asynchronicity of Precipitation and Potential Evapotranspiration in Mediterranean Climates. *Geophysical Research Letters*, *n/a*(n/a). https://doi.org/10.1029/2019GL085653

Freeze, R. A. (1972). Role of subsurface flow in generating surface runoff: 2. Upstream source areas. *Water Resources Research*, *8*(5), 1272–1283. https://doi.org/10.1029/WR008i005p01272

Gannon, J. P., Bailey, S. W., & McGuire, K. J. (2014). Organizing groundwater regimes and response thresholds by soils: A framework for understanding runoff generation in a headwater catchment. *Water Resources Research*, *50*(11), 8403–8419. https://doi.org/10.1002/2014WR015498

Gao, H., Hrachowitz, M., Schymanski, S. J., Fenicia, F., Sriwongsitanon, N., & Savenije, H. H. G. (2014). Climate controls how ecosystems size the root zone storage capacity at catchment scale. *Geophysical Research Letters*, *41*(22), 7916–7923. https://doi.org/10.1002/2014GL061668

Godsey, S., Elsenbeer, H., & Stallard, R. (2004). Overland flow generation in two lithologically distinct rainforest catchments. *Journal of Hydrology*, *295*(1), 276–290. https://doi.org/https://doi.org/10.1016/j.jhydrol.2004.03.014

Godsey, S. E., & Kirchner, J. W. (2014). Dynamic, discontinuous stream networks: hydrologically driven variations in active drainage density, flowing channels and stream order. *Hydrological Processes*, *28*(23), 5791–5803. https://doi.org/10.1002/hyp.10310

González-Ferreras, A. M., & Barquín, J. (2017). Mapping the temporary and perennial character of whole river networks. *Water Resources Research*, *53*(8), 6709–6724. https://doi.org/10.1002/2017WR020390

Grant, G. E., & Dietrich, W. E. (2017). The frontier beneath our feet. *Water*

Resources Research, *53*(4), 2605–2609. https://doi.org/10.1002/2017WR020835

Hahm, W. J., Rempe, D. M., Dralle, D. N., Dawson, T. E., Lovill, S. M., Bryk, A. B., et al. (2019). Lithologically controlled subsurface critical zone thickness and water storage capacity determine regional plant community composition. *Water Resources Research*, *0*(ja). https://doi.org/10.1029/2018WR023760

Hahm, W. J., Dralle, D. N., Rempe, D. M., Bryk, A. B., Thompson, S. E., Dawson, T. E., & Dietrich, W. E. (2019). Low Subsurface Water Storage Capacity Relative to Annual Rainfall Decouples Mediterranean Plant Productivity and Water Use From Rainfall Variability. *Geophysical Research Letters*, *46*(12), 6544–6553. https://doi.org/10.1029/2019GL083294

Hale, V. C., McDonnell, J. J., Stewart, M. K., Solomon, D. K., Doolitte, J., Ice, G. G., & Pack, R. T. (2016). Effect of bedrock permeability on stream base flow mean transit time scaling relationships: 2. Process study of storage and release. *Water Resources Research*, *52*(2), 1375–1397. https://doi.org/10.1002/2015WR017660

Hamon, W. R. (1963). Computation of direct runoff amounts from storm rainfall. *International Association of Scientific Hydrology Publication*, *63*, 52–62.

Hansen, W. F. (2001). Identifying stream types and management implications. *Forest Ecology and Management*, *143*(1), 39–46. https://doi.org/https://doi.org/10.1016/S0378-1127(00)00503-X

Hanson, P. J., Amthor, J. S., Wullschleger, S. D., Wilson, K. B., Grant, R. F., Hartley, A., et al. (2004). OAK FOREST CARBON AND WATER SIMULATIONS: MODEL INTERCOMPARISONS AND EVALUATIONS AGAINST INDEPENDENT DATA. *Ecological Monographs*, *74*(3), 443–489. https://doi.org/10.1890/03-4049

Harman, C. J., & Cosans, C. L. (2019). A low-dimensional model of bedrock weathering and lateral flow co-evolution in hillslopes: 2. Controls on weathering and permeability profiles, drainage hydraulics, and solute export pathways. *Hydrological Processes*, *0*(ja). https://doi.org/10.1002/hyp.13385

Hartmann, D. L., Tank, A. M. G. K., Rusticucci, M., Alexander, L. V, Brönnimann, S., Charabi, Y. A. R., et al. (2013). Observations: atmosphere and surface. In *Climate change 2013 the physical science basis: Working group I contribution to the fifth assessment report of the intergovernmental panel on climate change* (pp. 159–254). Cambridge University Press.

Hellwig, J., & Stahl, K. (2018). An assessment of trends and potential future changes in groundwater-baseflow drought based on catchment response times. *Hydrology and Earth System Sciences*, *22*(12), 6209–6224.

Herron, N., & Wilson, C. (2001). A water balance approach to assessing the hydrologic buffering potential of an alluvial fan. *Water Resources Research*, *37*(2), 341–351. https://doi.org/10.1029/2000WR900253

Hewlett, J. D., & Hibbert, A. R. (1963). Moisture and energy conditions within a sloping soil mass during drainage. *Journal of Geophysical Research*, *68*(4), 1081–1087.

Hewlett, J. D., & Hibbert, A. R. (1967). Factors affecting the response of small watersheds to precipitation in humid areas. *Forest Hydrology*, *1*, 275–290.

Hodges, C., Mallard, J., Markewitz, D., Barcellos, D., & Thompson, A. (2019). Seasonal and spatial variation in the potential for iron reduction in soils of the Southeastern Piedmont of the US. *CATENA*, *180*, 32–40. https://doi.org/https://doi.org/10.1016/j.catena.2019.03.026

Holbrook, W. S., Riebe, C. S., Elwaseif, M., L. Hayes, J., Basler-Reeder, K., L. Harry, D., et al. (2014). Geophysical constraints on deep weathering and water storage potential in the Southern Sierra Critical Zone Observatory. *Earth Surface Processes and Landforms*, *39*(3), 366–380. https://doi.org/10.1002/esp.3502

Holdridge, L. R. (1947). Determination of World Plant Formations From Simple Climatic Data. *Science*, *105*(2727), 367 LP – 368. https://doi.org/10.1126/science.105.2727.367

Hood, J. L., & Hayashi, M. (2015). Characterization of snowmelt flux and groundwater storage in an alpine headwater basin. *Journal of Hydrology*, *521*, 482–497. https://doi.org/https://doi.org/10.1016/j.jhydrol.2014.12.041

Hooke, R. L. (2000). On the history of humans as geomorphic agents. *Geology*, *28*(9), 843–846. https://doi.org/10.1130/0091-7613(2000)28<843:OTHOHA>2.0.CO;2

Horton, R. E. (1933). The Role of infiltration in the hydrologic cycle. *Eos, Transactions American Geophysical Union*, *14*(1), 446–460. https://doi.org/10.1029/TR014i001p00446

Horton, R. E. (1942). Remarks on hydrologic terminology. *Eos, Transactions American Geophysical Union*, *23*(2), 479–482.

Horton, R. E. (1945). EROSIONAL DEVELOPMENT OF STREAMS AND THEIR DRAINAGE BASINS; HYDROPHYSICAL APPROACH TO QUANTITATIVE MORPHOLOGY. *GSA Bulletin*, *56*(3), 275–370. https://doi.org/10.1130/0016-7606(1945)56[275:EDOSAT]2.0.CO;2

Hursh, C. R. (1936). Storm water and absorption. *Eos Trans. AGU*, *17*(2), 301–302.

Hursh, C. R. (1944). Water storage limitations in forest soil profiles. In *Proc. Soil Science Society of America* (Vol. 8, p. 412).

Jackson, C. R., Sun, G., Amatya, D., Swank, W. T., Riedel, M., Patric, J., et al. (2004). Fifty years of forest hydrology in the Southeast. *In: Ice, GG; Stednick, JD A Century of Forested and Wildland Watershed Lessons. Bethesda, MD: The Society of American Foresters. 33-112. Chapter 3.*

Jackson, C. R., Martin, J. K., Leigh, D. S., & West, L. T. (2005). A southeastern piedmont watershed sediment budget: Evidence for a multi-millennial agricultural legacy. *Journal of Soil and Water Conservation*, *60*(6), 298 LP – 310. Retrieved from http://www.jswconline.org/content/60/6/298.abstract

Jackson, C. R., Bitew, M., & Du, E. (2014). When interflow also percolates: downslope travel distances and hillsclope process zones.

Jaeger, K. L., Olden, J. D., & Pelland, N. A. (2014). Climate change poised to threaten hydrologic connectivity and endemic fishes in dryland streams. *Proceedings of the National Academy of Sciences*, *111*(38), 13894–13899.

Jaeger, K. L., Sando, R., McShane, R. R., Dunham, J. B., Hockman-Wert, D. P., Kaiser, K. E., et al. (2019). Probability of Streamflow Permanence Model (PROSPER): A spatially continuous model of annual streamflow permanence throughout the Pacific Northwest. *Journal of Hydrology X*, *2*, 100005. https://doi.org/https://doi.org/10.1016/j.hydroa.2018.100005

James, L. A. (2013). Legacy sediment: definitions and processes of episodically produced anthropogenic sediment. *Anthropocene*, *2*, 16–26.

Jefferson, A., Grant, G. E., Lewis, S. L., & Lancaster, S. T. (2010). Coevolution of hydrology and topography on a basalt landscape in the Oregon Cascade Range, USA. *Earth Surface Processes and Landforms*, *35*(7), 803–816. https://doi.org/10.1002/esp.1976

Jencso, K. G., McGlynn, B. L., Gooseff, M. N., Wondzell, S. M., Bencala, K. E., & Marshall, L. A. (2009). Hydrologic connectivity between landscapes and streams: Transferring reach- and plot-scale understanding to the catchment scale. *Water Resources Research*, *45*(4). https://doi.org/10.1029/2008WR007225

Kendall, K. A., Shanley, J. B., & McDonnell, J. J. (1999). A hydrometric and geochemical approach to test the transmissivity feedback hypothesis during snowmelt. *Journal of Hydrology*, *219*(3), 188–205. https://doi.org/https://doi.org/10.1016/S0022-1694(99)00059-1

Kim, H. J., Sidle, R. C., & Moore, R. D. (2005). Shallow lateral flow from a forested hillslope: Influence of antecedent wetness. *Catena*, *60*(3), 293–306.

Kirchner, J. W. (2009). Catchments as simple dynamical systems: Catchment characterization, rainfall-runoff modeling, and doing hydrology backward. *Water Resources Research*, *45*(2). https://doi.org/10.1029/2008WR006912

Kirkby, M. J., & Chorley, R. J. (1967). THROUGHFLOW, OVERLAND FLOW AND EROSION. *International Association of Scientific Hydrology. Bulletin*, *12*(3), 5–21. https://doi.org/10.1080/02626666709493533

Klaus, J., & Jackson, C. R. (2018). Interflow Is Not Binary: A Continuous Shallow Perched Layer Does Not Imply Continuous Connectivity. *Water Resources Research*, *54*(9), 5921–5932. https://doi.org/10.1029/2018WR022920

Kohler, M. A., & Linsley, R. K. (1951). *Predicting the runoff from storm rainfall* (Vol. 30). US Department of Commerce, Weather Bureau.

Landerer, F. W., & Swenson, S. C. (2012). Accuracy of scaled GRACE terrestrial water storage estimates. *Water Resources Research*, *48*(4).

Laseter, S. H., Ford, C. R., Vose, J. M., & Swift Jr, L. W. (2012). Long-term temperature and precipitation trends at the Coweeta Hydrologic Laboratory, Otto, North Carolina, USA. *Hydrology Research*, *43*(6), 890–901. https://doi.org/10.2166/nh.2012.067

Lawes, J. B., & Gilbert, J. H. (1888). On the present position of the question of the sources of the nitrogen of vegetation, with some new results, and preliminary notice of new lines of investigation. *Proceedings of the Royal Society of London*, *43*(258–265), 108–116.

Lohse, K. A., & Dietrich, W. E. (2005). Contrasting effects of soil development on hydrological properties and flow paths. *Water Resources Research*, *41*(12). https://doi.org/10.1029/2004WR003403

Lu, J., Sun, G., McNulty, S. G., & Amatya, D. M. (2005). A COMPARISON OF SIX POTENTIAL EVAPOTRANSPIRATION METHODS FOR REGIONAL

USE IN THE SOUTHEASTERN UNITED STATES1. *JAWRA Journal of the American Water Resources Association*, *41*(3), 621–633. https://doi.org/10.1111/j.1752-1688.2005.tb03759.x

Marchi, L., Borga, M., Preciso, E., & Gaume, E. (2010). Characterisation of selected extreme flash floods in Europe and implications for flood risk management. *Journal of Hydrology*, *394*(1–2), 118–133.

Markovich, K. H., Manning, A. H., Condon, L. E., & McIntosh, J. C. (2019). Mountain-Block Recharge: A Review of Current Understanding. *Water Resources Research*, *n/a*(n/a). https://doi.org/10.1029/2019WR025676

McDonnell, J. J. (1990). A Rationale for Old Water Discharge Through Macropores in a Steep, Humid Catchment. *Water Resources Research*, *26*(11), 2821–2832. https://doi.org/10.1029/WR026i011p02821

McGlynn, B. L., & McDonnell, J. J. (2003a). Quantifying the relative contributions of riparian and hillslope zones to catchment runoff. *Water Resources Research*, *39*(11). https://doi.org/10.1029/2003WR002091

McGlynn, B. L., & McDonnell, J. J. (2003b). Role of discrete landscape units in controlling catchment dissolved organic carbon dynamics. *Water Resources Research*, *39*(4). https://doi.org/10.1029/2002WR001525

McGlynn, B. L., McDonnell, J. J., Seibert, J., & Kendall, C. (2004). Scale effects on headwater catchment runoff timing, flow sources, and groundwater-streamflow relations. *Water Resources Research*, *40*(7). https://doi.org/10.1029/2003WR002494

McGuire, K. J., McDonnell, J. J., Weiler, M., Kendall, C., McGlynn, B. L., Welker, J. M., & Seibert, J. (2005). The role of topography on catchment-scale water residence time. *Water Resources Research*, *41*(5). https://doi.org/10.1029/2004WR003657

McNamara, J. P., Kane, D. L., & Hinzman, L. D. (1998). An analysis of streamflow hydrology in the Kuparuk River Basin, Arctic Alaska: a nested watershed approach. *Journal of Hydrology*, *206*(1), 39–57. https://doi.org/https://doi.org/10.1016/S0022-1694(98)00083-3

McNamara, J. P., Tetzlaff, D., Bishop, K., Soulsby, C., Seyfried, M., Peters, N. E., et al. (2011). Storage as a Metric of Catchment Comparison. *Hydrological Processes*, *25*(21), 3364–3371. https://doi.org/10.1002/hyp.8113

Meixner, T., Manning, A. H., Stonestrom, D. A., Allen, D. M., Ajami, H., Blasch,

K. W., et al. (2016). Implications of projected climate change for groundwater recharge in the western United States. *Journal of Hydrology*, *534*, 124–138. https://doi.org/https://doi.org/10.1016/j.jhydrol.2015.12.027

Meyer, J. L., Strayer, D. L., Wallace, J. B., Eggert, S. L., Helfman, G. S., & Leonard, N. E. (2007). The Contribution of Headwater Streams to Biodiversity in River Networks. *JAWRA Journal of the American Water Resources Association*, *43*(1), 86–103. https://doi.org/10.1111/j.1752-1688.2007.00008.x

Milly, P. C. D. (1994). Climate, interseasonal storage of soil water, and the annual water balance. *Advances in Water Resources*, *17*(1), 19–24. https://doi.org/https://doi.org/10.1016/0309-1708(94)90020-5

Montgomery, D. R., & Dietrich, W. E. (1988). Where do channels begin? *Nature*, *336*(6196), 232–234.

Nadeau, T.-L., & Rains, M. C. (2007). Hydrological Connectivity Between Headwater Streams and Downstream Waters: How Science Can Inform Policy1. *JAWRA Journal of the American Water Resources Association*, *43*(1), 118–133. https://doi.org/10.1111/j.1752-1688.2007.00010.x

Nippgen, F., McGlynn, B. L., & Emanuel, R. E. (2015). The spatial and temporal evolution of contributing areas. *Water Resources Research*, *51*(6), 4550–4573. https://doi.org/10.1002/2014WR016719

Nippgen, F., McGlynn, B. L., Emanuel, R. E., & Vose, J. M. (2016). Watershed memory at the Coweeta Hydrologic Laboratory: The effect of past precipitation and storage on hydrologic response. *Water Resources Research*, *52*(3), 1673–1695. https://doi.org/10.1002/2015WR018196

Novick, K., Oishi, C., & Stoy, P. (2016). *AmeriFlux US-Dk2 Duke Forest-hardwoods*. AmeriFlux; Indiana University; Montana State University; USDA Forest Service.

Penna, D., Tromp-van Meerveld, H. J., Gobbi, A., Borga, M., & Dalla Fontana, G. (2011). The influence of soil moisture on threshold runoff generation processes in an alpine headwater catchment. *Hydrology and Earth System Sciences*, *15*(3), 689–702.

Pereira, A. R., & De Camargo, Â. P. (1989). An analysis of the criticism of Thornthwaite's equation for estimating potential evapotranspiration. *Agricultural and Forest Meteorology*, *46*(1–2), 149–157.

Peters, N. E., & Aulenbach, B. T. (2011). Water storage at the Panola Mountain

Research Watershed, Georgia, USA. *Hydrological Processes*, *25*(25), 3878–3889. https://doi.org/10.1002/hyp.8334

Pfister, L., Martínez-Carreras, N., Hissler, C., Klaus, J., Carrer, G. E., Stewart, M. K., & McDonnell, J. J. (2017). Bedrock geology controls on catchment storage, mixing, and release: A comparative analysis of 16 nested catchments. *Hydrological Processes*, *31*(10), 1828–1845. https://doi.org/10.1002/hyp.11134

Porporato, A., D'Odorico, P., Laio, F., Ridolfi, L., & Rodriguez-Iturbe, I. (2002). Ecohydrology of water-controlled ecosystems. *Advances in Water Resources*, *25*(8), 1335–1348. https://doi.org/https://doi.org/10.1016/S0309-1708(02)00058-1

Pringle, C. M. (2001). Hydrologic connectivity and the management of biological reserves: a global perspective. *Ecological Applications*, *11*(4), 981–998.

Pringle, C. M. (2003). What is hydrologic connectivity and why is it ecologically important? *Hydrological Processes*, *17*(13), 2685–2689.

Puigdefabregas, J., del Barrio, G., Boer, M. M., Gutiérrez, L., & Solé, A. (1998). Differential responses of hillslope and channel elements to rainfall events in a semi-arid area. *Geomorphology*, *23*(2), 337–351. https://doi.org/https://doi.org/10.1016/S0169-555X(98)00014-2

Rasmussen, T. C., & Mote, T. L. (2007). Monitoring surface and subsurface water storage using confined aquifer water levels at the Savannah River Site, USA. *Vadose Zone Journal*, *6*(2), 327–335.

Rempe, D. M., & Dietrich, W. E. (2018). Direct observations of rock moisture, a hidden component of the hydrologic cycle. *Proceedings of the National Academy of Sciences*, *115*(11), 2664 LP – 2669. https://doi.org/10.1073/pnas.1800141115

Richards, L. A. (1931). Capillary conduction of liquids through porous mediums. *Physics*, *1*(5), 318–333.

Richter, D. D., Markewitz, D., Heine, P. R., Jin, V., Raikes, J., Tian, K., & Wells, C. G. (2000). Legacies of agriculture and forest regrowth in the nitrogen of old-field soils. *Forest Ecology and Management*, *138*(1–3), 233–248. https://doi.org/10.1016/S0378-1127(00)00399-6

Richter, D. D., Eppes, M.-C., Austin, J. C., Bacon, A. R., Billings, S., Brecheisen, Z., et al. (2019). Soil Production and the soil geomorphology legacy of Grove Karl Gilbert. *Soil Science Society of America Journal*.

Rinderer, M., van Meerveld, H. J., & Seibert, J. (2014). Topographic controls on shallow groundwater levels in a steep, prealpine catchment: When are the TWI assumptions valid? *Water Resources Research*, *50*(7), 6067–6080. https://doi.org/10.1002/2013WR015009

Rinderer, M., van Meerveld, H. J., & McGlynn, B. L. (2019). From Points to Patterns: Using Groundwater Time Series Clustering to Investigate Subsurface Hydrological Connectivity and Runoff Source Area Dynamics. *Water Resources Research*, *0*(0). https://doi.org/10.1029/2018WR023886

Rodell, M., Chen, J., Kato, H., Famiglietti, J. S., Nigro, J., & Wilson, C. R. (2007). Estimating groundwater storage changes in the Mississippi River basin (USA) using GRACE. *Hydrogeology Journal*, *15*(1), 159–166.

Rodriguez-Iturbe, I., D'Odorico, P., Porporato, A., & Ridolfi, L. (1999). On the spatial and temporal links between vegetation, climate, and soil moisture. *Water Resources Research*, *35*(12), 3709–3722. https://doi.org/10.1029/1999WR900255

Rose, S., & Peters, N. E. (2001). Effects of urbanization on streamflow in the Atlanta area (Georgia, USA): a comparative hydrological approach. *Hydrological Processes*, *15*(8), 1441–1457. https://doi.org/10.1002/hyp.218

Ryu, Y., Baldocchi, D. D., Ma, S., & Hehn, T. (2008). Interannual variability of evapotranspiration and energy exchange over an annual grassland in California. *Journal of Geophysical Research: Atmospheres*, *113*(D9). https://doi.org/10.1029/2007JD009263

Sayama, T., McDonnell, J. J., Dhakal, A., & Sullivan, K. (2011). How much water can a watershed store? *Hydrological Processes*, *25*(25), 3899–3908. https://doi.org/10.1002/hyp.8288

Schlesinger, W. H., & Jasechko, S. (2014). Transpiration in the global water cycle. *Agricultural and Forest Meteorology*, *189–190*, 115–117. https://doi.org/https://doi.org/10.1016/j.agrformet.2014.01.011

Schumacher, W. (1864). Soil physics. *German.) Wiegandt & Hempet, Berlin*.

Schymanski, S. J., Sivapalan, M., Roderick, M. L., Hutley, L. B., & Beringer, J. (2009). An optimality-based model of the dynamic feedbacks between natural vegetation and the water balance. *Water Resources Research*, *45*(1). https://doi.org/10.1029/2008WR006841

Seibert, J., Bishop, K., Nyberg, L., & Rodhe, A. (2011). Water storage in a till catchment. I: Distributed modelling and relationship to runoff. *Hydrological*

Processes, *25*(25), 3937–3949. https://doi.org/10.1002/hyp.8309

Selker, J. S., McCord, J. T., & Keller, C. K. (1999). *Vadose zone processes*. CRC Press.

Seyfried, M. S., Grant, L. E., Marks, D., Winstral, A., & McNamara, J. (2009). Simulated soil water storage effects on streamflow generation in a mountainous snowmelt environment, Idaho, USA. *Hydrological Processes*, *23*(6), 858–873. https://doi.org/10.1002/hyp.7211

Sidle, R. C., Tsuboyama, Y., Noguchi, S., Hosoda, I., Fujieda, M., & Shimizu, T. (2000). Stormflow generation in steep forested headwaters: a linked hydrogeomorphic paradigm. *Hydrological Processes*, *14*(3), 369–385.

Sidle, R. C., Noguchi, S., Tsuboyama, Y., & Laursen, K. (2001). A conceptual model of preferential flow systems in forested hillslopes: evidence of self-organization. *Hydrological Processes*, *15*(10), 1675–1692. https://doi.org/10.1002/hyp.233

Sittner, W. T., Schauss, C. E., & Monro, J. C. (1969). Continuous hydrograph synthesis with an API-type hydrologic model. *Water Resources Research*, *5*(5), 1007–1022.

Sklash, M. G., & Farvolden, R. N. (1979). The role of groundwater in storm runoff. In *Developments in water science* (Vol. 12, pp. 45–65). Elsevier.

Smith, T., Marshall, L., McGlynn, B., & Jencso, K. (2013). Using field data to inform and evaluate a new model of catchment hydrologic connectivity. *Water Resources Research*, *49*(10), 6834–6846.

Soulsby, C., Tetzlaff, D., & Hrachowitz, M. (2009). Tracers and transit times: windows for viewing catchment scale storage? *Hydrological Processes*, *23*(24), 3503–3507. https://doi.org/10.1002/hyp.7501

Spence, C. (2010). A Paradigm Shift in Hydrology: Storage Thresholds Across Scales Influence Catchment Runoff Generation. *Geography Compass*, *4*(7), 819–833. https://doi.org/10.1111/j.1749-8198.2010.00341.x

Staudinger, M., Stoelzle, M., Seeger, S., Seibert, J., Weiler, M., & Stahl, K. (2017). Catchment water storage variation with elevation. *Hydrological Processes*, *31*(11), 2000–2015. https://doi.org/10.1002/hyp.11158

Stephenson, N. L. (1990). Climatic Control of Vegetation Distribution: The Role of the Water Balance. *The American Naturalist*, *135*(5), 649–670. https://doi.org/10.1086/285067

Stoy, P. C., Katul, G. G., Siqueira, M. B. S., Juang, J., Novick, K. A., McCarthy, H. R., et al. (2006). Separating the effects of climate and vegetation on evapotranspiration along a successional chronosequence in the southeastern US. *Global Change Biology*, *12*(11), 2115–2135.

Swarowsky, A., Dahlgren, R. A., Tate, K. W., Hopmans, J. W., & O'Geen, A. T. (2011). Catchment-Scale Soil Water Dynamics in a Mediterranean-Type Oak Woodland. *Vadose Zone Journal*, *10*, 800–815. https://doi.org/10.2136/vzj2010.0126

Taylor, K. E., Stouffer, R. J., & Meehl, G. A. (2011). An Overview of CMIP5 and the Experiment Design. *Bulletin of the American Meteorological Society*, *93*(4), 485–498. https://doi.org/10.1175/BAMS-D-11-00094.1

Tetzlaff, D., Birkel, C., Dick, J., Geris, J., & Soulsby, C. (2014). Storage dynamics in hydropedological units control hillslope connectivity, runoff generation, and the evolution of catchment transit time distributions. *Water Resources Research*, *50*(2), 969–985. https://doi.org/10.1002/2013WR014147

Thornthwaite, C. W. (1948). An approach toward a rational classification of climate. *Geographical Review*, *38*(1), 55–94.

Tooth, S. (2000). Process, form and change in dryland rivers: a review of recent research. *Earth-Science Reviews*, *51*(1), 67–107. https://doi.org/https://doi.org/10.1016/S0012-8252(00)00014-3

Trimble, S. W. (1975). *A volumetric estimate of man-induced soil erosion on the southern Piedmont Plateau*. *Prospective technology for predicting sediment yields and sources*.

Trimble, S. W. (1981). Changes in sediment storage in the Coon Creek basin, driftless area, Wisconsin, 1853 to 1975. *Science*. https://doi.org/10.1126/science.214.4517.181

Tromp-van Meerveld, H. J., & McDonnell, J. J. (2006). Threshold relations in subsurface stormflow: 2. The fill and spill hypothesis. *Water Resources Research*, *42*(2). https://doi.org/10.1029/2004WR003800

Tsuboyama, Y., Sidle, R. C., Noguchi, S., & Hosoda, I. (1994). Flow and solute transport through the soil matrix and macropores of a hillslope segment. *Water Resources Research*, *30*(4), 879–890.

Tsukamoto, Y. (1963). Storm discharge from an experimental watershed. *Journal of the Japanese Forestry Society*, *45*(6), 186–190.

USBR. (2001). *Water measurement manual*. Denver, CO: US Government Printing Office.

Vidon, P. G. F., & Hill, A. R. (2004). Landscape controls on nitrate removal in stream riparian zones. *Water Resources Research*, *40*(3).

Vorosmarty, C. J., Federer, C. A., & Schloss, A. L. (1998). Potential evaporation functions compared on US watersheds: Possible implications for global-scale water balance and terrestrial ecosystem modeling. *Journal of Hydrology*, *207*(3), 147–169. https://doi.org/https://doi.org/10.1016/S0022-1694(98)00109-7

Vose, J. M., & Elliott, K. J. (2016). Oak, Fire, and Global Change in the Eastern USA: What Might the Future Hold? *Fire Ecology*, *12*(2), 160–179. https://doi.org/10.4996/fireecology.1202160

Wade, A. M., Richter, D. D., Cherkinsky, A., Craft, C. B., & Heine, P. R. (2020). Limited carbon contents of centuries old soils forming in legacy sediment. *Geomorphology*, *354*, 107018. https://doi.org/https://doi.org/10.1016/j.geomorph.2019.107018

Wagener, T., Sivapalan, M., Troch, P., & Woods, R. A. (2007). Catchment Classification and Hydrologic Similarity. *Geography Compass*, *1*(4), 901–931. https://doi.org/10.1111/j.1749-8198.2007.00039.x

Walsh, C. J., Roy, A., Feminella, J., Cottingham, P., Groffman, P., & Morgan II, R. (2005). The Urban Stream Syndrome: Current Knowledge and the Search For A Cure. *Am. Benthol. Soc*, *24*, 706–723. https://doi.org/10.1899/0887-3593(2005)024\[0706:TUSSCK\]2.0.CO;2

Walter, R. C., & Merritts, D. J. (2008). Natural streams and the legacy of water-powered mills. *Science*, *319*(5861), 299–304. https://doi.org/10.1126/science.1151716

Wang, D., & Cai, X. (2009). Detecting human interferences to low flows through base flow recession analysis. *Water Resources Research*, *45*(7). https://doi.org/10.1029/2009WR007819

Weiler, M., & McDonnell, J. J. (2007). Conceptualizing lateral preferential flow and flow networks and simulating the effects on gauged and ungauged hillslopes. *Water Resources Research*, *43*(3).

Weyman, D. R. (1970). THROUGHFLOW ON HILLSLOPES AND ITS RELATION TO THE STREAM HYDROGRAPH. *International Association of Scientific Hydrology. Bulletin*, *15*(3), 25–33.

https://doi.org/10.1080/02626667009493969

Weyman, D. R. (1973). Measurements of the downslope flow of water in a soil. *Journal of Hydrology*, *20*(3), 267–288.

Whittaker, R. H. (1970). *Communities and ecosystems. Communities and ecosystems.* New York, NY: MacMillan Publishing Company.

Wilson, J. L., & Guan, H. (2004). Mountain-block hydrology and mountain-front recharge. Wiley Online Library.

Wilson, K. B., & Baldocchi, D. D. (2000). Seasonal and interannual variability of energy fluxes over a broadleaved temperate deciduous forest in North America. *Agricultural and Forest Meteorology*, *100*(1), 1–18. https://doi.org/https://doi.org/10.1016/S0168-1923(99)00088-X

Wohl, E. (2019). Forgotten Legacies: Understanding and Mitigating Historical Human Alterations of River Corridors. *Water Resources Research*, *0*(ja). https://doi.org/10.1029/2018WR024433

Wolock, D. M., & McCabe, G. J. (1999). Explaining spatial variability in mean annual runoff in the conterminous United States. *Climate Research*, *11*(2), 149–159. Retrieved from https://www.int-res.com/abstracts/cr/v11/n2/p149-159/

Wondzell, S. M. (2011). The role of the hyporheic zone across stream networks. *Hydrological Processes*, *25*(22), 3525–3532. https://doi.org/10.1002/hyp.8119

Woodruff, J. F., & Hewlett, J. D. (1970). Predicting and Mapping the Average Hydrologic Response for the Eastern United States. *Water Resources Research*, *6*(5), 1312–1326. https://doi.org/10.1029/WR006i005p01312

Woods, R. A., & Rowe, L. (1996). The changing spatial variability of subsurface flow across a hillside. *Journal of Hydrology (New Zealand)*, *35*(1), 51–86. Retrieved from http://www.jstor.org/stable/43944761

Woods, S. W., MacDonald, L. H., & Westbrook, C. J. (2006). Hydrologic interactions between an alluvial fan and a slope wetland in the central Rocky Mountains, USA. *Wetlands*, *26*(1), 230–243. https://doi.org/10.1672/0277-5212(2006)26[230:HIBAAF]2.0.CO;2

Wooldridge, S. A., Franks, S. W., & Kalma, J. D. (2001). Hydrological implications of the Southern Oscillation: variability of the rainfall-runoff relationship. *Hydrological Sciences Journal*, *46*(1), 73–88.

https://doi.org/10.1080/02626660109492801

Xiao, D., Shi, Y., Brantley, S. L., Forsythe, B., DiBiase, R., Davis, K., & Li, L. (2019). Streamflow generation from catchments of contrasting lithologies: the role of soil properties, topography, and catchment size. *Water Resources Research*, *0*(ja). https://doi.org/10.1029/2018WR023736

Yokoo, Y., Sivapalan, M., & Oki, T. (2008). Investigating the roles of climate seasonality and landscape characteristics on mean annual and monthly water balances. *Journal of Hydrology*, *357*(3), 255–269. https://doi.org/https://doi.org/10.1016/j.jhydrol.2008.05.010

Zimmer, M. A., & McGlynn, B. L. (2017a). Bidirectional stream–groundwater flow in response to ephemeral and intermittent streamflow and groundwater seasonality. *Hydrological Processes*, *31*(22), 3871–3880. https://doi.org/10.1002/hyp.11301

Zimmer, M. A., & McGlynn, B. L. (2017b). Ephemeral and intermittent runoff generation processes in a low relief, highly weathered catchment. *Water Resources Research*, *53*(8), 7055–7077. https://doi.org/10.1002/2016WR019742

Zimmer, M. A., & McGlynn, B. L. (2018). Lateral, Vertical, and Longitudinal Source Area Connectivity Drive Runoff and Carbon Export Across Watershed Scales. *Water Resources Research*, *54*(3), 1576–1598. https://doi.org/10.1002/2017WR021718

Biography

John Mallard is a watershed hydrologist with interests that range across gradients and stream orders. His research has included studies of stream-groundwater exchange, stream nutrient dynamics, runoff generation, and shallow subsurface groundwater. He has generally favored work that creates or leverages intensively collected field data, remotely sensed landscape characteristics, and parsimonious models to generate new understanding of landscapes that extends beyond study sites. John studied Environmental Science at the University of North Carolina – Chapel Hill (2007) and obtained a Masters in Science from Montana State University (2012). He has worked on both sides of the Mississippi including the Sawtooth Mountains of central Idaho for his Masters degree and the Southern Piedmont of upstate South Carolina for his PhD. He has authored manuscripts in Water Resources Research, Hydrological Processes, and Catena. His work has been presented at multiple regional, national, and international conferences and has won presentation awards at the annual meetings of both the American and European Geophysical Unions.